

Wind-Electric Icemaking Project: Analysis and Dynamometer Testing Volume I

Rick Holz, P.E.
Vahan Gervorgian, Ph.D.
Steve Drouilhet, P.E.
Ed Muljadi, Ph.D.
*National Wind Technology Center
National Renewable Energy Laboratory
Golden, Colorado*



National Renewable Energy Laboratory
1617 Cole Boulevard
Golden, Colorado 80401-3393
A national laboratory of the U.S. Department of Energy
Managed by Midwest Research Institute
for the U.S. Department of Energy
under contract No. DE-AC36-83CH10093

Work performed under Task No. WE805020

July 1998

NOTICE

This report was prepared as an account of work sponsored by an agency of the United States government. Neither the United States government nor any agency thereof, nor any of their employees, makes any warranty, express or implied, or assumes any legal liability or responsibility for the accuracy, completeness, or usefulness of any information, apparatus, product, or process disclosed, or represents that its use would not infringe privately owned rights. Reference herein to any specific commercial product, process, or service by trade name, trademark, manufacturer, or otherwise does not necessarily constitute or imply its endorsement, recommendation, or favoring by the United States government or any agency thereof. The views and opinions of authors expressed herein do not necessarily state or reflect those of the United States government or any agency thereof.

Available to DOE and DOE contractors from:
Office of Scientific and Technical Information (OSTI)
P.O. Box 62
Oak Ridge, TN 37831
Prices available by calling (423) 576-8401

Available to the public from:
National Technical Information Service (NTIS)
U.S. Department of Commerce
5285 Port Royal Road
Springfield, VA 22161
(703) 487-4650



Abstract

The wind/hybrid systems group at the National Renewable Energy Laboratory has been researching the most practical and cost-effective methods for producing ice from off-grid wind-electric power systems. The first phase of the project, conducted in 1993-94, included full-scale dynamometer and field testing of two different electric ice makers directly connected to a permanent magnet alternator. The results of that phase were encouraging and the second phase of the project was launched in which steady-state and dynamic numerical models of these systems were developed and experimentally validated. The third phase of the project was the dynamometer testing of the North Star ice maker, which is powered by a 12-kilowatt Bergey Windpower Company, Inc., alternator. This report describes both the second and third project phases. Also included are detailed economic analyses and a discussion of the future prospects of wind-electric ice-making systems.

Acknowledgments

The U.S. Department of Energy funded this project through the National Renewable Energy Laboratory's National Wind Technology Center.

The authors would like to thank Bergey Windpower Company of Norman, Oklahoma; World Power Technologies, Inc., of Duluth, Minnesota; and North Star Ice Equipment Corporation of Seattle, Washington, for providing vital equipment for this project. We are also grateful to Jerry Bianchi for helping us with instrumentation and to Paul Gallipeau and Jim Adams for their timely and accurate machining of much-needed test equipment. We wish to offer special thanks to Holly Davis for her excellent thesis and other helpful comments on Phase 1 of the project.

Table of Contents

Volume 1

| | <u>Page</u> |
|--|-------------|
| 1. Executive Summary..... | 1 |
| 2. Background | 3 |
| 2.1 Wind-Electric Ice Making | 3 |
| 2.2 Investigations of Wind-Electric Ice Making at NREL | 4 |
| PART I: PHASE 1 | |
| 3. Phase 1: Concept Demonstration..... | 5 |
| 3.1 The Start-Up Problem..... | 6 |
| PART II: PHASES 2 AND 3 | |
| 4. Phase 2: Bench-Scale Testing and Model Validation | 8 |
| 4.1 Mathematical Models for Wind-Electric Ice-Making System..... | 8 |
| 4.1.1 Model Assumptions | 8 |
| 4.1.2 Steady-State Model..... | 9 |
| 4.1.3 Dynamic Model..... | 10 |
| 4.2 Bench-Scale Testing..... | 11 |
| 4.2.1 Equipment and Data Acquisition System Description..... | 11 |
| 4.2.2 Test Plan..... | 14 |
| 4.2.3 Test Results..... | 17 |
| 4.2.3.1 Parameter Determinations (Tests 1 and 2) | 17 |
| 4.2.3.2 Line-Connected Induction Motor (Tests 3 and 4) | 17 |
| 4.2.3.3 Alternator/Induction Motor System (Tests 5 and 6)..... | 18 |
| 4.3 Model Validation..... | 19 |
| 4.3.1 Line-Connected Induction Motor Steady-State Validation..... | 19 |
| 4.3.2 Alternator/Induction Motor System Steady-State Validation..... | 21 |
| 4.3.3 Alternator/Induction Motor System Dynamic Test Validation..... | 23 |
| 4.4 Characteristics of North Star Ice-Making Load..... | 28 |
| 4.5 Modeled Dynamic Behavior of Different Approaches to Start-Up Problem | 31 |
| 4.5.1 Basecase..... | 32 |
| 4.5.2 Series Capacitors..... | 33 |
| 4.5.3 Mechanical Clutch | 35 |
| 4.5.4 Centrifugal Compressor | 35 |
| 4.6 Phase 2 Conclusions | 37 |
| 5. Phase 3: Dynamometer Testing of North Star Ice Maker with 12-kW Bergey Alternator | 38 |
| 5.1 Experimental Setup and Data Acquisition System..... | 38 |
| 5.2 Test Plan | 40 |
| 5.3 Test Results | 40 |
| 5.3.1 Experimental Determination of Alternator Parameters..... | 40 |
| 5.3.2 Line-Connected Tests..... | 40 |
| 5.3.3 Alternator-Connected Tests | 42 |
| 5.3.3.1 Ice Maker Steady-State Performance | 42 |
| 5.3.3.2 Start-Up Characteristics | 43 |
| 5.3.4 Variable-Frequency Test..... | 49 |
| 5.3.5 Operating Problems Exposed during Testing..... | 51 |

Table of Contents (Continued)

| | <u>Page</u> |
|--|-------------|
| 5.4. Analysis of Ice Production as a Function of Wind Speed | 51 |
| 5.5 Phase 3 Conclusions | 53 |
| PART III: CONCLUSIONS AND FUTURE PLANS | |
| 6. Design Considerations for a Variable-Frequency Ice-Making System | 54 |
| 6.1 Problems with Running Commercial Ice Makers on Variable-Frequency AC | 54 |
| 6.1.1 The Start-Up Overload Problem | 54 |
| 6.1.2 Mechanical Vibrations at High Frequencies | 55 |
| 6.1.3 Poor Quality of Ice at Low Frequencies..... | 55 |
| 6.1.4 Control System Failures | 56 |
| 6.2 “Strawman” Specification for a Commercial Ice Maker Powered by a PMA Wind Turbine | 56 |
| 6.2.1 Power Source Characterization | 56 |
| 6.2.2 Ambient and Water Source Conditions..... | 56 |
| 6.2.3 Ice Maker Characterization | 57 |
| 6.2.4 Performance Goals..... | 57 |
| 7. The Present and Future of Wind-Electric Ice Making..... | 58 |
| 7.1 Estimated Cost of Ice for Wind-Electric Ice-Making Systems..... | 58 |
| 7.1.1 Hybrid2 Performance Simulations | 61 |
| 7.1.2 Cost-of-Ice Calculations..... | 62 |
| 7.2 The Characteristics of Good Sites for Directly Connected Wind Ice-Making Systems | 63 |
| 7.3 Conclusions and Future Plans..... | 64 |
| 8. Bibliography..... | 65 |

Volume 2

| | |
|---|-----|
| Appendix A: Mathematical Description of Steady-State Model..... | A-1 |
| Appendix B: Mathematical Description of Dynamic Model | B-1 |
| Appendix C: Bench-Scale Test Machinery Specifications | C-1 |
| Appendix D: Detailed Results for Tests 1 and 2 (Machine Parameter Determinations)..... | D-1 |
| Appendix E: Detailed Results for Test 3 (Steady-State Line-Connected Induction Motor)..... | E-1 |
| Appendix F: Detailed Results for Test 4 (Dynamic Line-Connected Induction Motor) | F-1 |
| Appendix G: Detailed Results for Test 5 (Steady-State Alternator/Induction Motor System) | G-1 |
| Appendix H: Detailed Results for Test 6 (Dynamic Alternator/Induction Motor System)..... | H-1 |
| Appendix I: Validation Results for Dynamic Tests of Alternator/Induction Motor System | I-1 |

Table of Contents (Concluded)

| | <u>Page</u> |
|--|-------------|
| Appendix J: Simulations of Different Approaches to Start-Up Problem..... | J-1 |
| Appendix K: Results of Cost-of-Ice Calculations..... | K-1 |

List of Figures

| | <u>Page</u> |
|---|-------------|
| Figure 4.1: Block diagram of wind turbine/ice-making system | 8 |
| Figure 4.2: Electrical equivalent diagram with series capacitor..... | 9 |
| Figure 4.3: Three-phase diagram of “PM Alternator-Induction Motor” electromechanical system | 10 |
| Figure 4.4: Schematic of bench-scale test apparatus (Tests 5 and 6)..... | 12 |
| Figure 4.5: Schematic of bench-scale test apparatus (Tests 3 and 4)..... | 13 |
| Figure 4.6: Dynamometer configuration and torque-speed characteristics | 13 |
| Figure 4.7: Motor speed during start-up of line-connected induction motor (106 VAC @ 60 Hz) with series capacitors: “low”-inertia case | 18 |
| Figure 4.8: Motor speed during start-up of line-connected induction motor (106 VAC @ 60 Hz) with series capacitors: “high”-inertia case | 18 |
| Figure 4.9: “High”-inertia induction motor speed history—started up by alternator (capacitors switched into circuit at 1.25 s)..... | 19 |
| Figure 4.10: Current vs. slip for steady-state operation of line-connected induction motor (load motor) | 20 |
| Figure 4.11: Real power vs. slip for steady-state operation of line-connected induction motor (load motor) | 20 |
| Figure 4.12: Torque vs. slip for steady-state operation of line-connected induction motor (load motor) | 21 |
| Figure 4.13: Model/experiment comparisons for steady-state no-load and locked-rotor tests..... | 21 |
| Figure 4.14: Comparison of line current for no-load start-up | 23 |
| Figure 4.15: Comparison of alternator-phase voltage for no-load start-up | 24 |
| Figure 4.16: Comparison of alternator output power for no-load start-up | 24 |
| Figure 4.17: Comparison of line frequency for no-load start-up..... | 24 |
| Figure 4.18: Comparison of load motor speed for no-load start-up | 25 |
| Figure 4.19: Comparison of load motor electromagnetic torque for no-load start-up..... | 25 |
| Figure 4.20: Comparison of alternator electromagnetic torque for no-load start-up..... | 25 |
| Figure 4.21: Comparison of line current for loaded start-up..... | 26 |
| Figure 4.22: Comparison of alternator-phase voltage for loaded start-up..... | 26 |
| Figure 4.23: Comparison of alternator output power for loaded start-up..... | 27 |
| Figure 4.24: Comparison of line frequency for loaded start-up | 27 |
| Figure 4.25: Comparison of load motor speed for loaded start-up..... | 27 |
| Figure 4.26: Comparison of load motor electromagnetic torque for loaded start-up..... | 28 |
| Figure 4.27: Comparison of alternator electromagnetic torque for loaded start-up | 28 |
| Figure 4.28: Phase currents (North Star start-up test) | 29 |
| Figure 4.29: Phase currents (North Star steady-state test) | 30 |
| Figure 4.30: Input power (North Star start-up test)..... | 30 |
| Figure 4.31: Input power (North Star steady-state test) | 30 |
| Figure 4.32: Input power Fourier transform for North Star start-up test..... | 31 |
| Figure 4.33: Input power Fourier transform for North Star steady-state test..... | 31 |
| Figure 4.34: Compressor motor electromagnetic torque..... | 32 |
| Figure 4.35: Motor rpm (constant-load start) | 33 |
| Figure 4.36: Motor electromagnetic torque (constant-load start)..... | 33 |
| Figure 4.37: Motor start-up torque as a function of alternator frequency at different capacitances | 34 |

List of Figures (Concluded)

| | <u>Page</u> |
|---|-------------|
| Figure 4.38: Motor rpm (constant-load/switched capacitor)..... | 34 |
| Figure 4.39: Motor and load torques (constant-load/switched capacitor)..... | 34 |
| Figure 4.40: Motor rpm (constant-load/clutch)..... | 35 |
| Figure 4.41: Motor and load torques (constant-load/clutch)..... | 35 |
| Figure 4.42: Torque vs. speed load curve for centrifugal compressor..... | 36 |
| Figure 4.43: Motor rpm (scroll compressor)..... | 36 |
| Figure 4.44: Motor and load torques (scroll compressor)..... | 36 |
| Figure 5.1: Dynamometer test setup..... | 39 |
| Figure 5.2: Ice/water circulation diagram..... | 39 |
| Figure 5.3: Measured currents for “warm” and “cold” start-up tests..... | 41 |
| Figure 5.4: Measured power for “warm” and “cold” start-up tests..... | 41 |
| Figure 5.5: Results of 3-minute line-connected tests..... | 42 |
| Figure 5.6a: Results from alternator-connected steady-state test..... | 43 |
| Figure 5.6b: Results from alternator-connected steady-state test..... | 44 |
| Figure 5.7: “Warm” start-up test without series capacitors (25 Hz)..... | 45 |
| Figure 5.8: “Warm” start-up test without series capacitors (30 Hz)..... | 45 |
| Figure 5.9: “Warm” start-up test without series capacitors (35 Hz)..... | 46 |
| Figure 5.10: “Warm” start-up test without series capacitors (40 Hz)..... | 46 |
| Figure 5.11: “Warm” start-up test without series capacitors (45 Hz)..... | 47 |
| Figure 5.12: “Warm” start-up test without series capacitors (50 Hz)..... | 47 |
| Figure 5.13: Alternator-connected “warm” start-up with 750- μ F series capacitor (50 Hz)..... | 48 |
| Figure 5.14: Alternator-connected “warm” start-up with 500- μ F series capacitor (60 Hz)..... | 48 |
| Figure 5.15: Alternator frequency during variable-frequency test..... | 49 |
| Figure 5.16: Mechanical and electrical power during variable-frequency test..... | 49 |
| Figure 5.17: Evaporator and suction temperatures during variable-frequency test..... | 50 |
| Figure 5.18: Cumulative ice production rate during variable-frequency test..... | 50 |
| Figure 5.19: Alternator and wind rotor power..... | 52 |
| Figure 5.20: Ice production versus wind speed..... | 52 |
| Figure 7.1: Cost of ice versus ice production for fuel cost = U.S.\$1.25/gallon..... | 59 |
| Figure 7.2: Cost of ice versus ice production for fuel cost = U.S.\$1.75/gallon..... | 60 |

List of Tables

| | |
|---|----|
| Table 3.1: Description of Ice Makers..... | 5 |
| Table 4.1: Summary of Measurement Transducers and Signal Conditioners..... | 15 |
| Table 4.2: Data Acquisition Parameters..... | 15 |
| Table 4.3: Bench-Scale Test Descriptions..... | 16 |
| Table 4.4: Machine Parameters Used in Numerical Models..... | 17 |
| Table 4.5: Model/Experiment Comparisons for Steady-State Load Tests at 35 Hz..... | 22 |
| Table 4.6: Model/Experiment Comparisons for Steady-State Load Tests at 65 Hz..... | 22 |
| Table 7.1: Ice Production versus Wind Speed for Directly Connected Systems..... | 61 |
| Table 7.2: Estimated Capital Costs for Various Ice-Making Systems..... | 63 |

1. Executive Summary

The primary purpose of this report is to describe the results of Phases 2 and 3 of the National Renewable Energy Laboratory's investigation of directly connected, wind-electric ice-making systems (i.e., in which a vapor-compression refrigeration system ice maker is powered directly from the variable-frequency output of a permanent magnet alternator [PMA] wind turbine). Phase 2 was a follow-on from Phase 1, which was conducted from September 1993 through December 1994. In Phase 1, dynamometer and field tests on two different ice makers, a Scotsman and a North Star, demonstrated that a vapor-compression refrigeration system could operate adequately from an intermittent and variable-frequency power source such as a PMA wind turbine. However, there were some problems with starting the larger of the two ice makers, the North Star. The Phase 2 objective was to develop and validate numerical models that could be used to (1) select the best solutions to the start-up problem, and (2) determine the long-term performance of wind-electric ice-making systems. The Phase 3 objective was to resume full-scale dynamometer tests of the North Star ice maker to verify an electrical start-up solution and collect more operational data.

In Phase 2, a steady-state numerical model was developed for predicting the performance of wind-electric ice-making systems. The model included the wind turbine rotor performance curve, the equivalent circuit equations for the permanent magnet alternator and the induction motor, and the compressor's torque-speed curve. We programmed the model using the MathCad 5.0 software package. A dynamic model, which was also developed in Phase 2, captured the complete dynamic interaction of the alternator, induction motor, and capacitors. We used steady-state torque-speed curves for the wind turbine rotor and compressor load, and programmed the model using the MatLab 4.2 software package.

We used a 1/3- to 1/2-horsepower (hp) "bench-scale" test apparatus to validate the numerical models. The first set of tests was used to determine the equivalent circuit parameters of the PMA and the induction motor (i.e., the load motor). With only a few minor changes, that set of machine parameters was used in all modeling that followed. The validation tests were of two types. The first isolated the induction motor by "line-connecting" it to a variable-voltage, constant-frequency alternating current (AC) power supply. The second had the alternator powering the induction motor directly, as in the actual ice-making system. We used a 2-hp inverter and a 3-hp induction motor to drive the alternator at any desired speed. We then successfully validated the models for all configurations, including those in which capacitors were connected in series between the alternator and induction motor.

After validating the model, we then used it to investigate the following possible solutions to the start-up problem: (1) adding series capacitors between the alternator and the compressor motor, (2) adding a mechanical clutch between the motor and the compressor, and (3) using a different type of compressor such as a centrifugal compressor. The load used in this modeling effort was experimentally determined for the North Star. For all three of these system modifications, the model indicated that the alternator had no problem starting the North Star, provided that the relevant component parameters were correctly sized and/or controlled.

In the Phase 3 dynamometer testing, the North Star ice maker was powered by a Bergey Windpower Company, Inc., 12-kilowatt (kW) PMA in both dynamic and steady-state conditions. Even though the new, 12-kW PMA did not require modification to start the ice maker, several tests were run with series capacitors to collect data, as well as to identify potential problems associated with the altered electrical system. The other major portion of Phase 3 consisted of steady-state testing of the ice-making system over a wide range of operating frequencies. We used these data coupled with known wind turbine characteristics to develop an ice production versus wind-speed curve for the North Star system. Phase 3 revealed more electrical and mechanical problems during steady-state operation and start-up of the

ice maker, many of which were not discovered during the Phase 1 dynamometer and field testing. The most significant problems involved mechanical vibrations of the ice-making equipment at 70–80 hertz (Hz) and poor ice quality over the lower range of frequencies.

Aside from addressing the technical details of the wind-electric ice-making systems, we also discuss the institutional and economical issues. Using the ice production curve from Phase 3 and Hybrid2, the cost of flake ice produced by wind-electric means has been estimated at under \$0.04 per pound of ice. This cost is competitive under certain conditions with the price that many villagers in Mexico and Central America are currently paying for delivered block ice. We also devised some guidelines that will help to screen out potential project sites for wind-electric ice-making.

The North Star D-12 ice maker, which has been the focus of the Phase 2 and 3 investigations, would require extensive modifications to operate from a variable-voltage/variable-frequency power source. We suspect that most other commercially available ice makers would also require some modification. Although modifications are certainly technically feasible, their impact on the cost-effectiveness of the ice-making system has yet to be determined.

Thus, in addition to a definitive ice-maker modification proposal, there is also a continuing need for a detailed market study. However, all of the evidence contained in this report leads us to conclude that further development of directly connected wind ice-making systems could be a worthwhile joint business venture for a small wind turbine manufacturer and a commercial ice-maker manufacturer.

2. Background

2.1 Wind-Electric Ice Making

Many development organizations have identified the need of rural communities in tropical and subtropical climate zones for refrigeration and ice making. Among such communities the most important uses of the latter are for food and vaccine preservation. Food preservation could significantly help to limit malnutrition and the spread of disease. Vaccine preservation also has obvious benefits for the health of a community. Less necessary, but nonetheless important, economic uses of refrigeration or ice include soft-drink chilling and ice-candy preparation. The latter has been documented as playing a significant role in the economies of rural Indonesian villages.³

One subset of food preservation that appears to have synergy with wind energy is fish harvest preservation. In many coastal, tropical, and rural communities around the world, there exist both a good wind resource and a strong dependence on fishing for income and nutrition. In many of these communities where fishing is often the largest industry, ice is purchased at very high prices for their fish harvests. The ice is typically purchased from distant, more-developed towns that have grid electricity. Wind-powered ice makers are a possible source of cheaper and better quality ice for some of these communities.

A study was conducted in 1994–1995 to evaluate the likelihood of successful wind-electric ice-making projects along the coasts of Honduras.¹⁴ Five fishing villages—Miami, Río Tinto, Los Cerritos, Guapinol, and Prumnitara—were each visited for several days by rural-development specialists. In the first three villages, ice was purchased in nominal 100-lb. blocks. The amount of ice used in these three villages varied from 2,000 to 7,000 lbs. per week depending on the fishing season, air temperature, and ice requirements for other uses. In general, the ice-to-fish ratio appeared to vary from about 1.5 to 2.5 lbs. of block ice per pound of fish. In Guapinol, ice was trucked in in very large volumes. (Average weekly deliveries were 45,000 lbs.) In Prumnitara, almost all of the fish harvest was dried and salted, a process which takes at least six hours for each 100 lbs. of fish. This study did not result in conclusive feasibility analyses because the costs of making ice from wind power were not known then. The study did, however, conclude that two of the five villages would make good wind-powered ice-maker project sites.

The cost of ice for comparative economic studies is very difficult to determine from the Honduran study. The primary reasons are that all costs were given in terms of the Honduran currency, the Lempira, and that the study is now more than two years old. Using the official foreign currency exchange rates for the time of the study, the cost of ice would fall in the range of U.S. \$0.0095 to U.S. \$0.0214 per pound of ice. These figures are not thought to be representative of the current cost of block ice in Central America for the following three reasons: (1) the exchange rate of the Honduran Lempira changed radically between 1990 and 1997, (2) the converted cost of kerosene during the study was half of what it is today, and (3) current cost of ice in Mexican fishing villages is approximately U.S. \$0.04 per pound. A further complication stems from evidence that as much as 40% of the block ice could melt during transport and still the villagers paid the same price for the ice. The option of fish drying was particularly not cost effective because 60%–75% of the original weight is lost in the drying process, the price per pound is much lower for dried fish than for fresh fish, and there is a much larger year-round market for fresh fish.

Aside from project site identification and cost of ice, several other factors must be considered, including the type of ice produced. The different types of ice are block, plate, and flake. Of the three types, flake ice has the greatest surface area-to-weight ratio, making it the most efficient type of ice for certain types of food (e.g., fish) preservation. Another consideration is use of hazardous materials. Avoidance or minimization of the use of products such as ammonia, chlorofluorocarbons, lead-acid batteries, and fuels

such as diesel, gasoline, and kerosene are beneficial to a remote community. An ice maker's ability to use salt-water is advantageous because of the abundance of the latter in coastal areas. Also, because many of these systems will be placed in tropical coastal areas, it is important that they be resistant to the corrosive effects of saltwater and tolerant of the violent tropical weather.

2.2 Investigations of Wind-Electric Ice Making at NREL

Because there was a need to identify the lowest-cost, wind-powered ice-making option for remote fishing villages, the National Renewable Energy Laboratory (NREL) began to investigate "directly connected" wind-electric ice-making systems. The "directly connected" system is one in which the variable-frequency/voltage output of a permanent magnet wind generator is used to directly power a vapor compression refrigeration (VCR) ice maker. This system architecture avoids the energy losses and costs of a rectifier, batteries, and an inverter. Although there were obvious technical hurdles to be overcome with this architecture, the motivation behind NREL's investigation stems from the success of variable-frequency/voltage water pumping, which is common throughout the world.

NREL's investigation has involved three phases of testing and simulation. Phase 1, run from September 1993 until December 1994, successfully demonstrated the viability of the "direct-connect" concept. Two commercial ice makers connected to wind turbines were field-tested and did produce ice. Many of the anticipated problems of running a VCR system at variable speed never materialized. However, one problem did arise that had to be solved. Surge currents during start-up of the larger ice maker caused it to stall out on several occasions. This was a significant problem because sizing the wind turbine to the starting currents of the ice maker would result in an uneconomical system. Consequently, Phase 2 was launched.

The main objective of Phase 2 was to develop and validate numerical models, both dynamic and steady-state, of the wind turbine-ice-making system. A dynamic model could be used to select the best solutions to the start-up problem as well as help design dynamometer and field tests for verification of the start-up solutions. A steady-state model could be used to predict the long-term performance of wind-electric ice-making systems. In order to meet this objective, a small-scale (1/3- to 1/2-hp) laboratory dynamometer test apparatus was assembled and used to validate the steady-state and dynamic numerical models. There was some concern that the small size of the test equipment would hinder the validation effort because of magnetic saturation and other non-linearities commonly associated with small electric machines. It made sense, however, to attempt the tests on small equipment in order to save time and funds. Phase 2 was completed in October 1995.

In Phase 3, the experimental follow-on to Phase 2, NREL conducted its investigation of the North Star ice maker, which is powered by a 12-kilowatt (kW) permanent magnet alternator (PMA). The system was dynamometer-tested for both steady-state and dynamic conditions. NREL tested different sizes of series capacitors to improve the ice maker's start-up characteristics. We also tested the steady-state performance in a wide range of operating frequencies. This project phase revealed a set of problems unforeseen during the previous two phases. The system demonstrated poor performance for both steady-state and start-up conditions. Thus, the results of Phase 3 testing have demonstrated that a commercial ice maker could not operate satisfactorily when directly coupled to a variable-frequency wind turbine. Continued development is needed to address the problems revealed during testing. Additional study of other commercial ice makers and custom-designed ice makers is also needed.

PART I: PHASE 1

3. Phase 1: Concept Demonstration

The first phase of NREL's investigation of wind-electric ice making started in September 1993 and concluded in December 1994. It was a joint project between NREL and the University of Colorado in Boulder. The project culminated in Holly Davis' Master's thesis.² The Bergey Windpower Company, Inc., supplied the dynamometer and field-test facilities and equipment.

The six major activities in Phase 1 were:

- 1) Literature search
- 2) Development of a methodology for determining ice requirements for rural fishing
- 3) Selection of the ice maker
- 4) Full-scale dynamometer tests
- 5) Full-scale field tests
- 6) Development of a numerical ice-making system model.

Two ice makers were investigated in Phase 1. Both are described in Table 3.1. For purposes of identification, the ice makers will be referred to by their manufacturers, i.e., Scotsman (Vernon Hills, Illinois) and North Star (Seattle, Washington). The Scotsman is actually two FM1200 units connected to the same ice bin. The rated capacity and electrical inputs in Table 3.1 are based on the two Scotsman units. The North Star ice maker acquired by NREL contains a Maneurop hermetic motor/compressor unit, Model MT-64-HM-3.

Table 3.1 Description of Ice Makers

| | Scotsman | North Star |
|--|---|---|
| Model Number | FM2400WE-3A | Model 5/ Coldisc D-12 |
| General Classification | Commercial | Industrial |
| Type of Ice | Flake | Flake |
| Rated Capacity (lbs. ice/24 h) | 2,390 | 2,200 |
| Condenser Type | Water-Cooled | Air-Cooled |
| Compressor Type | Hermetic/ Reciprocating | Hermetic/ Reciprocating |
| Compressor Size (hp) | 2 x 1.5 | 4.8 |
| Electrical Input (per Phase 1 testing @ 60 Hz) | 3 ϕ , 230 VAC, 10.2 Amps, 2.6 kW | 3 ϕ , 230 VAC, 14.8 Amps, 4.2 kW |
| Compressor Pump Down | No | No |
| Evaporator Configuration | Stationary Cylinder/ Moving Helical Auger | Rotating Disk/ Stationary Auger |
| Refrigeration System | R22 or R502, Thermostatic Expansion Valve | R22 or R502, Fixed-Size Orifice Expansion Valve, Liquid Overfeed |
| Water Type for Ice | Fresh | Salty |

Two PMAs were used in the dynamometer and field tests. Both are manufactured by the Bergey Windpower Company (Norman, Oklahoma). One was nominally rated at 10 kW and the other at 12 kW. The designs of both PMAs are essentially the same, the only differences being in the magnet and stator winding sizes.

One of the primary objectives of the Phase 1 testing was to determine whether a vapor-compression refrigeration system would work well with an intermittent and variable-frequency power source such as a PMA wind turbine. The biggest concerns about the intermittency of the power source were:

- Manual resets when power is lost
- Incomplete start-up and shutdown sequences
- Cutter-bar or auger freezing to ice-making surface and not having enough time to free itself
- Intermittent operation of crankcase heaters (applicable only to cold climates).

The variable-frequency concerns were:

- Dynamic instability of expansion valve
- Low refrigerant flow could compromise compressor lubrication (refrigerant-oil solution in compressor).
- Control circuitry could be affected by variable frequency and voltage.

Fortunately, many of these anticipated problems never materialized. However, a few of the problems did arise, whereas for others the testing was probably insufficient to expose them. The control system of the Scotsman ice maker was severely affected by low voltage. The contactors were bypassed because the voltage was insufficient to hold them closed. The compressor lubrication problem did not show up in the Phase 1 tests, but may be a cumulative effect that could take weeks or months of operation to manifest itself. The biggest problem, however, was encountered during the start-up of the ice makers. Section 3.1 describes that problem in detail.

The other primary objective of Phase 1 was to build a database from the dynamometer and field tests and incorporate the data into a steady-state numerical model that could be used to predict the long-term performance of the wind turbine/ice maker system. The model consisted of three components: the wind turbine model (a torque-tip speed ratio curve), the alternator model (a simple torque-power-speed relationship), and the ice maker model (derived from the dynamometer data). The model results were in good agreement with the field-test data.

3.1 The Start-Up Problem

During the Phase 1 dynamometer testing, only one of the two ice-making units of the Scotsman could be started from the 10-kW PMA. The 12-kW PMA was able to start both Scotsman units. The 10-kW PMA could not run the North Star at all and the 12-kW PMA was not able to run the North Star in many of the test conditions.

The difficulty in starting an induction motor-driven reciprocating compressor powered by a permanent magnet alternator is a result of the high torque required to turn the compressor shaft (even at low speed), combined with a poor impedance match between the alternator and the motor when first connected. Initially, the motor has a very low impedance and demands a high starting current from the alternator. Because of the relatively high source impedance (both inductive and resistive) of the alternator, however, the alternator cannot deliver the required current, and the terminal voltage on both the alternator and motor drops. At reduced voltage and current, the motor does not develop sufficient torque to turn the compressor shaft.

There are several ways—either electrical or mechanical—to address the ice maker start-up problem. The electrical solutions would include electrical alterations of the alternator and/or compressor motor windings or the addition of electrical components between the alternator and motor. Any such solution would attempt either to reduce the effective alternator impedance or to increase the effective motor impedance so as to increase the power transfer under starting conditions. The most promising approach, and one that was pursued in Phase 2, is to add capacitors in series between the PMA and the induction motor. The capacitors effectively reduce the starting impedance of the PMA. However, these capacitors must be switched out of the system immediately after start-up because even with the compressor motor at running speed, the reduced circuit impedance leads to excessive alternator and motor current, possibly to the extent that the alternator and motor windings may burn out.

The mechanical solution is to alter the motor load, either by adding a mechanical component between the motor and the load (the compressor) or by changing the load characteristics, thus reducing the load torque below the motor's starting electromagnetic torque. The type of motor/compressor system will largely determine which mechanical solutions are feasible. Closed or hermetic systems do not allow access to the motor and compressor or to the shaft connecting them. Only the refrigeration system apart from the compressor could be used to alter the load. In an open-drive system, many alterations are possible. A fluid coupling or a friction clutch/flywheel system could be added between the motor and compressor. The former would gradually increase the load torque whereas the latter would increase torque more abruptly but would use the flywheel inertia to "smooth" the torque pulse. Another possibility with open systems is to change out the compressor altogether. Reciprocating positive-displacement compressors produce a load comparable to the running load the instant that the shaft begins to rotate. Scroll compressors, another positive-displacement component, do not begin to create a pressure differential (and therefore a reaction torque) until the scroll reaches a certain minimum level of revolutions per minute (rpm), beyond which the compressor has a fairly flat torque/speed characteristic, similar to that of the reciprocating compressor. Centrifugal compressors produce load torques that increase as the square of the shaft speed.

PART II: PHASES 2 AND 3

4. Phase 2: Bench-Scale Testing and Model Validation

4.1 Mathematical Models for Wind-Electric Ice-Making System

4.1.1 Model Assumptions

A block diagram of a wind turbine ice maker system is shown in Fig. 4.1. The system consists of the following major components: a wind turbine rotor, a three-phase permanent magnet synchronous alternator, and a VCR system. The refrigeration (ice-making) system is comprised of an evaporator, a condenser, a throttling valve, and a compressor. Because our main goal was to develop solutions for improving system start-up, it was expedient for modeling purposes to consider only the compressor unit of the ice maker.

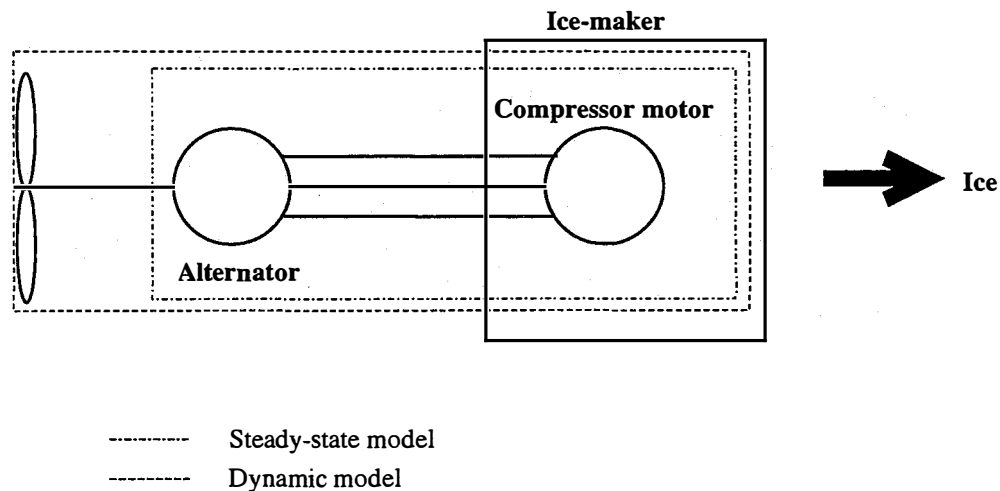


Figure 4.1. Block diagram of wind turbine/ice-making system

In order to predict the behavior and performance of the above-mentioned system, as well as to estimate the advantages of various solutions for start-up improvement, we needed to develop a computer model of the system. The two major purposes of system modeling are:

1. Long-term prediction of system behavior: evaluation of the ice maker's site-specific performance for different system configurations and control strategies.
2. Modeling of system dynamic response to possible perturbations (e.g., wind gusts, compressor load variations): evaluation of possible instabilities in the system due to the introduction of additional components (such as capacitors and mechanical devices) and compressor load oscillations, as well as calculations of magnitude and duration of overcurrent and overvoltage conditions for different start-up options.

The first purpose can be achieved using a steady-state model, the second by using a more sophisticated and more detailed dynamic model that describes all mechanical and electrical transients occurring in the system. Diagrams, assumptions, and brief descriptions of the model will follow.

4.1.2 Steady-State Model

The system steady-state model (see Fig. 4.1) includes the wind turbine rotor performance curve (i.e., C_p vs. tip-speed ratio), alternator and compressor motor electrical steady-state models, and the compressor's torque-speed curve. The per-phase electrical-equivalent diagram of the alternator/induction motor system with series capacitors in the circuit is shown in Fig. 4.2.

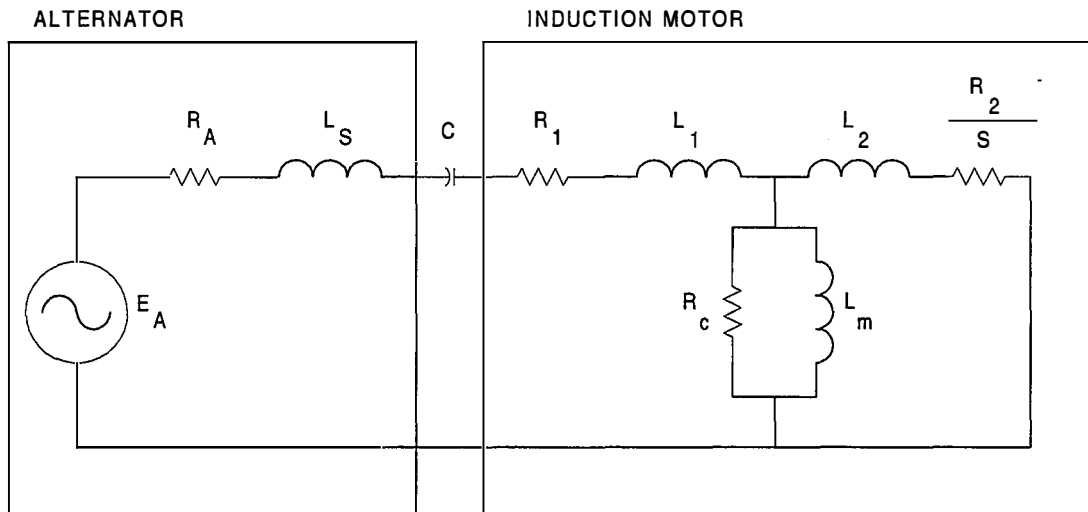


Figure 4.2. Electrical-equivalent diagram with series capacitor

The following symbolic conventions have been adopted: E_A —phase electromotive force induced by resultant air-gap flux; R_A —alternator stator winding effective resistance; L_S —alternator synchronous inductance; C —capacitance of series capacitor; R_1 , R_2 —motor stator and rotor effective resistance; L_1 , L_2 —motor stator and rotor leakage inductance; L_m —motor mutual inductance; R_c —electrical resistance, simulating magnetic losses in motor core; S —motor slip.

All motor/rotor parameters are referred to the stator. The induction-motor squirrel-cage rotor is represented by a three-phase equivalent winding (transformer analog). The following model assumptions have been universally adopted and incorporated into the steady-state model:

- Alternator has proportional air gap.
- Alternator magnetic-circuit saturation is not considered (i.e., constant voltage per hertz ratio).
- Motor magnetic-circuit saturation is not considered.
- Skin effect in motor squirrel-cage rotor is neglected.
- Alternator and motor windings are considered balanced.

The model is based on the steady-state equations of electrical equilibrium as well as power balance equations. The mathematical description of the steady-state model is given in Appendix A. The model has been programmed using MathCad 5.0 software.

4.1.3 Dynamic Model

The system dynamic model includes the alternator and load motor electromechanical dynamic models (see Fig. 4.1). Dynamic models of the wind turbine rotor and compressor load can be easily included; however, in this version, they are represented by steady-state torque/speed curves. (This was the only available data.) The three-phase diagram of the modeled electromechanical system is shown in Fig. 4.3.

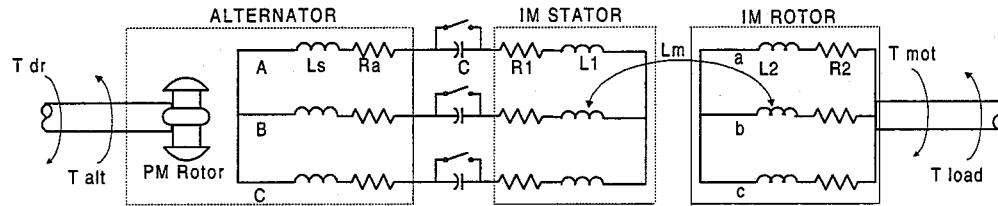


Figure 4.3. Three-phase diagram of "PM Alternator-Induction Motor" electromechanical system

All of the symbol conventions and modeling assumptions that were used for the steady-state model also apply to the dynamic model. Additional symbol conventions are: T_{dr} —driving torque; T_{alt} —alternator electromagnetic torque; T_{mot} —motor electromagnetic torque; and T_{load} —motor load torque. Driving and load torques are referred to alternator and motor shafts, respectively. The model is based on universally accepted, nonlinear differential equations of electrical equilibrium in an "ABC" coordinate system. The mechanical equations (1 and 2) of motion are given below in their basic form:

$$U := I \cdot R + \frac{d}{dt} \psi \quad (1)$$

$$\Delta T := J \cdot \left(\frac{d}{dt} \Omega \right) \quad (2)$$

where:

- U = voltage
- I = current
- R = resistance
- ψ = flux linkage
- Ω = angular mechanical speed
- ΔT = difference between electrical machine and mechanical device torques
- J = mechanical moment of inertia.

All equations in the model are given in "per" units and are represented in vector form. The analytical solution of the above-mentioned system of differential equations is impossible because of the presence of periodic coefficients (i.e., mutual inductances between stator and rotor windings are periodic functions of rotor angle). So the system of equations can only be solved numerically. (We used the Fourth-order Runge-Kutta method with adaptive step-size.) The model, which has been programmed in the MatLab 4.2 software package, is flexible and can simulate system dynamic behavior under practically any condition. The model allows the inclusion of various electrical and mechanical switching functions in order to simulate electrical switches, mechanical clutches, and other components. It also is possible to model both nonsalient- and salient-pole alternators. The system of base values and the mathematical description of the model are given in Appendix B.

4.2 Bench-Scale Testing

The "bench-scale" testing took place in the power electronics laboratory at the National Wind Technology Center (NWTC). The objective of these tests was to validate the electrical portion of the steady-state and dynamic mathematical models. In other words, these tests focused on the electrical interaction between a mechanically driven permanent magnet alternator and a loaded induction motor, which represented the compressor motor of the actual ice-making system.

4.2.1 Equipment and Data Acquisition System Description

Schematics of the bench-scale test apparatus are shown in Figures 4.4 and 4.5. Figure 4.4 shows the "alternator-driven" system and Figure 4.5 shows the "line-connected" system. The following is a description of the former. Three-phase electric power was supplied to a variable-frequency AC drive via a fused disconnect box. A Magtrol (Model 4614) polyphase power analyzer was inserted between the AC drive and the drive motor. The drive motor was an AC induction machine. A timing gearbelt and pulley system was used to reduce the speed from the drive motor to the PMA. The speed reduction ratio most commonly used for these tests was 2.25:1. The three-phase electrical output from the PMA was used to drive the load motor, another AC induction machine. The load motor was directly coupled (with a flexible coupling between their shafts) to a DC machine, which served as a dynamometer. Rigidly attached to the outer housing of the dynamometer was a steel arm, which was used to measure the reaction torque to the load motor. (Note that the reaction torque is only representative of the load motor torque during steady-state operation.) Detailed specifications for the variable-frequency drive, drive motor, PMA, load motor, and dynamometer are given in Appendix C.

The dynamometer was used to apply shaft loads to the load motor. The general configuration of the dynamometer is shown in Figure 4.6a. The torque-speed characteristic of the DC machine configured in this way is also shown. Equation 3 describes the torque produced by this system:

$$T := \underbrace{\left[\frac{(k\phi)^2}{R_a + R_L} \right]}_{\text{slope}} \cdot \omega + \underbrace{\left[\frac{(k\phi) \cdot V_a}{R_a + R_L} \right]}_{\text{offset}} \quad (3)$$

where:

- $k\phi$ = field strength
- T = torque
- ω = shaft rotational speed
- R_a = armature resistance
- R_L = load resistance
- V_a = applied armature voltage.

The field strength is proportional to the current in the field winding and can be adjusted with the field rheostat and the applied field voltage. For a constant field strength, torque varies linearly with speed where the offset or "standing" torque is given by the right-hand bracketed term in the equation, and the slope is given by the left-hand bracketed term. The "standing" torque is most easily adjusted with the applied armature voltage and the slope with the field strength. Figure 4.6b shows three different torque-speed characteristics. The first has no applied armature voltage and therefore no "standing" torque. The second has a large applied armature voltage, but a very small field strength.

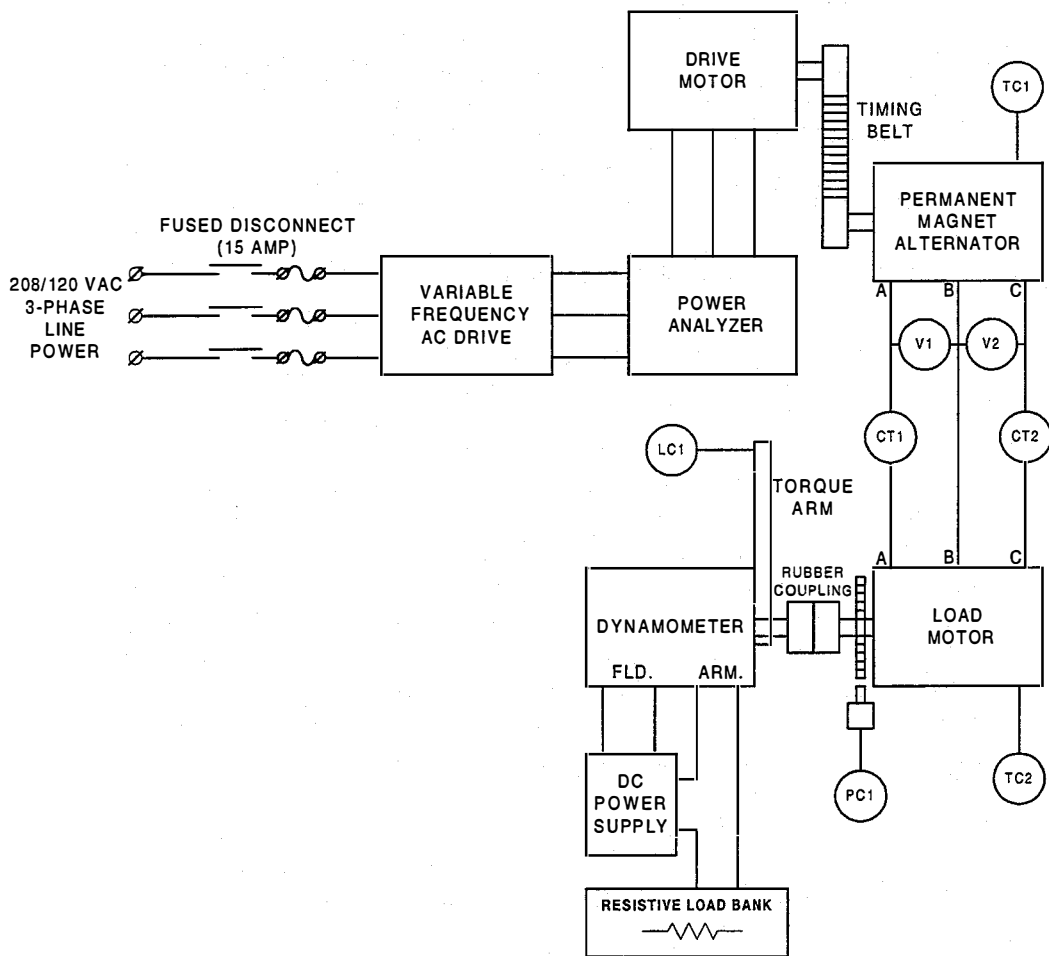


Figure 4.4. Schematic of bench-scale test apparatus (Tests 5 and 6)

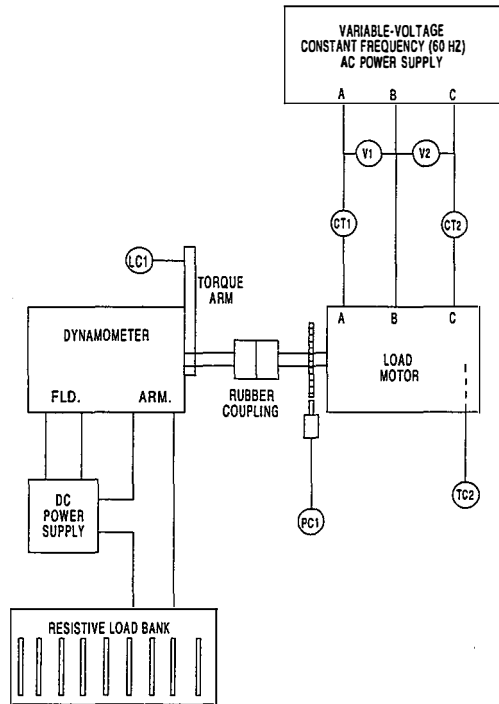


Figure 4.5. Schematic of bench-scale test apparatus (Tests 3 and 4)

Consequently, a "standing" torque is present and the slope is close to horizontal. The third uses a strong field and a large voltage applied to the armature circuit. The loads described by the latter two cases more closely resemble the load from the positive-displacement compressor in the North Star ice maker than the first case. The increase in load as the compressor speeds up is due to the effect of friction. In actual practice, there may also be a small oscillation (a function of compressor crank angle) about the mean torque as shown in Figure 4.6b. For the purposes of model validation, however, the dynamometer torque-speed characteristic described above is adequate. The shaft of the dynamometer can also be "locked" to its housing for locked-rotor testing of the load motor. In this case, there are no electrical connections required for the dynamometer.

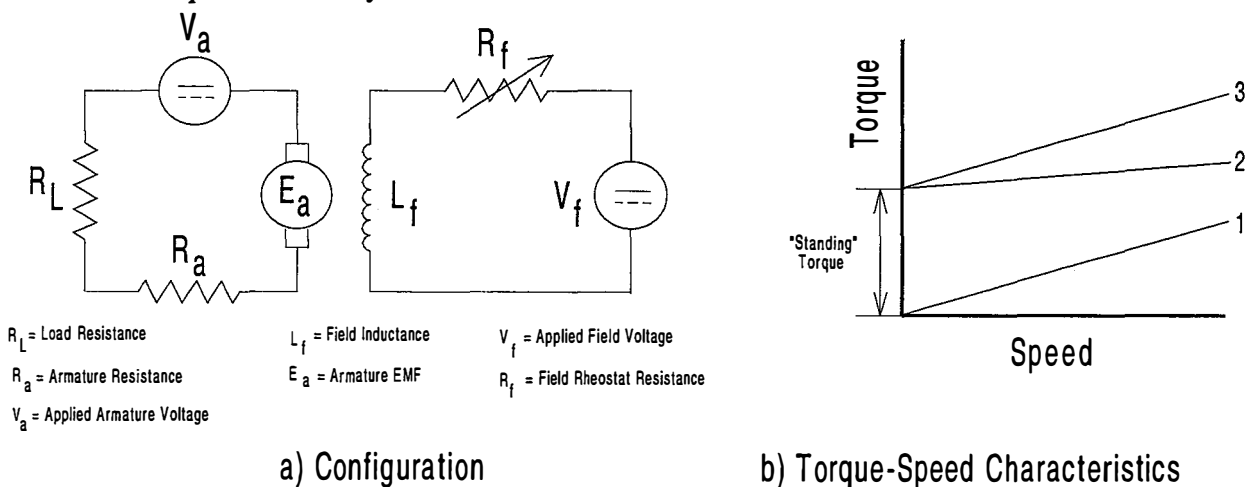


Figure 4.6. Dynamometer configuration and torque-speed characteristics

Referring back to Figures 4.4 and 4.5, the measurements taken during each test are shown with a circle and a two- or three-letter designation. Table 4.1 summarizes these measurements and any type of signal conditioning that was used. The conditioned signals were routed through shielded cable to a National Instruments SCXI-1300 terminal block module. From the terminal blocks, the signals were then sent to a 32-channel multiplexer amplifier, a National Instruments *SCXI-1100*. The analog-to-digital conversions are done on a National Instruments AT-MIO-16E-2 plug-in I/O board in a Pentium computer. National Instruments' Labview Version 3.1.1 software was used to control data acquisition and postprocessing. Two separate data acquisition programs were prepared, one for the steady-state tests and the other for the dynamic tests. All measured data could be viewed as well as four calculated parameters: real power, reactive power, power factor, and line frequency. In both the steady-state and dynamic test programs, the data acquisition parameters were adjustable, but the ones used most frequently are given in Table 4.2. The scan rate and acquisition time in the dynamic test program were limited by the internal memory of the Pentium computer. To eliminate electrical noise and the effect of extraneous mechanical vibrations, a numerical low-pass filter with a cut-off frequency of 8 Hz was applied to the torque signal.

4.2.2 Test Plan

The bench-scale testing covered three different types of tests: 1) machine parameter determinations (Tests 1 and 2), 2) "line-connected" induction motor tests (Tests 3 and 4), and 3) alternator/induction motor system tests (Tests 5 and 6). These are summarized in Table 4.3. The first type consisted only of steady-state testing. We intended that the machine parameter determination tests be fairly simple to conduct so that they could be easily repeated in any number of settings (in other words, not necessarily at a research facility). The particular tests we used to determine the machine parameters comprised a subset of the complete and more rigorous tests recommended by the Institute of Electrical and Electronics Engineers (IEEE).¹³ The second set of tests, the "line-connected" induction motor tests, isolated the operation of the induction motor with and without series capacitors in the circuit. The power source for these tests was a constant-frequency (60-Hz), variable-voltage, sinusoidal-wave AC power supply. These tests were not only an important step in the model validation process, but they also enhanced our understanding of the electrical interaction between the induction motor and series capacitors. The final set of tests of the alternator/induction motor system were the most important because they verified whether or not the single set of machine parameters derived from Tests 1 and 2 could be used to model the complex alternator/series capacitor/induction motor interactions. Test 6, the dynamic tests, also provided some evidence that the series capacitor solution to the start-up problem was indeed a valid one.

Throughout Table 4.3 there are references to "no-load" conditions as well as "low" and "high" inertia conditions. The term "no-load" is used loosely to mean that no torque load was intentionally applied to the induction motor shaft. However, because of friction in the bearings of both the induction motor and the dynamometer, many of these conditions were not actually "no-load." The terms "low" and "high" inertia refer to systems with nothing connected to the shaft of the induction motor and with the unloaded dynamometer (i.e., the dynamometer is not electrically connected in any way) connected to the shaft of the induction motor, respectively. Both are referred to as "no-load" conditions.

Table 4.1. Summary of Measurement Transducers and Signal Conditioners

| Desig. | Measurement Description | Transducer/Signal Conditioner Description | Estimated Accuracy |
|---------------|---------------------------------------|--|---------------------------|
| CT1 | Line Current (Phase A) | Ohio Semitronics Inc. (OSI) CTL-50 Hall Effect Current Transducer and OSI CTA-101 Signal Conditioner | +/- 0.1% |
| CT2 | Line Current (Phase B) | Ohio Semitronics Inc. (OSI) CTL-50 Hall Effect Current Transducer and OSI CTA-101 Signal Conditioner | +/- 0.1% |
| V1 | Line-to-Line Voltage (Phases A and B) | Inverpower L109-VIB 100:1 Voltage Reducer/Isolator | +/- 2% |
| V2 | Line-to-Line Voltage (Phases B and C) | Inverpower L109-VIB 100:1 Voltage Reducer/Isolator | +/- 2% |
| LC1 | Load (Dynamometer) Torque | Transducer Techniques MDB-10 Load Cell & OSI CTA-101 Signal Conditioner | N/a |
| PC1 | Load Motor Speed | 60-Tooth Gear & Red Lion Controls Proximity Sensor/ PRA1-3021 Pulse Rate to Analog Converter | +/- 0.25% |
| TC1 | Alternator Stator Winding Temperature | Type J Thermocouple | +/- 2°F |
| TC2 | Load Motor Stator Winding Temperature | Type J Thermocouple | +/- 2°F |

Table 4.2. Data Acquisition Parameters

| Steady-State Tests | |
|---------------------------|------|
| Acquisition Time (s) | 0.5 |
| Scan Rate (Hz) | 2000 |
| Sampling Interval (s) | 2.0 |
| Dynamic Tests | |
| Acquisition Time (s) | 4.0 |
| Scan Rate (Hz) | 600 |

Table 4.3. Bench-Scale Test Descriptions

| Test No. | Test Name | Test Conditions |
|-----------------|---|--|
| 1 | Load Motor Parameter Determination | |
| 1a | No-Load Test | Line-connected; 60 Hz; "low"-inertia configuration; line-to-line voltage varied from 100 to 208 VAC in 10-VAC increments. |
| 1b | Locked Rotor Test | Line-connected; 60 Hz; motor shaft "locked"; line-to-line voltages were varied from 0 to 100 VAC in increments of 10 VAC. |
| 1c | Leakage Inductance Test | Rotor removed from motor; 60 Hz; voltages applied to stator winding were 5, 9, and 14 VAC. |
| 1d | Stator Resistance Test | Measured stator winding resistance. |
| 2 | Alternator Parameter Determination | |
| 2a | Open-Circuit Test | Unconnected alternator operated at 30, 60, and 90 Hz. Induced voltage measured. |
| 2b | Resistive-Load Test | Alternator operated at 46, 75, and 103 Hz; resistive load directly connected to alternator; resistances varied from 99 to 2000 ohms at each frequency. |
| 2c | Stator Resistance Test | Measured stator winding resistance. |
| 3 | Induction Motor Steady-State Operation | Line-connected; 60 Hz; line-to-line voltages were 60, 104, and 209.5 VAC; capacitors were not used. Loads applied with dynamometer. |
| 4 | Induction Motor Dynamic Operation | Line-connected, 60 Hz, 79 VAC with "low" inertia configuration only; 106 VAC with "low" and "high" inertia; with capacitors. |
| 5 | Alternator/Induction Motor System Steady-State Operation | |
| 5a | No-Load Test | "Low"-inertia configuration; system operated at 26, 35, 40, 46, 61, and 75 Hz. |
| 5b | Load Test | System operated at 35, 50, and 65 Hz; with and without series capacitors; dynamometer applied three different loads for each configuration. |
| 5c | Locked-Rotor Test | System operated at 22, 25, 34, and 44 Hz; no capacitors; load motor shaft "locked." |
| 6 | Alternator/Induction Motor System Dynamic Operation | |
| 6a | No-Load Test | Alternator operated at 35, 45, 55, and 65 Hz; with and without series capacitors; "low"-inertia configuration. |
| 6b | Load Test | Alternator operated at 35, 45, 55, and 65 Hz; with and without series capacitors; dynamometer applied constant torques to load motor. |

4.2.3 Test Results

The following sections give a brief overview of the test results and describe some of the more interesting results. The validation comparisons of modeled and test data can be found in Chapter 6.3.

4.2.3.1 Parameter Determinations (Tests 1 and 2)

The detailed results for Tests 1 and 2 and the calculations of the equivalent circuit parameters for the load motor (an induction motor) and the permanent magnet alternator are given in Appendix D. The parameters that were finally used for both the steady-state and dynamic numerical models are listed in Table 4.4 below. Three of these parameters, R_2 , L_2 , and L_m , could not be calculated directly and were consequently estimated at first and then adjusted in order that the numerical model results would better fit the experimental data for Tests 3 through 6.

Table 4.4. Machine Parameters Used in Numerical Models

| Machine Parameter | |
|--------------------------------------|-------------|
| Load Motor | |
| Stator-Leakage Inductance, L_1 | 0.018 henry |
| Stator Resistance, R_1 | 5.8 ohm |
| Rotor-Leakage Inductance, L_2 | 0.22 henry |
| Rotor Resistance, R_2 | 2.5 ohm |
| Magnetic-Core Loss Resistance, R_c | 600 ohm |
| Magnetizing Inductance, L_m | 0.2 henry |
| Permanent Magnet Alternator | |
| Line-to-Line Voltage/Frequency Ratio | 5.0 VAC/Hz |
| Stator Resistance, R_a | 36.067 ohm |
| Stator Inductance, L_s | 0.18 henry |

4.2.3.2 Line-Connected Induction Motor (Tests 3 and 4)

Both steady-state and dynamic testing of the "line-connected" induction load motor was conducted. The dynamic tests incorporated 72- μ F capacitors in series with the stator winding whereas the steady-state tests did not. Tabulated results for the steady-state tests can be found in Appendix E. As explained in the appendix, the torque measurements are the least reliable of all the data. This was due to the small magnitude of the torque relative to the range of the torque transducer used and to unquantifiable mechanical friction.

The dynamic tests are of particular interest because they reveal some important characteristics of the resonant circuit created by the motor inductance and the series capacitors. Figure 4.7 shows the speed data when the induction motor was started at 106 VAC with a "low" inertia connected load. Figure 4.8 shows the same data for the case of a 106 VAC start with a "high" inertia load. The "low" and "high" inertia nomenclature is discussed in Section 4.2.2. With "low" inertia, the motor accelerates, overshoots synchronous speed (1,800 rpm for 60 Hz) slightly, and then settles around a somewhat lower speed, 1,794 rpm, due to some shaft friction. With "high" inertia, by contrast, the motor accelerates to almost 1,700 rpm, suddenly decelerates and its speed begins to oscillate. The average motor speed during the oscillation is about 1,210 rpm, corresponding to the synchronous speed of a 40-Hz rather than a 60-Hz

excitation. This lower frequency is probably a harmonic of the resonant frequency. Thus, it appears that the "high"-inertia system is closer to resonance than its "low"-inertia counterpart.

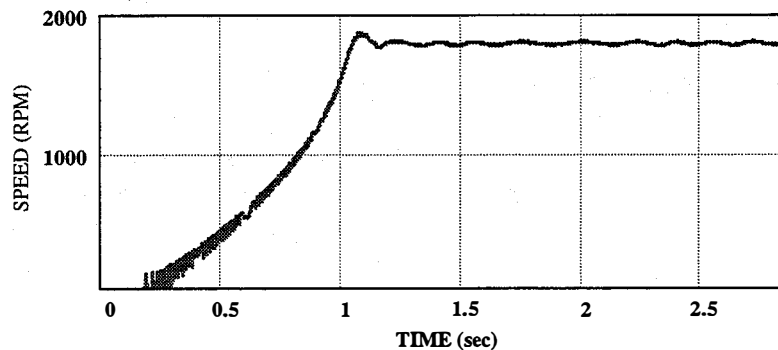


Figure 4.7. Motor speed during start-up of line-connected induction motor (106 VAC @ 60 Hz) with series capacitors: "low"-inertia case

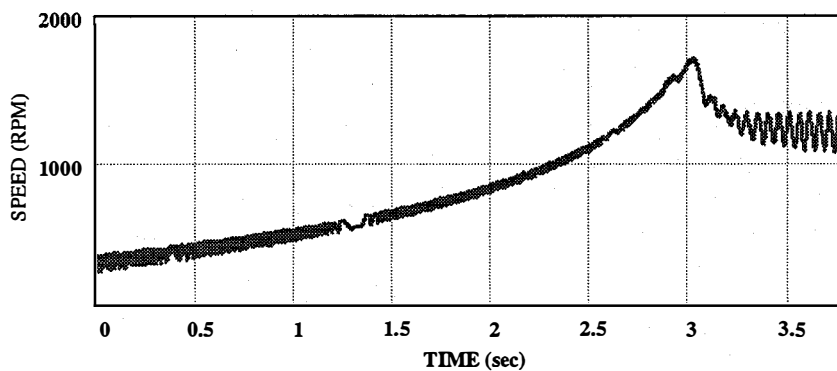


Figure 4.8. Motor speed during start-up of line-connected induction motor (106 VAC @ 60 Hz) with series capacitors: "high"-inertia case

4.2.3.3 Alternator/Induction Motor System (Tests 5 and 6)

We tested the alternator/induction motor system under several steady-state conditions: "no-load" ("low"-inertia configuration), load, and locked-rotor. The detailed results for these tests are in Appendix G.

We also thoroughly tested the alternator/induction motor system dynamically. The load induction motor was started up from a standstill under "low"- and "high"-inertia conditions. The start-ups were conducted at 35, 45, 55, and 65 Hz. The time traces for all of the cases appear in Appendix H. Of particular interest are the "high"-inertia cases. In each test, the alternator was unable to accelerate the motor while the capacitors were not switched into the circuit. Once the capacitors were switched into the circuit, the motor accelerated quickly to nearly synchronous speed. Figure 4.9 shows an example motor-speed time trace for 45 Hz. For the first 1.25 seconds the motor did not start. The capacitors were then

switched into the circuit and the motor accelerated to its final speed in about 1.2 seconds. This is direct proof that series capacitors can improve the ability of a permanent magnet alternator to start an induction machine.

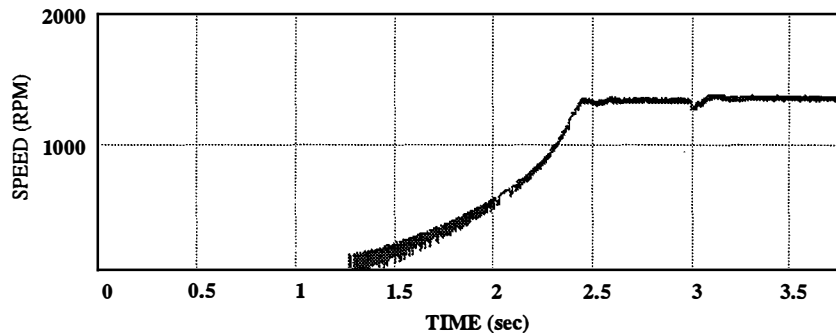


Figure 4.9. "High"-inertia induction motor speed history—started up by alternator (capacitors switched into circuit at 1.25 s)

4.3 Model Validation

The following three sections show comparisons of the experimentally and numerically generated behavior of the laboratory-scale machines. The parameters used for the numerical models are listed in Table 4.4 in Section 4.2.3.1. Despite the wide range of conditions over which the machines were operating, a single set of machine parameters worked quite well in the models. This was somewhat surprising because small machines are often prone to nonlinear saturation effects, and temperature can have a significant impact on component resistances. As a general rule, most of the modeled results were within $\pm 20\%$ of the measured data. This was considered an acceptable error band for the bench-scale machinery. We expect to have fewer errors with the full-scale equipment.

4.3.1 Line-Connected Induction Motor Steady-State Validation

Figures 4.10 through 4.12 show comparisons of the modeled (as shown by the lines) and measured (as shown by the symbols) behavior of the "line-connected" (60-Hz) induction motor. The agreement is quite good for the line current and real power consumption; the differences in torque can be explained by the problems with the torque measurement and friction losses. Based on these results we concluded that the complex nature of the induction motor was being adequately modeled. We didn't run the locked-rotor test at 209.5 VAC because the high line currents tripped the motor circuit breaker before a good steady-state result could be attained.

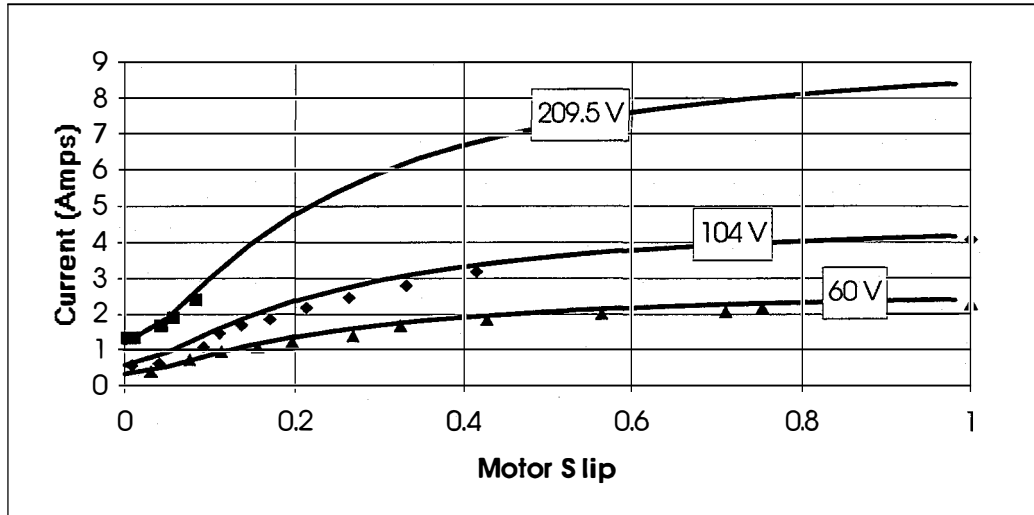


Figure 4.10. Current vs. slip for steady-state operation of line-connected induction motor (load motor)

$$\text{Motor_Slip} := \frac{\omega_s - \omega_a}{\omega_s}$$

where ω_s = synchronous speed, ω_a = actual speed

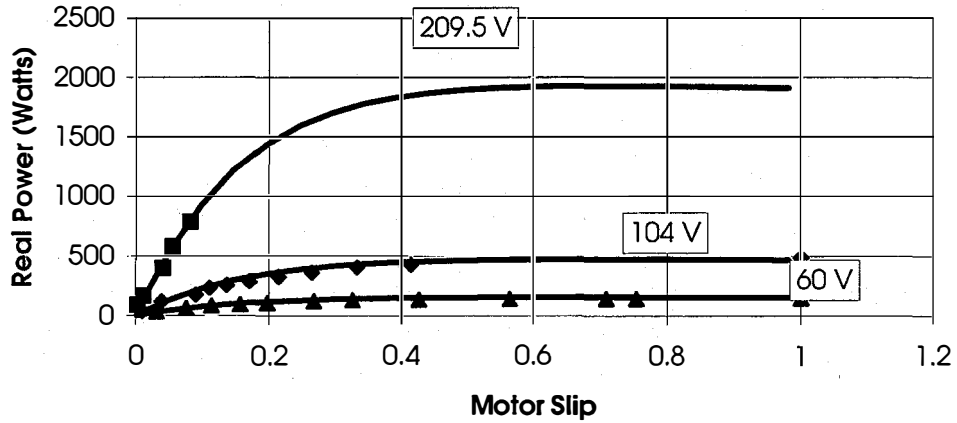


Figure 4.11. Real power vs. slip for steady-state operation of line-connected induction motor (load motor)

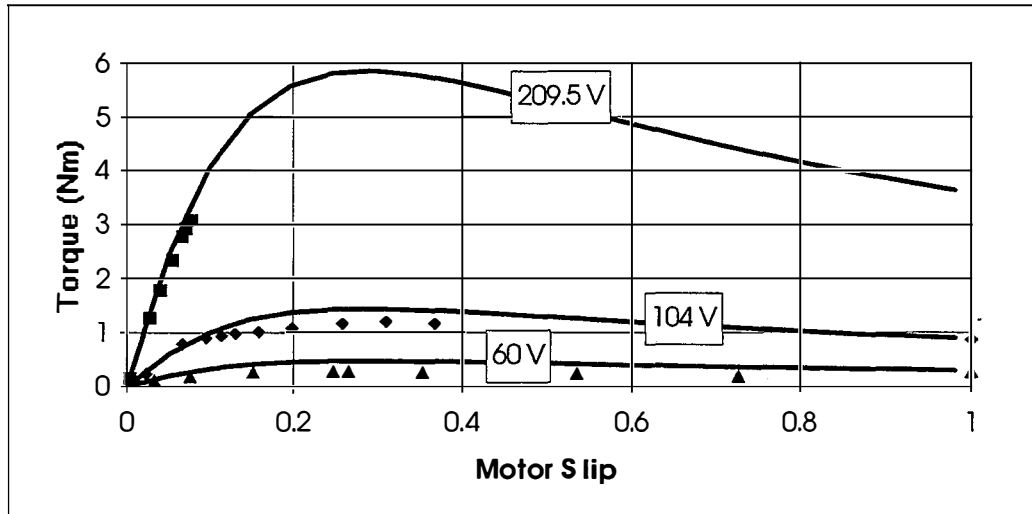


Figure 4.12. Torque vs. slip for steady-state operation of line-connected induction motor (load motor)

4.3.2 Alternator/Induction Motor System Steady-State Validation

Figure 4.13 shows comparisons of numerically and experimentally generated line currents for the alternator/induction motor system under steady-state "no-load" ("high"-inertia configuration) and locked-rotor conditions. Six different alternator speeds, and thus frequencies, were tested at "no-load" and four speeds for the locked-rotor condition. The RMS error is 1.1% for the no-load cases and 3.6% for the locked-rotor cases.

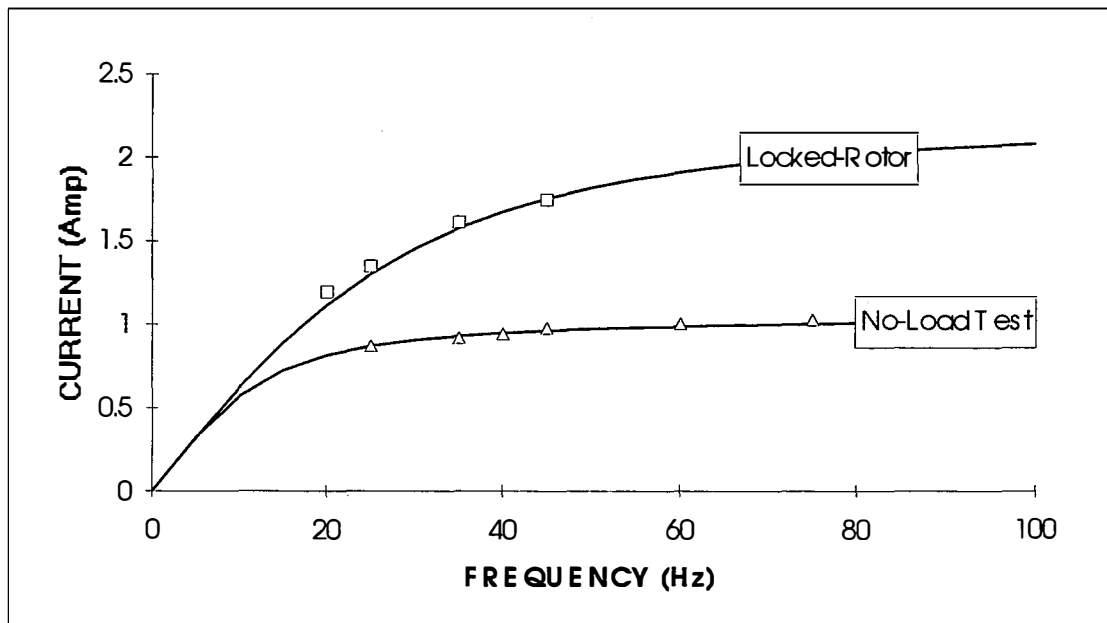


Figure 4.13. Model/experiment comparisons for steady-state no-load and locked-rotor tests

Tables 4.5 and 4.6 show the validation comparisons for the alternator/induction motor system under "loaded" steady-state conditions. Two nominal frequencies, 35 and 65 Hz, were tested and 72 μ F series capacitors were used in half of the cases. Three different dynamometer loading conditions were applied to each frequency/capacitor combination. The model runs were matched to the experimental runs by forcing the motor slip in the model to be the same as that in the experiment. The RMS errors for all of these cases for the line current, line-to-line voltage, and real power differences are 4.7%, 15.0%, and 17.2%, respectively.

Table 4.5. Model/Experiment Comparisons for Steady-State Load Tests at 35 Hz

| | Frequency (Hz) | 34.3 | 34.1 | 35.1 | 32.8 | 33.4 | 33.7 |
|----------------------|------------------|-------|-------|-------|-------|-------|-------|
| | Capacitors ? | No | No | No | Yes | Yes | Yes |
| | Load | 1 | 2 | 3 | 1 | 2 | 3 |
| Current (Amp) | Test | 0.970 | 1.120 | 0.920 | 1.590 | 1.380 | 1.140 |
| | Model | 0.978 | 1.188 | 0.923 | 1.626 | 1.345 | 1.260 |
| | Error (%) | +0.8 | +3.1 | +0.3 | +2.3 | -2.5 | +10.5 |
| Voltage (VAC) | Test | 52.07 | 43.71 | 58.31 | 41.00 | 38.10 | 53.12 |
| | Model | 47.23 | 36.50 | 54.72 | 22.49 | 37.02 | 58.57 |
| | Error (%) | -9.3 | -16.5 | -6.2 | -45.1 | -2.8 | +10.3 |
| Power (Watts) | Test | 92.4 | 116.5 | 36.5 | 97.0 | 113.7 | 138.6 |
| | Model | 89.1 | 110.3 | 39.7 | 52.1 | 121.0 | 147.9 |
| | Error (%) | -3.6 | -5.3 | +8.8 | -46.3 | +6.4 | +6.7 |

Table 4.6. Model/Experiment Comparisons for Steady-State Load Tests at 65 Hz

| | Frequency (Hz) | 65.1 | 64.6 | 64.8 | 65.4 | 64.9 | 64.6 |
|----------------------|------------------|--------|--------|-------|-------|-------|-------|
| | Capacitors ? | No | No | No | Yes | Yes | Yes |
| | Load | 1 | 2 | 3 | 1 | 2 | 3 |
| Current (Amp) | Test | 0.990 | 1.070 | 1.220 | 1.270 | 1.250 | 1.340 |
| | Model | 0.994 | 1.086 | 1.313 | 1.191 | 1.220 | 1.355 |
| | Error (%) | +0.4 | +1.5 | +7.6 | -6.2 | -2.4 | +1.1 |
| Voltage (VAC) | Test | 112.00 | 102.76 | 91.80 | 86.03 | 86.60 | 84.29 |
| | Model | 107.30 | 98.52 | 84.27 | 91.07 | 88.25 | 84.76 |
| | Error (%) | -4.2 | -4.1 | -8.2 | +5.9 | +1.9 | +0.6 |
| Power (Watts) | Test | 66.7 | 184.6 | 247.2 | 93.5 | 214.0 | 304.0 |
| | Model | 83.2 | 184.9 | 258.2 | 111.9 | 189.6 | 286.2 |
| | Error (%) | +24.7 | +0.2 | +4.5 | +19.7 | -11.4 | -5.9 |

4.3.3 Alternator/Induction Motor System Dynamic Test Validation

The model/experiment comparisons for "low"-inertia start-up validation are shown in Figures 4.14 through 4.20. This particular case had an initial frequency of 45 Hz and the 72 μF series capacitors were in the circuit for the entirety of the run. In the numerical model, the drive motor (an induction machine) was represented by a constant-torque/slip-slope and, consequently, the alternator frequency was allowed to drop appropriately and relatively accurately in response to the electrical loading of the alternator. Initially we had fixed the speed of the alternator in the model and this produced an unstable system; when a realistic torque/speed characteristic was used for the drive motor, the system stiffness decreased and stability resulted. The high-frequency oscillations in the experimentally generated frequency curve may be an artifact of the spectral-analysis algorithm used by the data acquisition system to calculate frequency. A 0.2-second window is needed for each calculation of frequency; this may be introducing an "aliasing" error in the first half of the one-second run. Notice that the steady-state frequencies are both very close to 44.5 Hz. The alternator electromagnetic torque curves also differ somewhat. The experimental torque was derived from the following equation:

$$\text{Alternator Torque} = [(\text{Power to Motor}) + (I^2 R_{\text{alt}} \text{ Losses})] / \text{Alternator Speed} \quad (4)$$

where the all quantities on the right-hand side of the equation were measured directly. The alternator resistance, R_{alt} , is considered to be constant. However, in reality, this parameter changes with alternator stator temperature. Therefore, the real alternator electromagnetic torque can differ slightly from the value obtained from the numerical model. Nevertheless, the deviation between the model and the test results is acceptable.

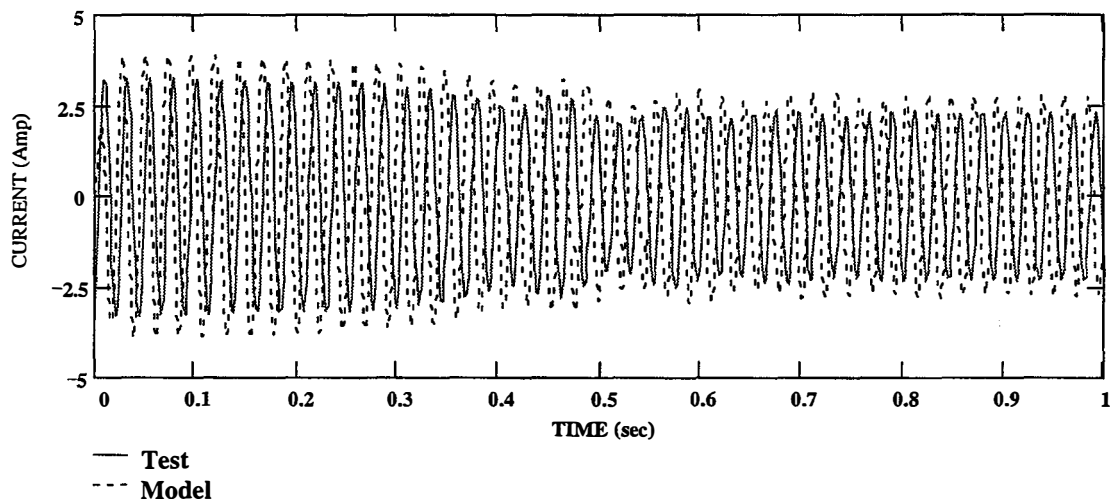


Figure 4.14. Comparison of line current for no-load start-up

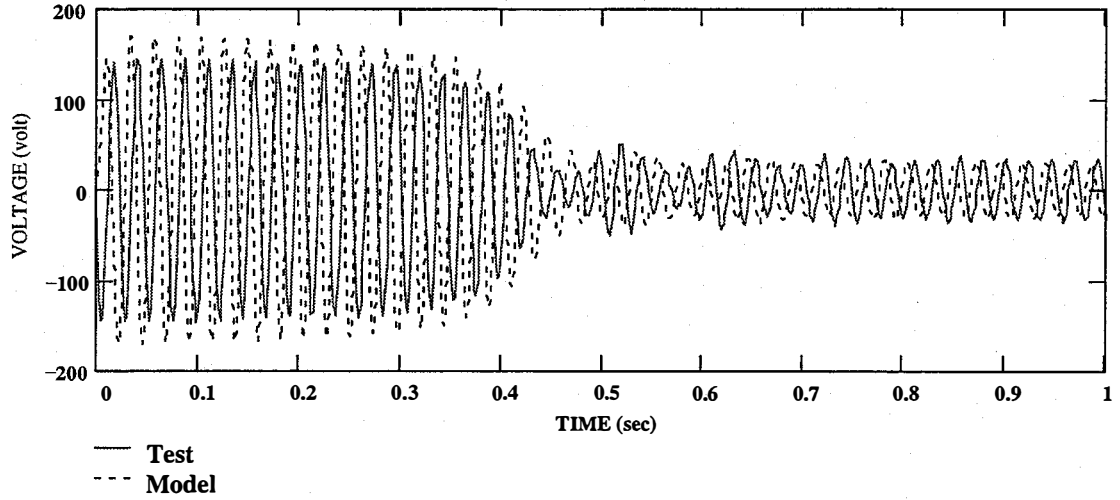


Figure 4.15. Comparison of alternator-phase voltage for no-load start-up

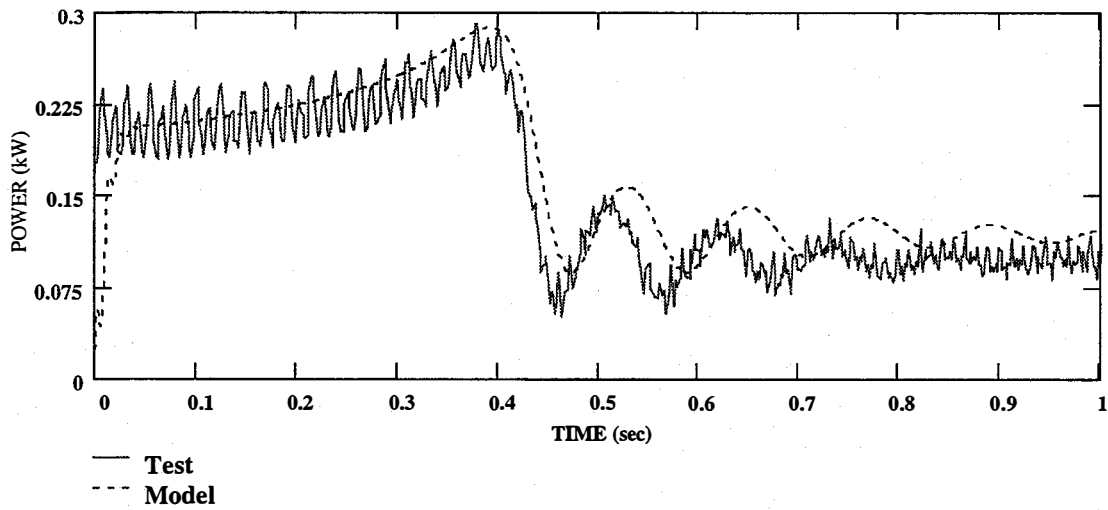


Figure 4.16. Comparison of alternator output power for no-load start-up

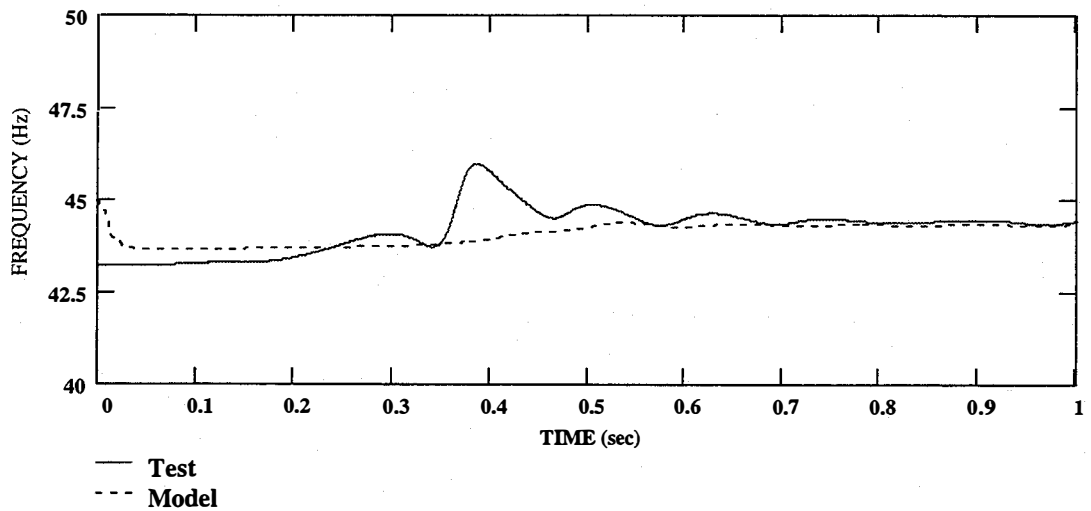


Figure 4.17. Comparison of line frequency for no-load start-up

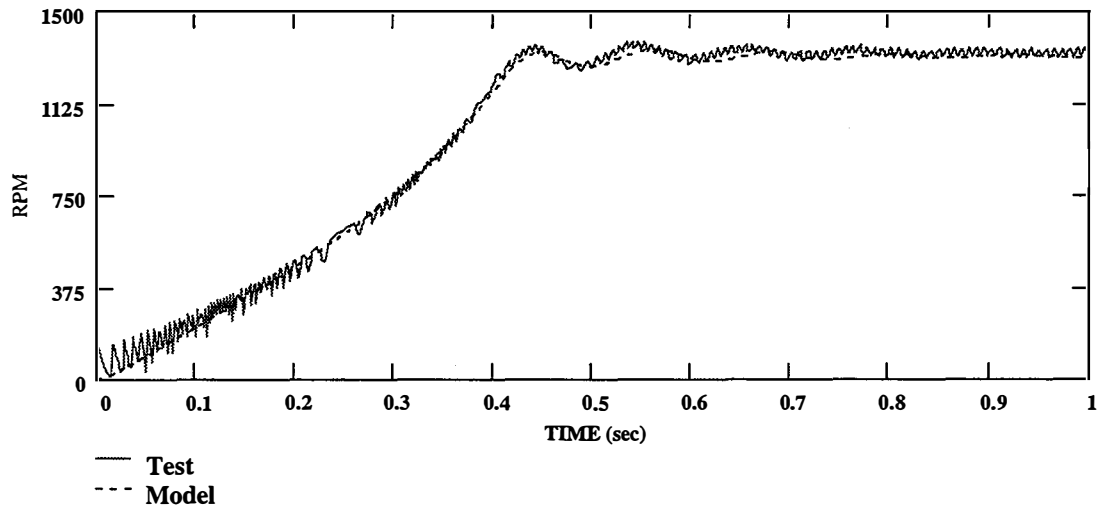


Figure 4.18. Comparison of load motor speed for no-load start-up

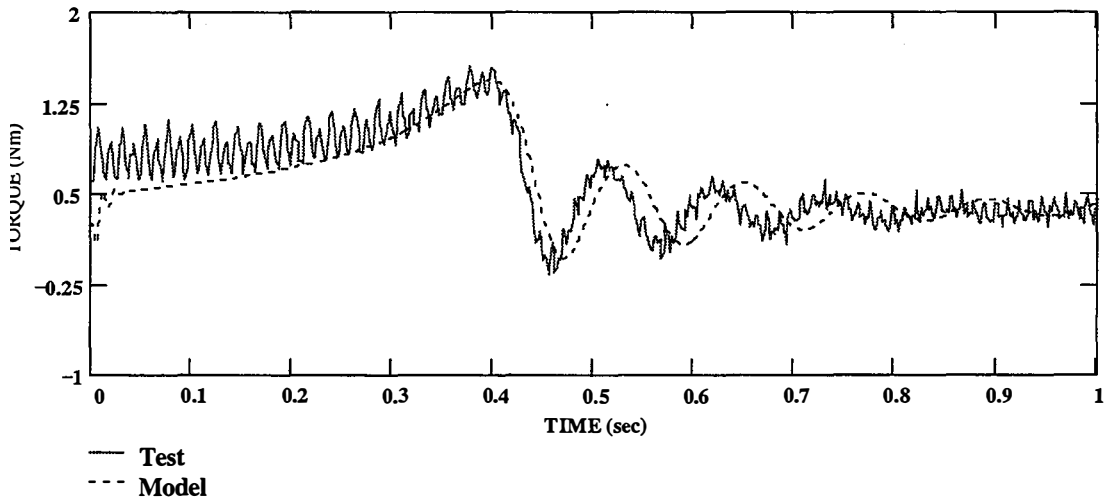


Figure 4.19. Comparison of load motor electromagnetic torque for no-load start-up

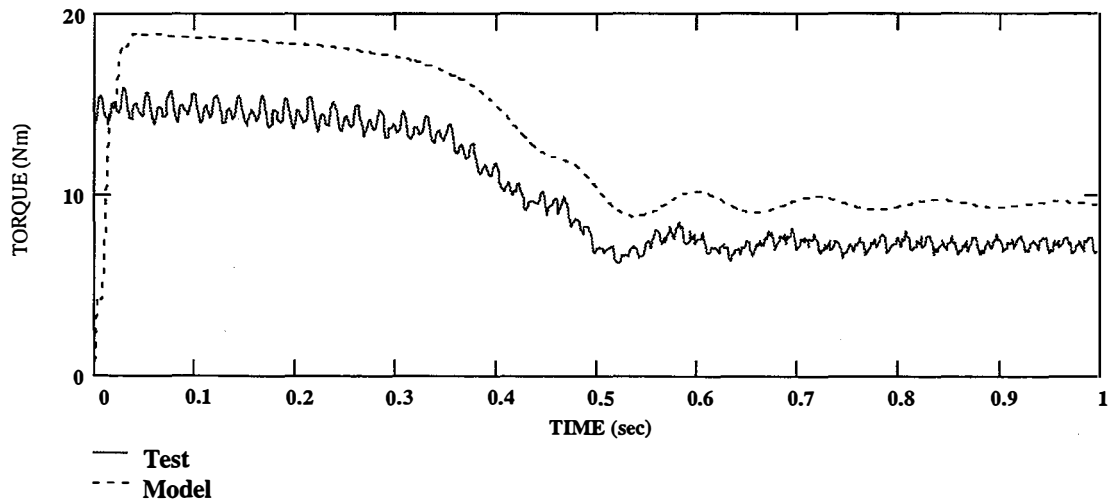


Figure 4.20. Comparison of alternator electromagnetic torque for no-load start-up

The model/experiment comparisons for the "high"-inertia start-up validation case are shown in Figures 4.12 through 4.27. Like the "low"-inertia validation case, this case also had an initial frequency of 45 Hz. The 72- μ F series capacitors were switched into the circuit after about 0.4 s and were left in the circuit for the remainder of the run. Once again, the modeled dynamic behavior of the alternator/induction motor system is extremely similar to that of the system under test.

All of the dynamic-validation cases for the alternator/induction motor system are shown in their entirety in Appendix I.

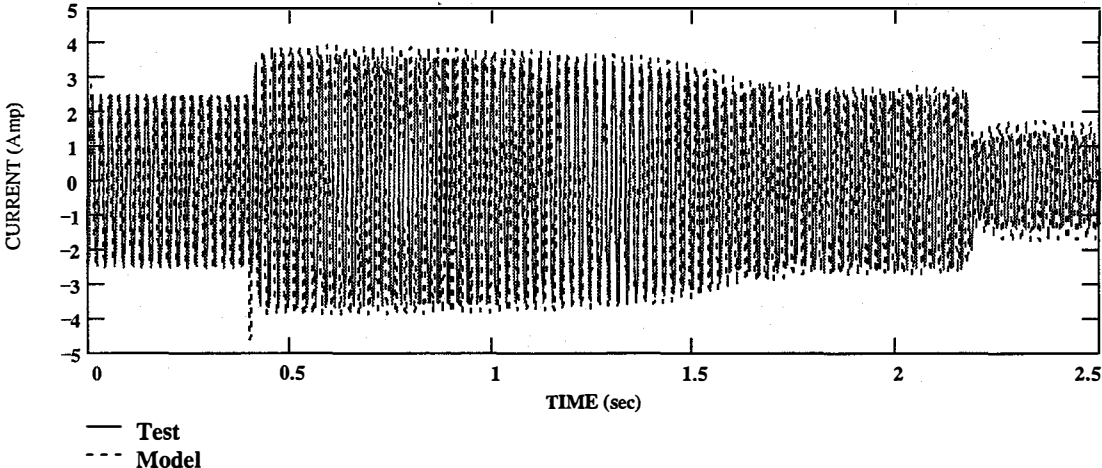


Figure 4.21. Comparison of line current for loaded start-up

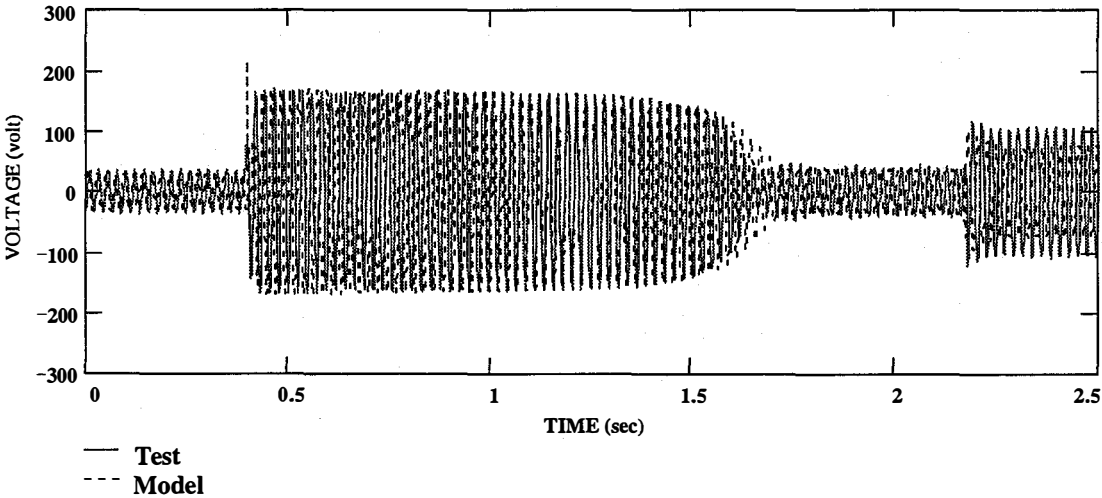


Figure 4.22. Comparison of alternator-phase voltage for loaded start-up

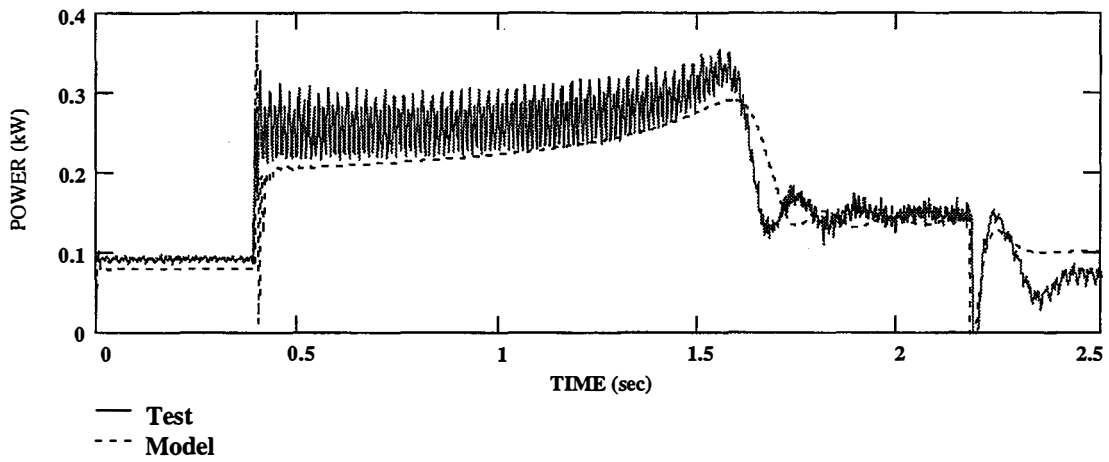


Figure 4.23. Comparison of alternator output power for loaded start-up

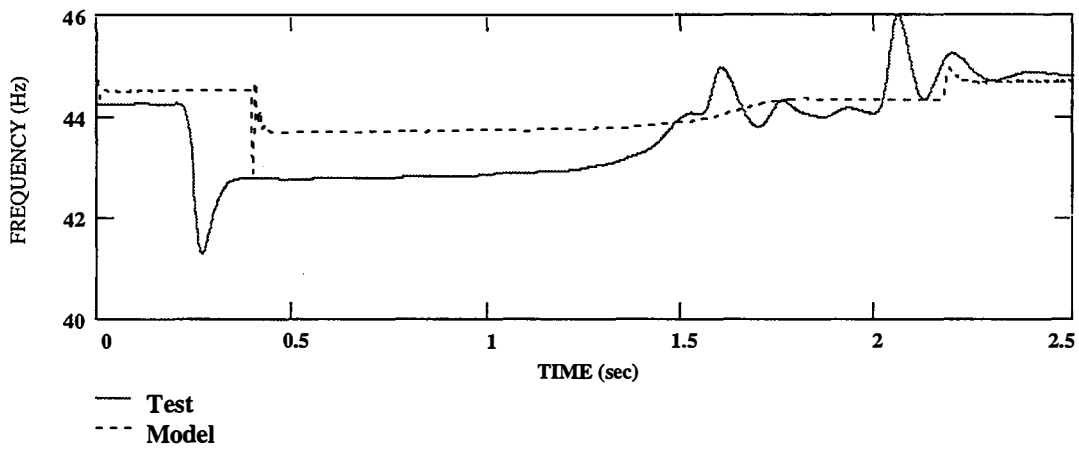


Figure 4.24. Comparison of line frequency for loaded start-up

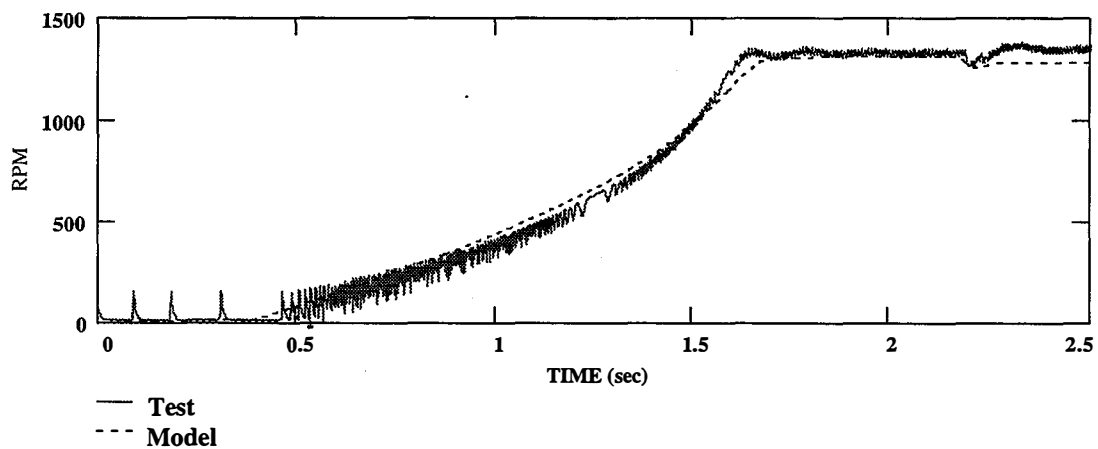


Figure 4.25. Comparison of load motor speed for loaded start-up

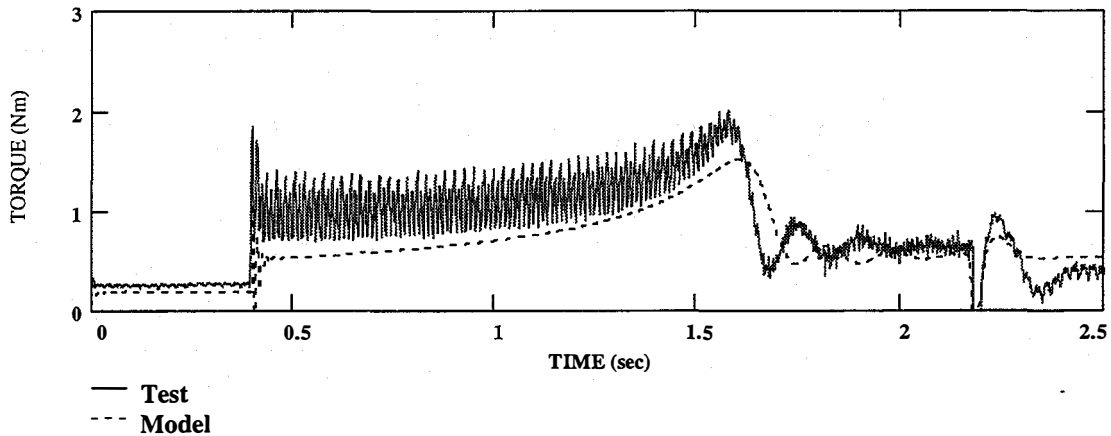


Figure 4.26. Comparison of load motor electromagnetic torque for loaded start-up

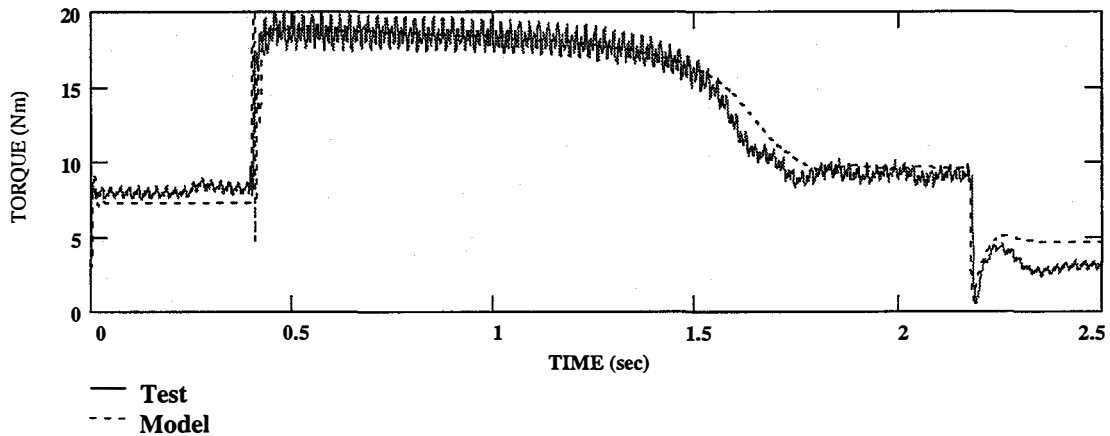


Figure 4.27. Comparison of alternator electromagnetic torque for loaded start-up

4.4 Characterization of North Star Ice-Making Load

In order to characterize the compressor load of the North Star ice-making unit as well as attempt to determine its system parameters, R. Holz and V. Gevorgian visited Bergey Windpower Company in Norman, Oklahoma, during February 27–March 1, 1995. Several successful start-up and steady-state tests were run. All the tests were accomplished with the ice maker connected to the 208 VAC three-phase grid. During the tests, two currents and two line-to-line voltages were measured. Shunts were initially used to measure the line currents. However, because of excessive noise picked up by the shunts, they were replaced by a Tektronics current clamp. The voltages were reduced and isolated with a Tektronics voltage isolator. Both the current and voltage signals were fed into a LeCroy oscilloscope where they could be monitored and analyzed in real time. The oscilloscope was also able to store the data on floppy disks. Because only two line currents were measured, the current in the third phase was calculated using the following equation:

$$I_C := -(I_A + I_B) \quad (5)$$

The voltage of the third phase was calculated assuming a 120° phase shift. The instantaneous ice maker input power could then be calculated from:

$$P := I_A \cdot U_A + I_B \cdot U_B + I_C \cdot U_C \quad (6)$$

The start-up tests were of two types, "warm" and "cold." The "warm" start-ups refer to times when the ice maker had been turned off for some time and the ice disk was near room temperature. A "cold" start-up means that the ice maker had been producing ice only a short time before it was restarted. The "warm" start-ups put the greatest load on the power source. The usual start-up test was begun when the main ice maker contactors were manually closed. At that time, the compressor motor and the condenser fans would start. For the next 5 minutes or so, the ice disk would cool down. Then, after a time-delayed relay closed, the disk motor would start and water would be sprayed over the disk. The steady-state data was recorded when the ice maker was producing ice.

Figures 4.28 through 4.33 show the results of one steady-state and one "warm" start-up test. Figures 4.32 and 4.33 show that the dominant frequency of input power oscillations was 120 Hz, which corresponds to the two compression strokes per revolution of a dual-piston reciprocating compressor operated at 3,600 rpm. The average amplitude of the oscillating power component during steady-state operation was 1.4 kW. This is rather large compared to the average power consumption of about 6 kW. There are several single-phase electrical components in the ice maker (fans, pumps, and disk-driving motor) that produce a somewhat unbalanced electrical load. This can be seen in the unequal line currents in Figure 4.29. As is seen from Figure 4.30, the start-up time for the line-connected system is about 0.05 s. By running our model under similar conditions, we found that the moment of inertia corresponding to such a short acceleration period should be on the order of 0.01 kilogram (kg) × m².

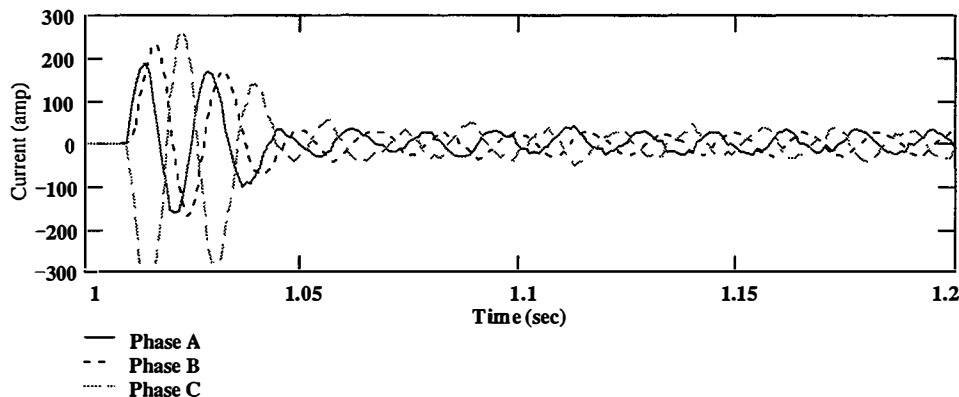


Figure 4.28. Phase currents (North Star start-up test)

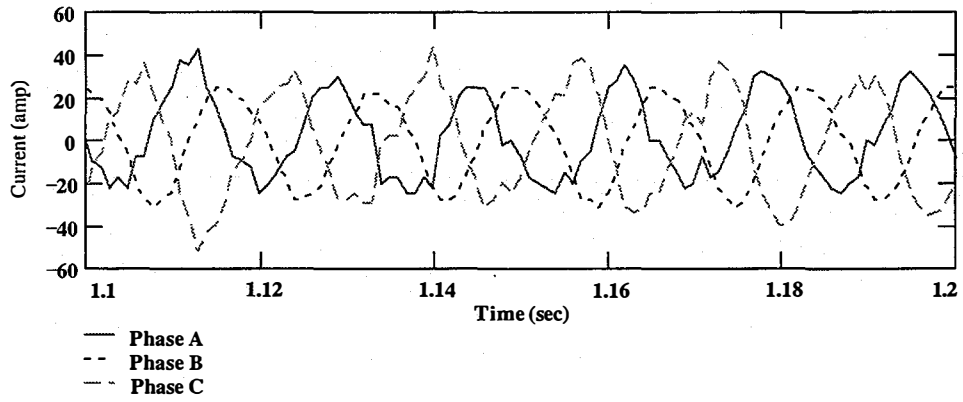


Figure 4.29. Phase currents (North Star steady-state test)

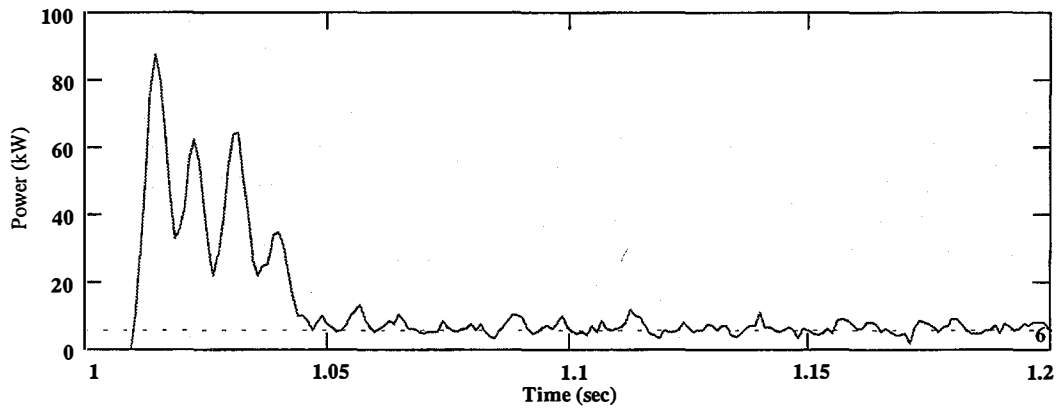


Figure 4.30. Input power (North Star start-up test)

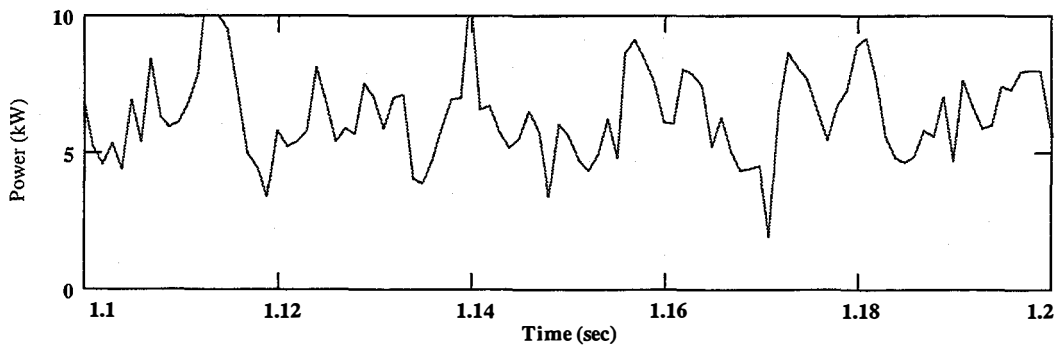


Figure 4.31. Input power (North Star steady-state test)

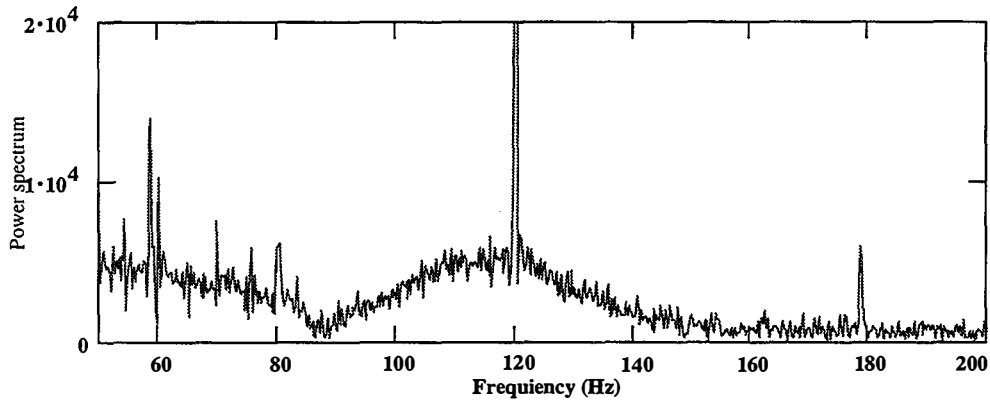


Figure 4.32. Input power Fourier transform for North Star start-up test

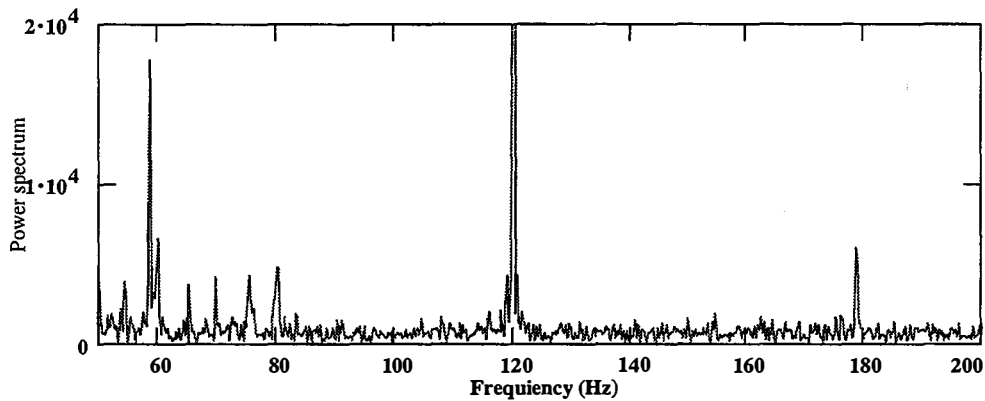


Figure 4.33. Input power Fourier transform for North Star steady-state test

4.5 Modeled Dynamic Behavior of Different Approaches to the Start-Up Problem

Figure 4.34 shows the North Star ice maker's compressor torque as a function of slip at different output frequencies of the Bergey alternator. As is seen from Figure 4.34, the maximum motor start-up torque at slip equal to one is 2 newton meters (Nm). However, our calculations show that the load torque is more likely in the range of 4–5 Nm. The system will not start under such conditions. Also, the motor start-up torque is higher at lower frequencies. This can be explained by the fact that at higher frequencies, motor reactances are higher; consequently, motor power factor is lower and motor real input power is lower, too.

Three approaches to this start-up problem were introduced in Chapter 3. They were: (1) switched-series capacitors, (2) a mechanical clutch or fluid coupling, and (3) a nonreciprocating compressor such as a scroll or centrifugal compressor. The second solution applies only if there is access to the motor shaft (i.e., an open-drive compressor as opposed to a hermetic compressor). Each of these methods was examined with the help of our validated numerical models. The dynamic model described in Chapter 3 and Appendix B was used for these simulations. Modeling results are given in Appendix J. The following cases were simulated:

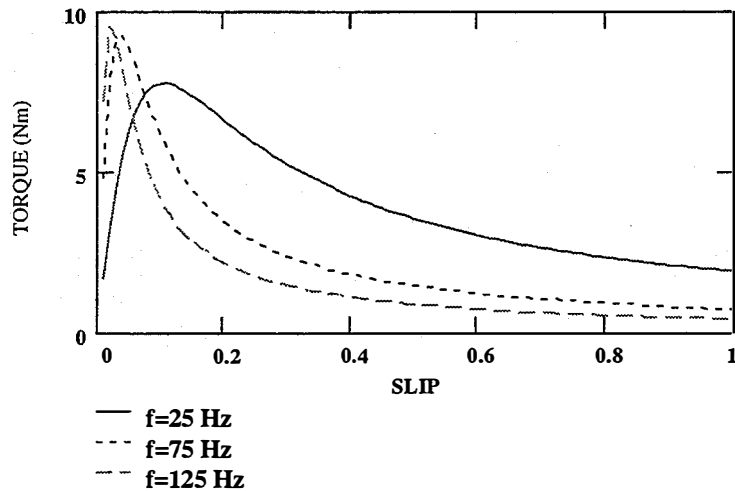


Figure 4.34. Compressor motor electromagnetic torque

| Alternator frequency—80 Hz | | Alternator frequency—30 Hz | |
|----------------------------|--|----------------------------|--|
| Basecase: | 1. No-load 2. Constant load | Basecase: | 1. No-load 2. Constant load |
| Switched capacitor: | 1. Constant load 2. Sinusoidal load | Switched capacitor: | 1. Constant load 2. Sinusoidal load |
| Clutch: | 1. Constant load 2. Sinusoidal load | Clutch: | 1. Constant load 2. Sinusoidal load |
| | | Centrifugal compressor: | 1. Constant load |

The following parameters were used in the model:

Alternator: $L_s=0.0205$ henry, $R_a=1.08$ ohm, $J=100 \text{ kg} \times \text{m}^2$, poles=19

Motor: $L_1=0.00125$ henry, $L_2=0.00125$ henry, $L_m=0.0634$ henry, $R_1=0.135$ ohm, $R_2=0.306$ ohm, $J=0.01 \text{ kg} \times \text{m}^2$, poles=1

For all cases, the wind speed was assumed constant at 6 m/s. More detailed analysis of the modeling results, as well as the selection of the most promising approaches to the start-up problem, are given in the following sections.

4.5.1 Basecase

The "basecase" represented the unassisted ("as-is") start-up of the ice maker's compressor motor, which was assumed to have a torque versus speed characteristic similar to Curve 2 in Figure 4.6b. The case shown here is for a constant load of 2 Nm. As shown in Figures 4.35 and 4.36, the starting torque of the motor cannot match the load torque and the motor consequently cannot start. This is the situation that was encountered in Phase 1 of this project.

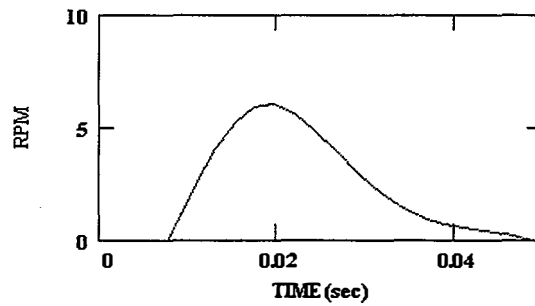


Figure 4.35. Motor rpm (constant-load start)

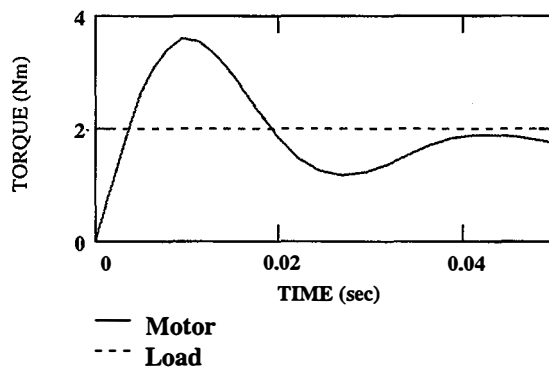


Figure 4.36. Motor electromagnetic torque (constant-load start)

4.5.2 Series Capacitors

One way to improve the motor's power factor is to connect a series capacitor between the alternator and motor. As is seen from Figure 4.37, there is a significant increase of motor start-up torque. But the obvious problem here is that by using constant capacitance, the torque increase can be obtained only within a certain range of alternator frequencies. Another problem is that the current in the circuit is excessive, even when the motor reaches its rated slip. It is therefore necessary to disconnect the capacitor from the circuit after the system has reached its synchronous speed, which requires only a contactor to bypass the capacitor. The contactor coil would be activated at some specified frequency or after a suitable time delay.

Figures 4.38 and 4.39 demonstrate the effect of adding the series capacitors to the basecase described in the previous section. The motor electromagnetic torque far exceeds the load torque and the motor accelerates to nearly synchronous speed very quickly. At 0.2 s, the capacitors are switched out of the circuit. The motor torque rapidly becomes negative, but because of inertia the motor speed does not decrease significantly and it recovers to synchronous speed.

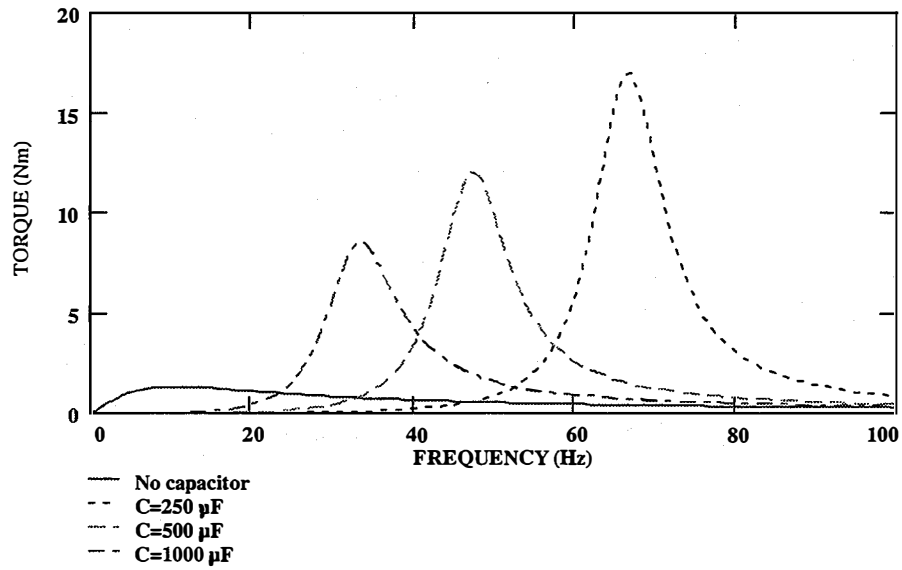


Figure 4.37. Motor start-up torque as a function of alternator frequency at different capacitances

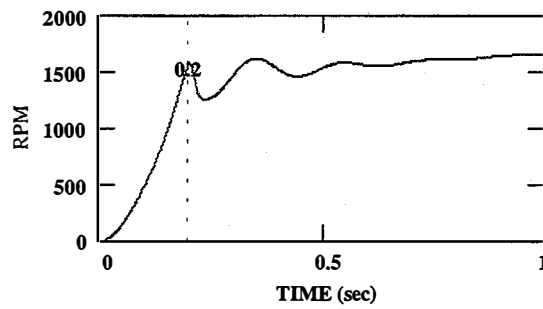


Figure 4.38. Motor rpm (constant-load/switched capacitor)

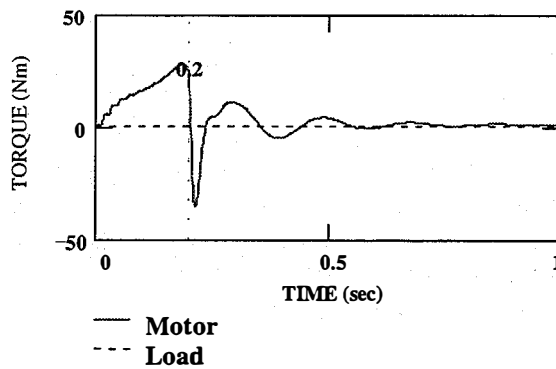


Figure 4.39. Motor and load torques (constant-load/switched capacitor)

4.5.3 Mechanical Clutch

The mechanical or friction clutch was modeled in an idealized sense where the compressor torque and inertia were not present until 1.12 s had elapsed, after which the torque suddenly jumped to 5 Nm and the inertia doubled from its initial value. In reality, the clutch would not impose such a perfect step increase in torque, but this is representative of the worst-case effect. Figures 4.40 and 4.41 show that a clutch would allow the motor to start. The clutch should engage at the point where the motor electromagnetic torque is sufficient to overcome both the load torque and the inertial acceleration force, as shown in Figure 4.41.

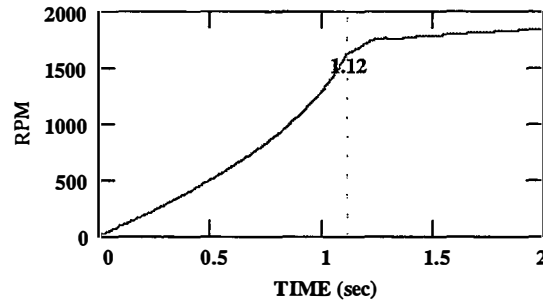


Figure 4.40. Motor rpm (constant-load/clutch)

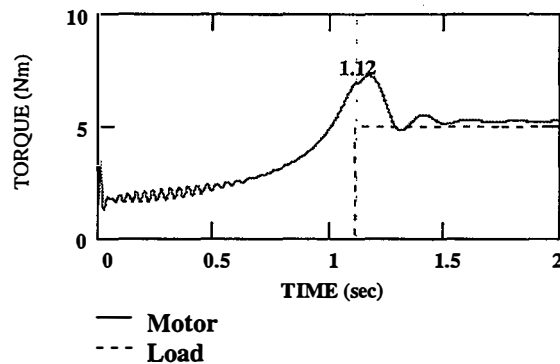


Figure 4.41. Motor and load torques (constant-load/clutch)

4.5.4 Centrifugal Compressor

The centrifugal compressor was modeled simply by making its load torque proportional to the square of the motor speed (see Figure 4.42). Figures 4.43 and 4.44 show that this system starts the slowest of all the previous ones. It takes nearly 4 s for the motor to reach synchronous speed, which suggests that even a system using a centrifugal compressor might require some intervention to improve start-up performance.

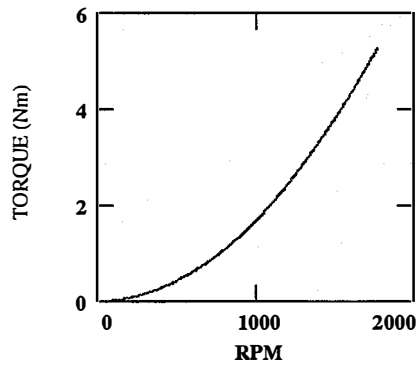


Figure 4.42. Torque vs. speed load curve for centrifugal compressor

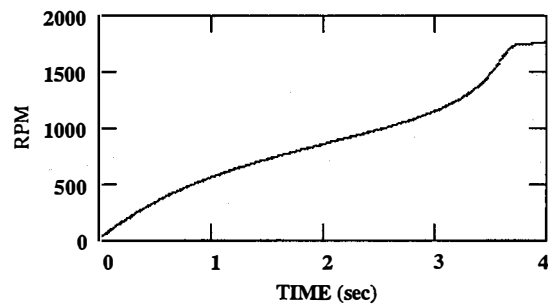


Figure 4.43. Motor rpm (centrifugal compressor)

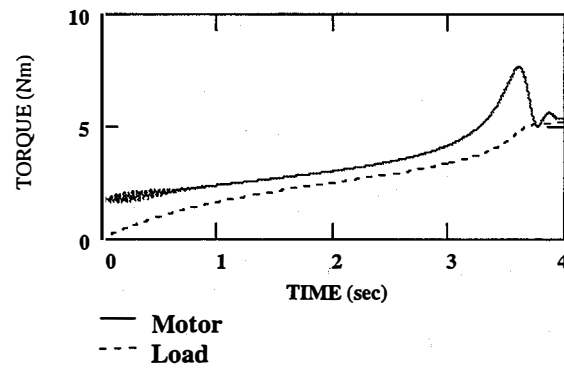


Figure 4.44. Motor and load torques (centrifugal compressor)

4.6 Phase 2 Conclusions

We concluded the following from Phase 2 of NREL's completed investigation of directly connected wind-electric ice-making systems:

- Both of the numerical models (steady-state and dynamic) developed in Phase 2 were experimentally validated using "bench-scale" equipment for a wide range of operating conditions.
- Testing of the dynamic numerical model revealed that the three ice maker start-up solutions (i.e., series capacitors, mechanical clutch, and centrifugal compressor) are effective provided that the systems are sized and controlled correctly.
- The series capacitor start-up appears to be the simplest of the solutions to implement.
- Another full-scale dynamometer and field testing phase will be required in order to verify the field readiness of a prototype directly connected wind-electric ice-making system.

5. Phase 3: Dynamometer Testing of North Star Ice Maker with 12-kW Bergey Alternator

The purpose of Phase 3 of the wind-electric ice-making project was to test the North Star ice maker's steady-state and dynamic performance while operating in variable voltage/frequency. We were strongly motivated by the promising modeling and bench-testing results from Phases 1 and 2 to begin Phase 3 dynamometer testing of the North Star ice maker with 12-kW Bergey alternator. The main objectives of the testing were to better understand the application of wind turbines to ice-making systems, to improve the ice maker's start-up characteristics and steady-state performance, and to prepare recommendations for field-testing.

5.1 Experimental Setup and Data Acquisition System

The dynamometer test setup consists of the following major components:

- Variable-speed 75-kW DC drive (Emerson VIP motor-speed control, 100-hp WER DC motor, two gearboxes, and torque/rpm transducer)
- 12-kW, 230-V Bergey permanent magnet alternator
- North Star Coldisc D-12 Flake Ice Maker (230 V, 60 Hz, and 3 phase.)
- Water tank with ice-melting, ice-mixing, and water-pumping accessories (designed and assembled at the NWTC)
- LabView data acquisition system (DAS) and miscellaneous measuring equipment.

The ice maker used for this test was a North Star Coldisc D-12, which uses a low-pressure receiver and liquid-overfeed system. When connected to a line with standard voltage and frequency, it produces 1.1 tons/day of ice using a 15-in.-diameter rotating disk through which cold refrigerant passes. Ice forms as water sprays on the disk's surface and is scraped off by stationary blades when the disk rotates.

We instrumented the ice maker to measure several performance parameters. We used a National Instrument's LabView to record the data, and thermocouples to measure temperatures for the inlet water, evaporator, and condenser. We also measured ice production by using an Omega FTB6100 flowmeter to monitor the amount of water flowing into the ice maker. Figure 5.1 shows the location of the sensors used in the data acquisition system. The ice maker is represented by single- and three-phase AC motors. LabView calculated alternator frequency, active and reactive power to the ice maker, and power factor using measured line-to-line voltages and line currents. Mechanical torque on the alternator shaft was measured with a torque transducer.

We installed switchable-series motor-start capacitors (250–750 μf) in order to improve the start-up characteristics of the ice maker. A bank of parallel motor-run capacitors was added to improve steady-state performance of the ice-making unit.

Figure 5.2 shows an ice/water circulation schematic. The water tank with saltwater was mounted underneath the test bed, where a North Star ice maker was installed. We filled the water tank with water containing 300 parts per million (ppm) salt, an amount that was maintained at a relatively constant level during the entire testing period. The saltwater from the water tank flowed through the flowmeter and plastic hose into the ice maker, with the use of a 1/10-hp water pump (Little Giant Pump Company).

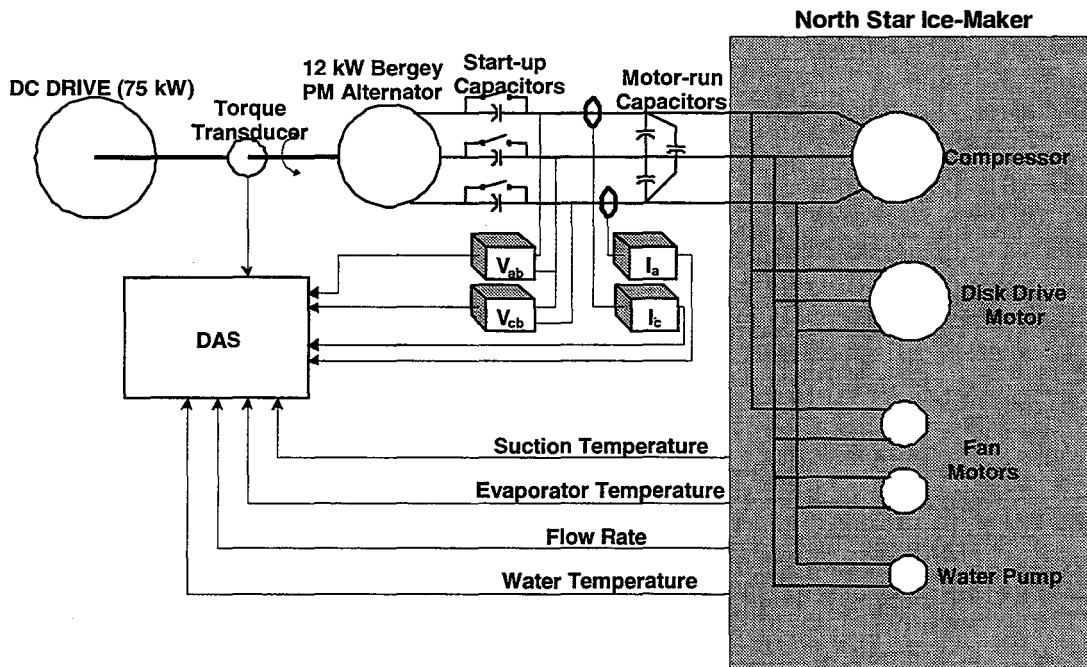


Figure 5.1. Dynamometer test setup

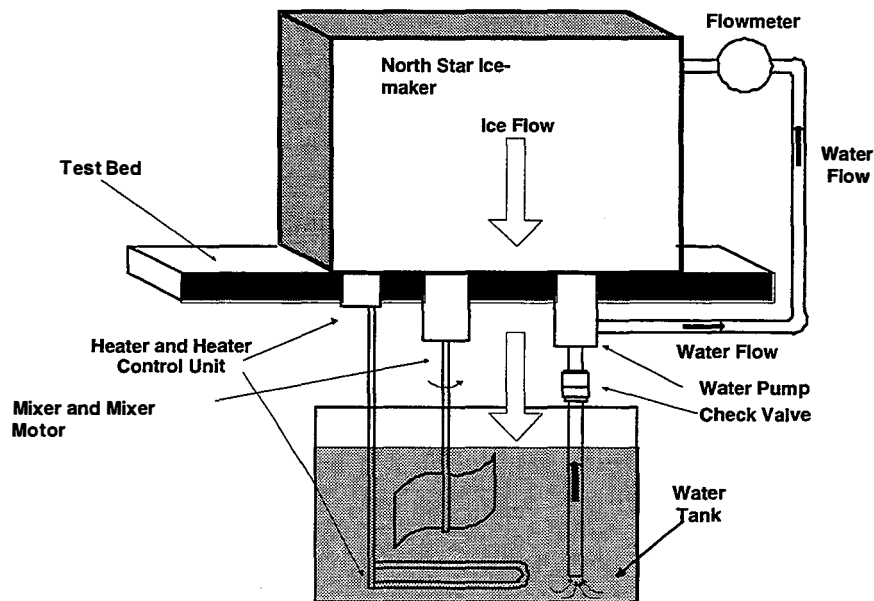


Figure 5.2. Ice/water circulation diagram

Flake ice dropped back into the water tank after being scraped off the disk. The Chromalox 6-kW heater with Omega CN8500 heater controller maintained constant water temperature in the tank according to a preset value (~20°C). A Dayton 1/10-hp motor with blades on its shaft was used to mix the water in the water tank. Thus, uninterrupted ice/water circulation provided for continuous unattended testing.

5.2 Test Plan

All Phase 3 testing activities were carried out according to the following test plan:

- (a) Line-connected start-up and steady-state tests of North Star ice maker
- (b) Alternator-connected start-up tests of North Star ice maker with and without series capacitors
- (c) Alternator-connected steady-state tests of North Star ice maker with and without parallel capacitors
- (d) Alternator-connected variable-frequency test.

5.3 Test Results

5.3.1 Experimental Determination of Alternator Parameters

We performed direct measurements for alternator resistance R_A and volt/hertz ratio k . A three-phase, Y-connected, 5.4-kW resistive load bank was used for the alternator's load test. The alternator frequency f and line current I were measured. Alternator inductance L_S was calculated from load test results using the following equation:

$$L_S = \frac{\sqrt{(kf)^2 - I^2(R_A + R_{load.bank})^2}}{2\pi f I} \quad (7)$$

The alternator parameters were obtained as follows:

| | |
|---------------------------|-------------------------------|
| Volt/hertz ratio (phase): | $k = 2.703 \text{ V/Hz}$ |
| Phase resistance: | $R_A = 1.1 \text{ ohm}$ |
| Phase inductance: | $L_S = 0.0112 \text{ henry.}$ |

5.3.2 Line-Connected Tests

The purpose of these tests was to evaluate the performance and electrical characteristics of the North Star ice maker, which was connected to a conventional 208-V, 60-Hz grid. The grid-connected start-up test was performed under two different conditions:

- The "warm" start-up test. In this case both evaporator and suction temperatures were close to ambient temperature ($t_{\text{evap}} = 27^\circ\text{C}$, $t_{\text{suct}} = 23^\circ\text{C}$).
- The "cold" start-up test. In this case both evaporator and suction temperatures were relatively low ($t_{\text{evap}} = 4^\circ\text{C}$, $t_{\text{suct}} = 0^\circ\text{C}$).

Both line current and active power were measured during "warm" and "cold" start-up tests. The results are shown in Figures 5.3 and 5.4. The ambient temperature during both tests was 28°C.

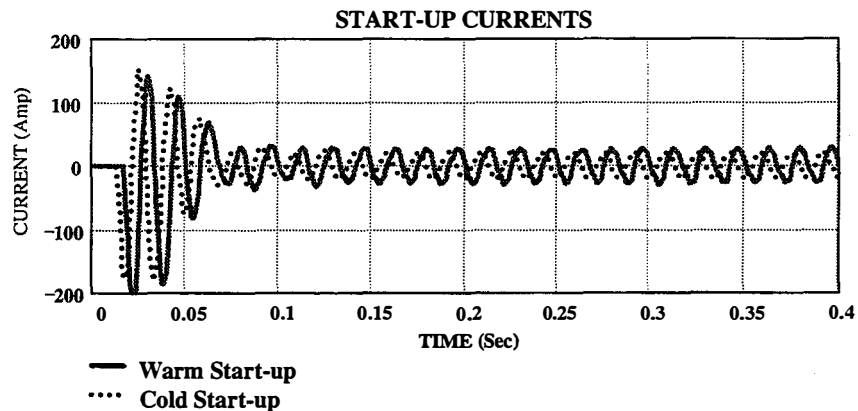


Figure 5.3. Measured currents for “warm” and “cold” start-up tests

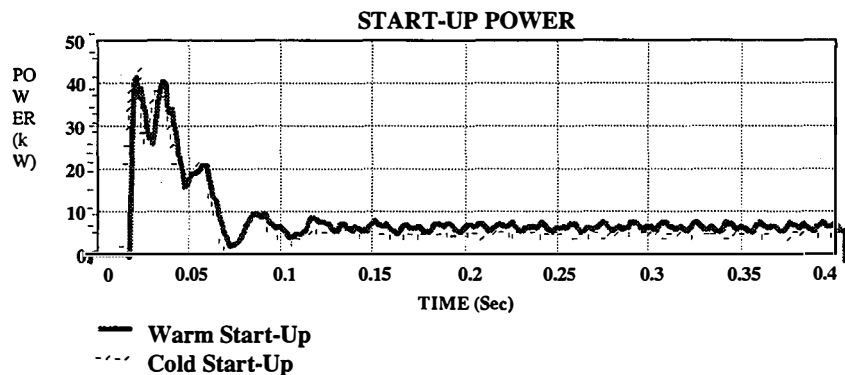


Figure 5.4. Measured power for “warm” and “cold” start-up tests

The maximum start-up current and power were about the same for both start-up conditions. It took about 0.8 s for the ice maker to start up, after which it operated at a steady state. (Even though the temperatures were changing, within the time interval of 0.4 s they were assumed to be constant.) As Figure 3 shows, the steady-state current and power for “warm” start-up were about 25% higher because of a higher load on the compressor. Active power in the steady-state regime was not constant, and was oscillating because of a phase imbalance in the ice maker.

Results for other continuous line-connected tests (3 min) are shown in Figure 5.5. The ice maker was started up at “warm” conditions, at which point the ice maker consumed about 8 kW of active power from the grid. As it continued to operate, both suction and evaporator temperatures kept decreasing. Compressor load kept decreasing as well, resulting in lower power consumption by the ice maker. The system stabilized both electrically and thermally in about 3 min, at which point both power and current were measured at 3.8 kW (which is about 35%–40% less than it was at start-up).

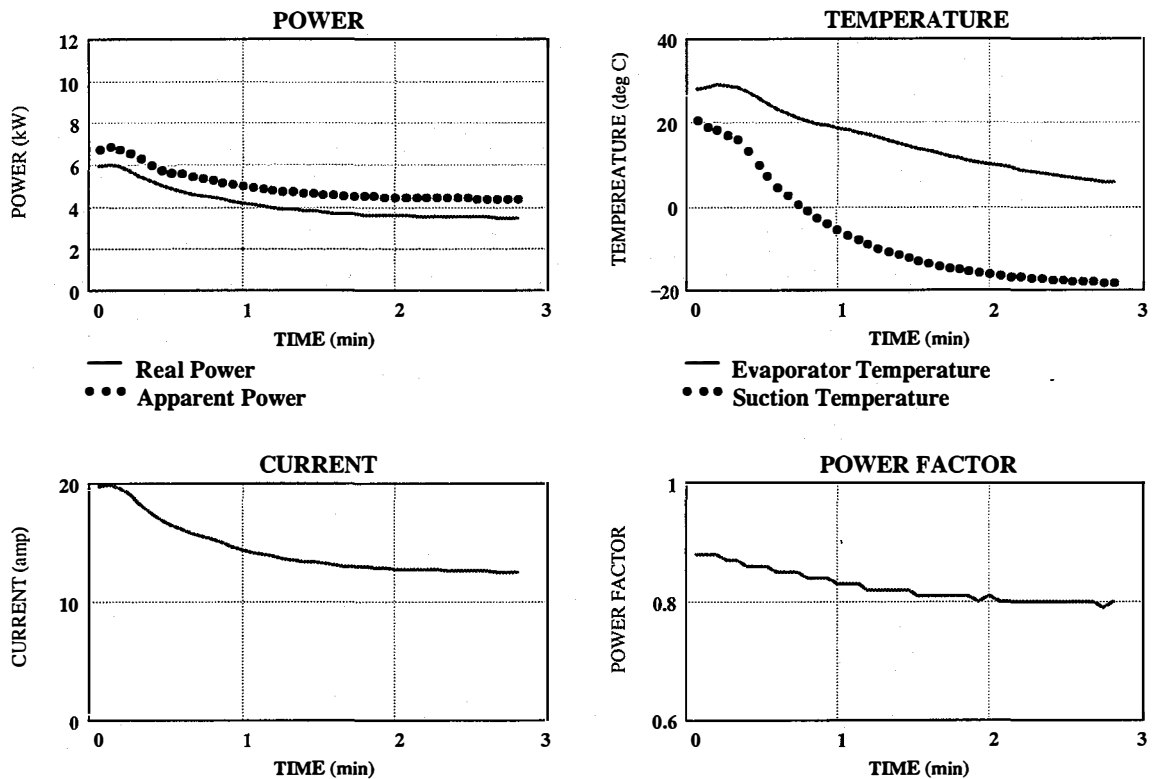


Figure 5.5. Results of 3-min line-connected tests

5.3.3 Alternator-Connected Tests

5.3.3.1 Ice Maker Steady-State Performance

The steady-state test was carried out for different alternator frequencies at the ambient temperature of 28°C. The system was running for at least 30 min at each frequency before the measurements were taken. Test results are shown in Figures 5.6a and b. Ice production increased almost linearly with the alternator frequency, as did electrical power and voltage. Line current is nearly independent of frequency, which can be explained by the fact that total impedance also increases proportionally with frequency. Thus, the resistive losses in the alternator and ice maker are constant and do not depend on frequency, which gives the ice maker a higher electrical efficiency at higher frequencies.

Because of lower refrigerant pressure at lower frequencies, both suction and evaporator temperatures became higher. It affected not only the ice production rate but also the ice quality. In order to determine the share of compressor and other auxiliary loads (fan, disk and pump motors) in the overall power consumption of the North Star ice maker, this test was conducted with the compressor disconnected. As seen in the above figures, the auxiliary load share is about 25%; however, this load is not balanced.

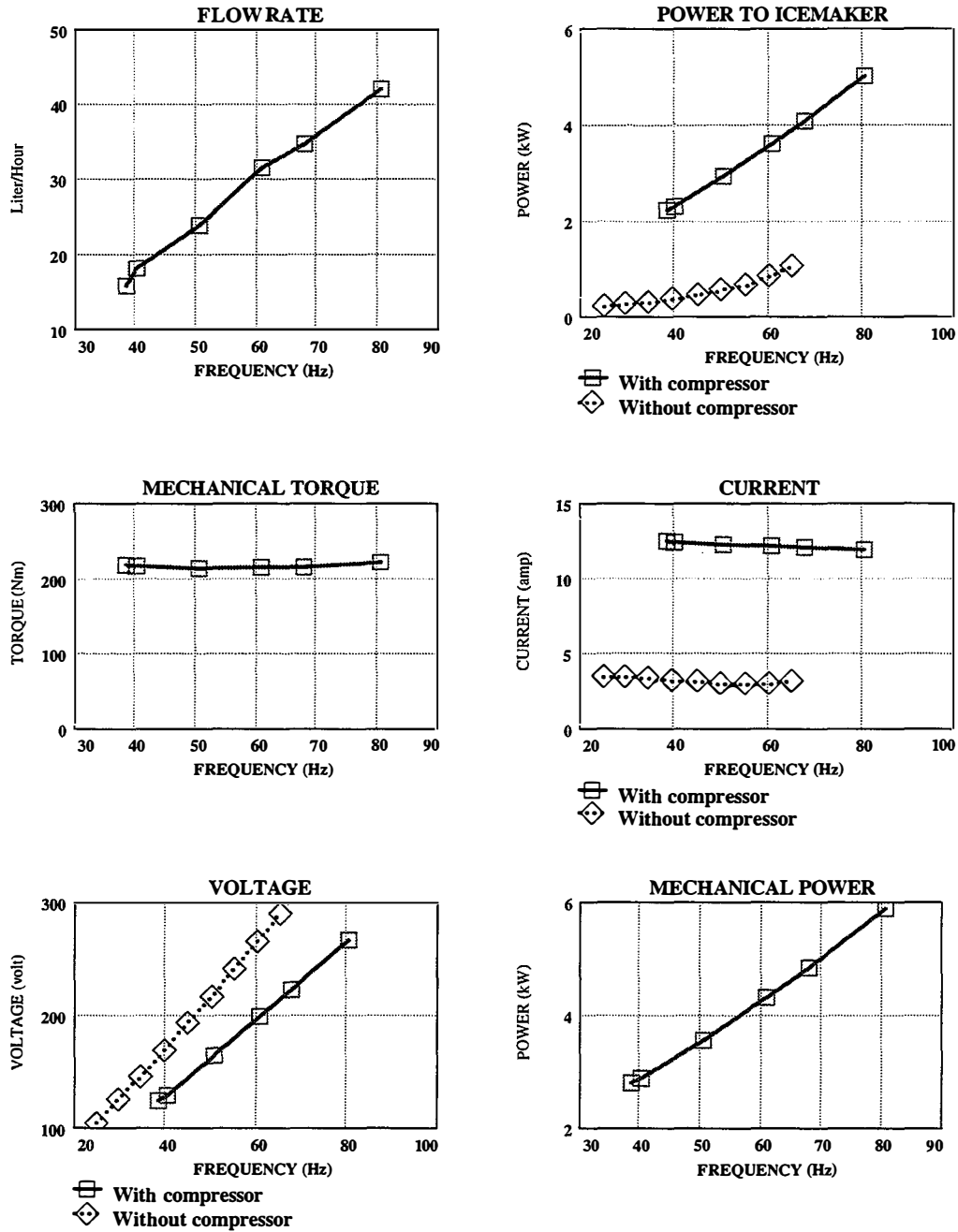


Figure 5.6a. Results from alternator-connected steady-state test

5.3.3.2 Start-Up Characteristics

Alternator-connected start-up tests were performed at different alternator frequencies for both “cold” and “warm” start-up conditions. Because the “warm” start-up is harder for the system, only the results for this test are shown below. Figures 5.7–5.12 show results for “warm” start-up tests (without series capacitors) at 25-, 30-, 35-, 40 -, 45- and 50-Hz alternator frequencies. Ambient temperature during this test was 28°C. The North Star ice maker starts at frequencies within the range of 25–45 Hz. However, sometimes it was not able to start under similar test

conditions, which means that the ice maker was operating at the boundary of operation. It never starts at the higher frequencies (50 Hz and higher).

The average ice-maker start-up time was 0.3–0.4 s. Maximum start-up current (peak-to-peak) varies from 30 to 40 amps depending on frequency. Maximum power during start-up is within a range of 1.5–3.5 kW. Alternator frequency drops after start-up, but right after that the system accelerates back to the preset dynamometer driving frequency.

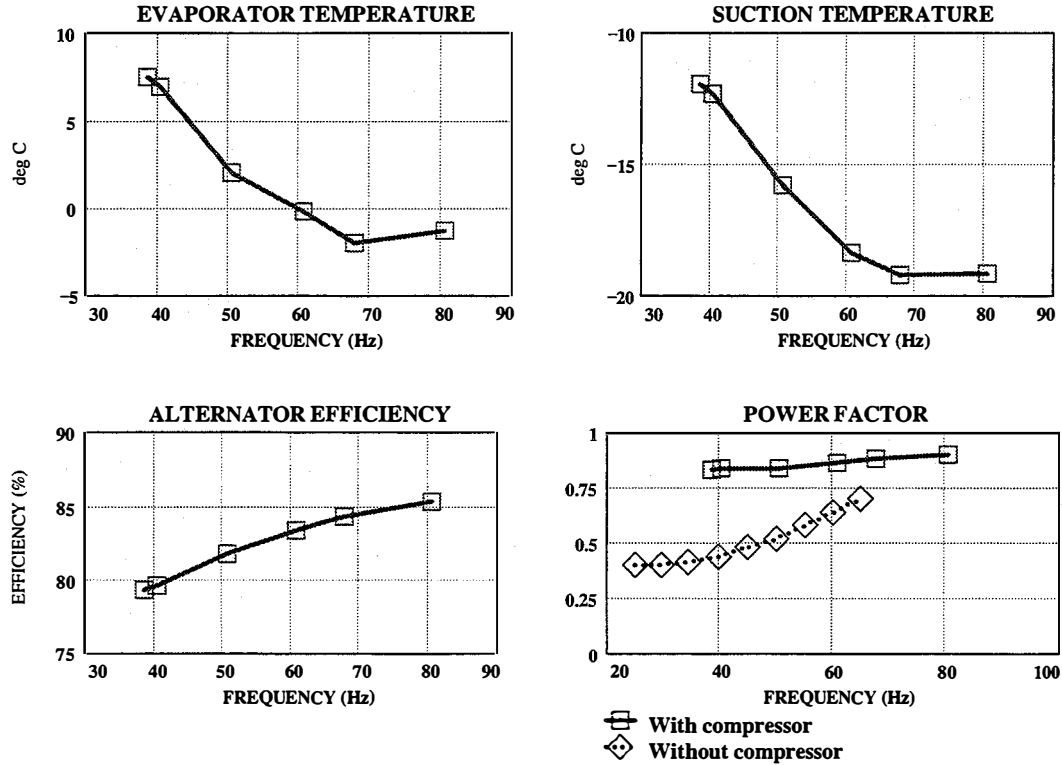


Figure 5.6b. Results from alternator-connected steady-state test

In order to improve the ice maker start-up characteristics, tests were conducted using various sizes of motor-start series capacitors. The capacitors compensate for motor inductance during start-up, thus allowing more active power and higher start-up current to be delivered by the alternator. After the motor reaches synchronous speed the capacitors are bypassed.

In order to conduct this test, we installed a bank of capacitors with bypass contactor controlled by time-delay relay. Some results from this test are shown in Figures 5.13 and 5.14. The series capacitors helped to boost start-up current and power significantly. In some cases, depending on capacitance and frequency, the start-up process was accompanied by alternator frequency oscillations. Despite the fact that there was a significant increase in power, the ice maker stalled after it was bypassed. This might be explained by the fact that there are other motors with quite different characteristics connected in parallel with the compressor. The North Star ice maker consists of five single- and three-phase induction motors. The optimum sizes of start-up for the capacitors were selected based on modeling results using the compressor motor parameters. In reality, however, the other different motors interact with the capacitors and the overall impedance of the ice maker is different from the one used in the model. This problem can be solved by implementing a special start-up sequence algorithm in the system. The start-up capacitors, with their bypass switch, should be connected in series with the compressor only downstream of the main contactor in the ice-maker control box, where all electrical connections and main contactors

are located. First, only the compressor should be started with series capacitors. After the compressor is started up the capacitors should be bypassed and the rest of the ice-maker motors connected. This method would use the capacitors effectively and improve the start-up characteristics of the ice maker. Because of other problems encountered, we did not implement this configuration.

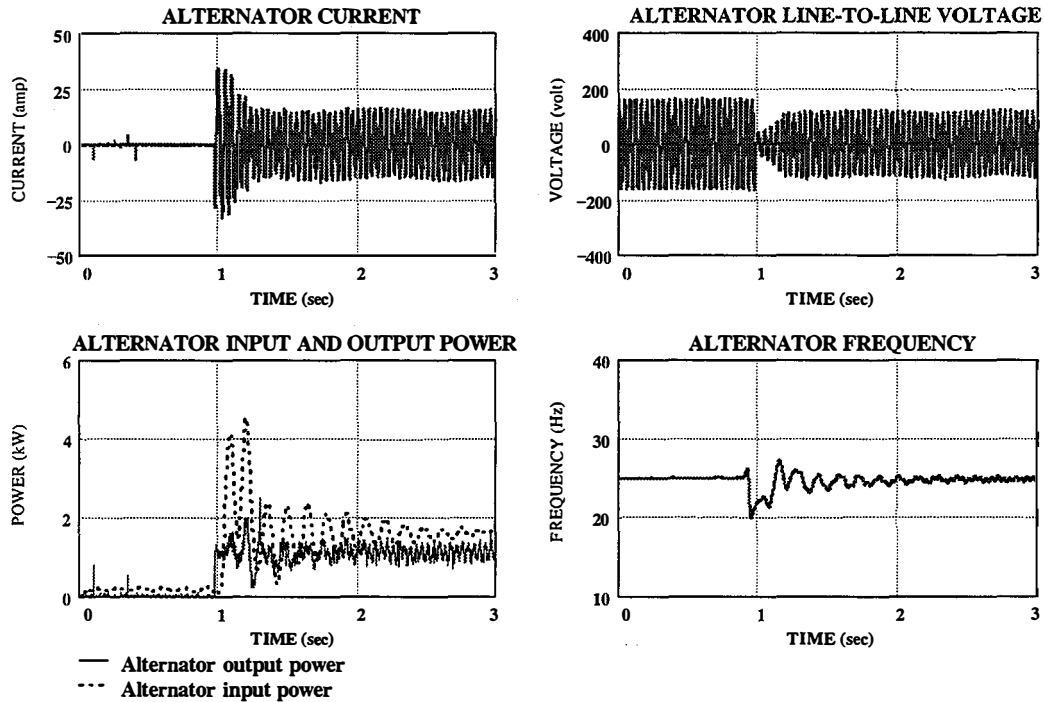


Figure 5.7. "Warm" start-up test without series capacitors (alternator frequency—25 Hz)

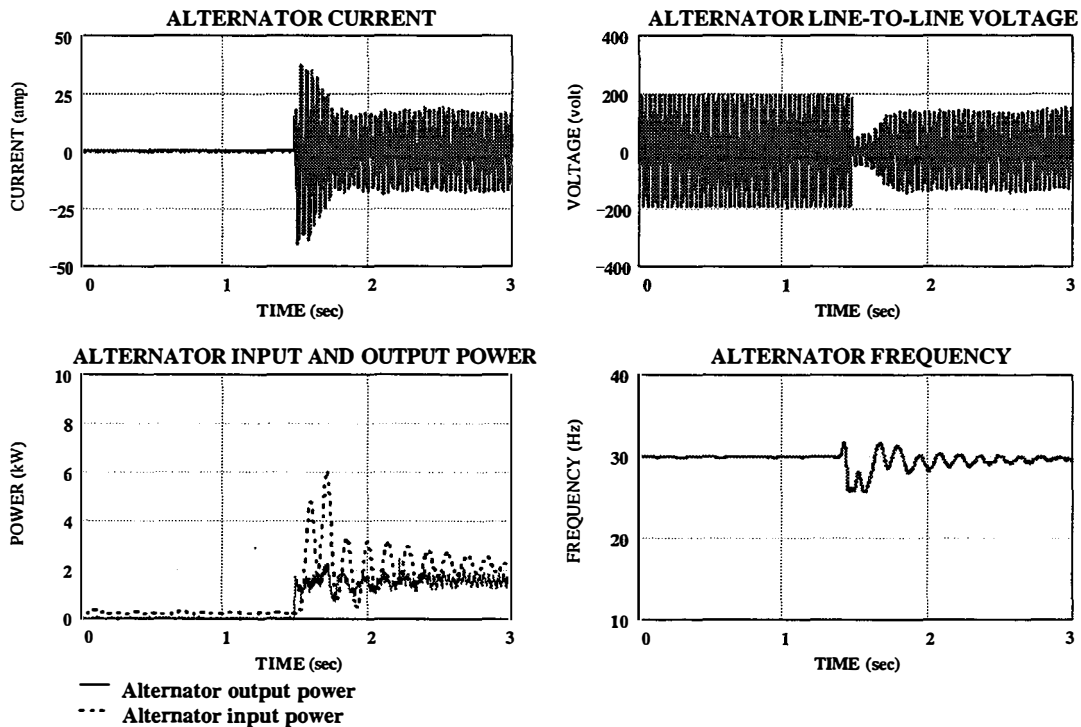


Figure 5.8. "Warm" start-up test without series capacitors (alternator frequency—30 Hz)

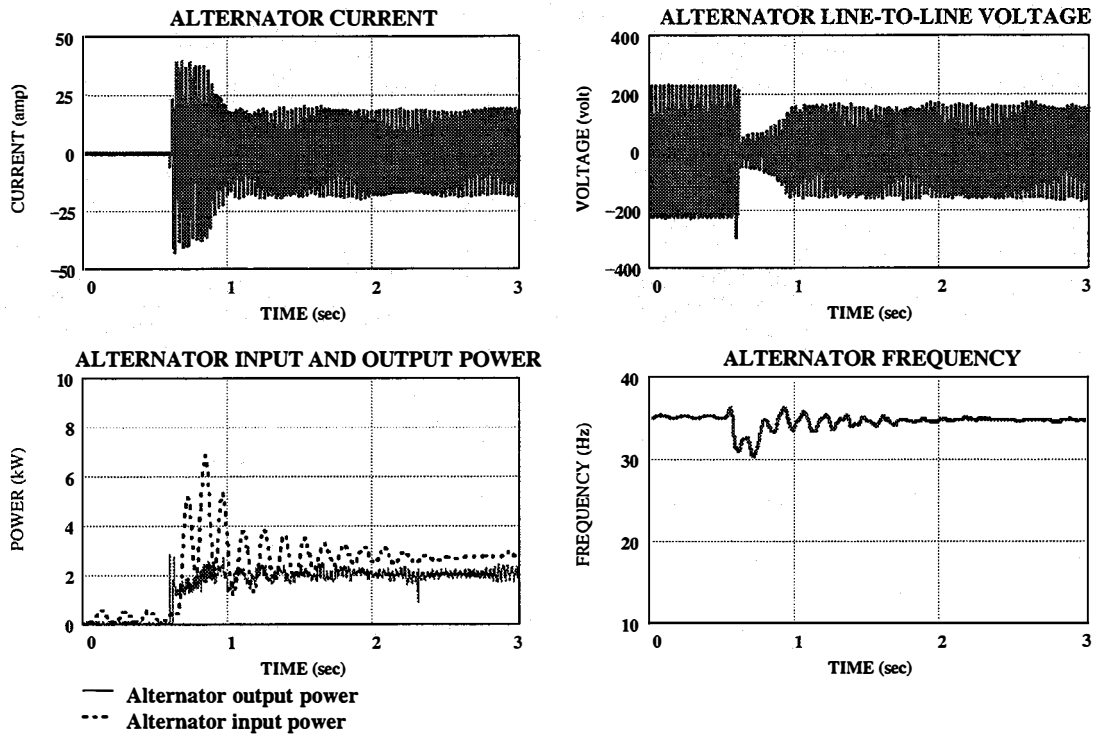


Figure 5.9. “Warm” start-up test without series capacitors (alternator frequency—35 Hz)

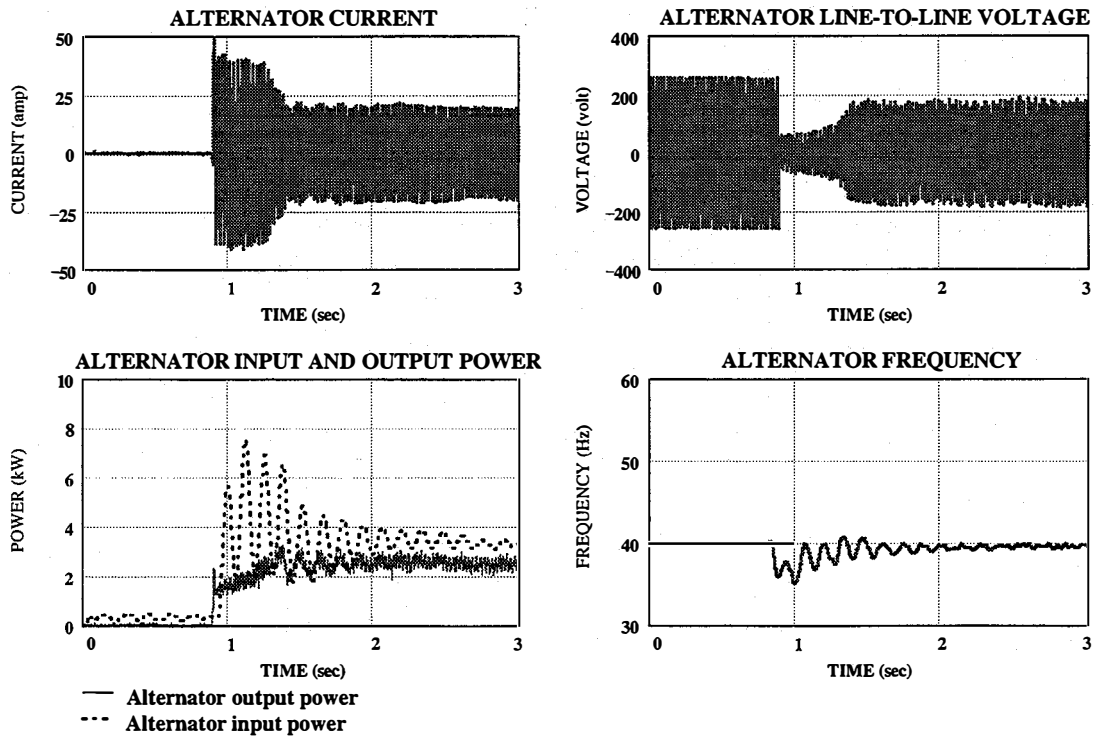


Figure 5.10. “Warm” start-up test without series capacitors (alternator frequency—40 Hz)

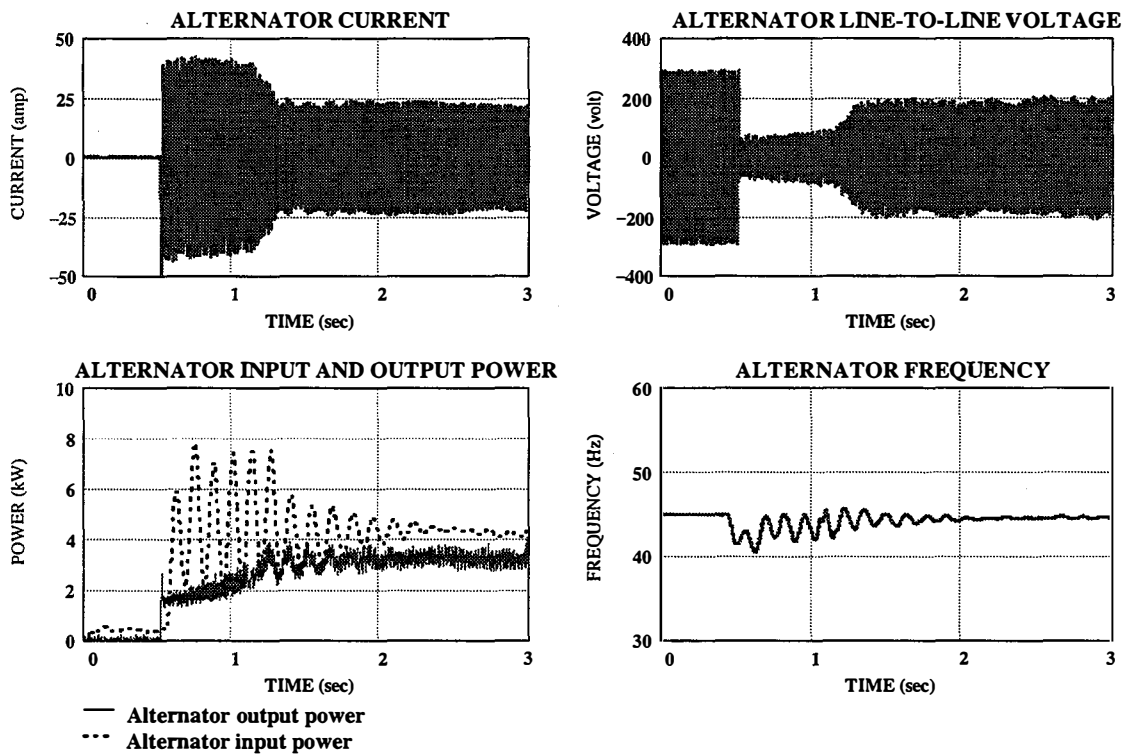


Figure 5.11. “Warm” start-up test without series capacitors (alternator frequency—45 Hz)

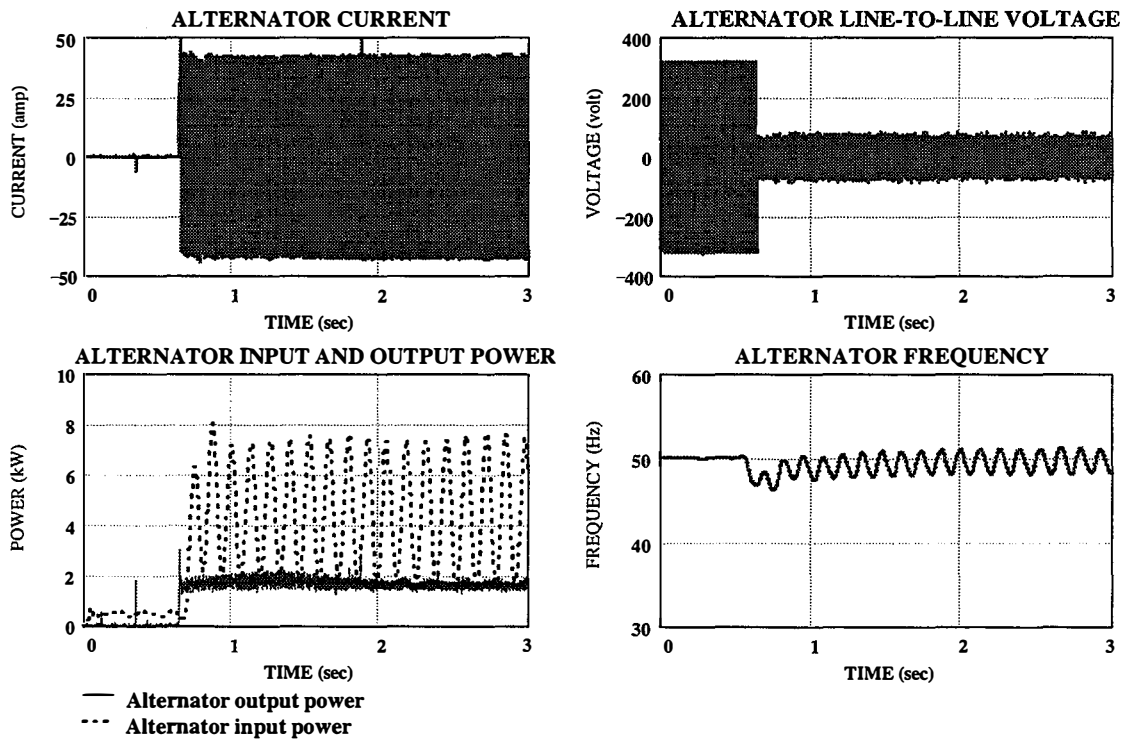


Figure 5.12. “Warm” start-up test without series capacitors (alternator frequency—50 Hz)

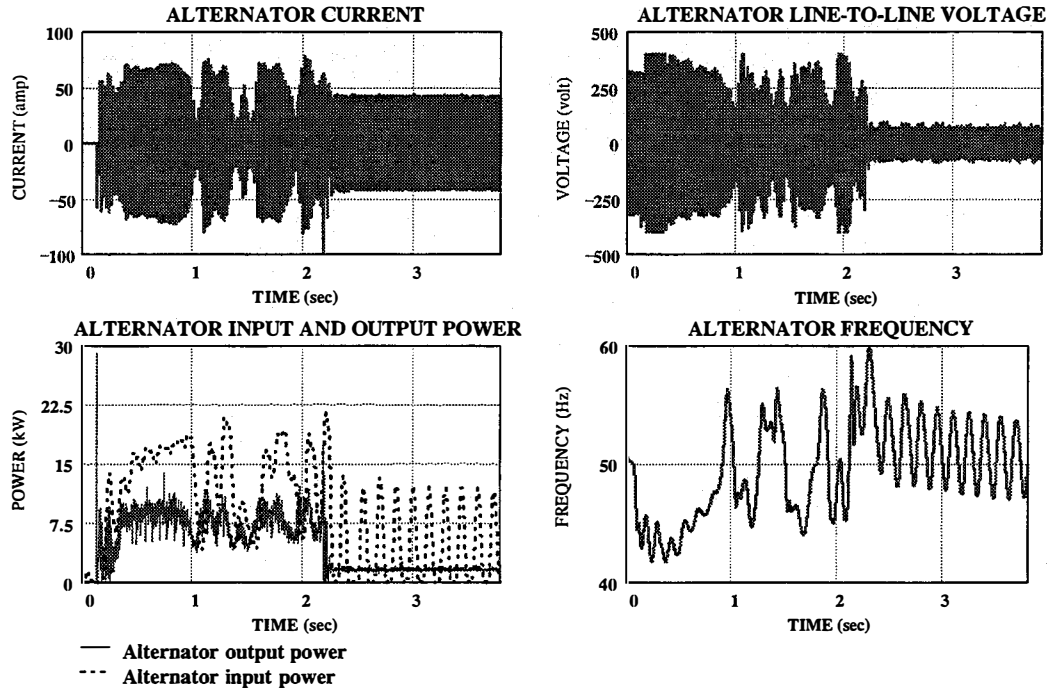


Figure 5.13. Alternator-connected “warm” start-up with 750- μ F series capacitor (alternator frequency—50 Hz)

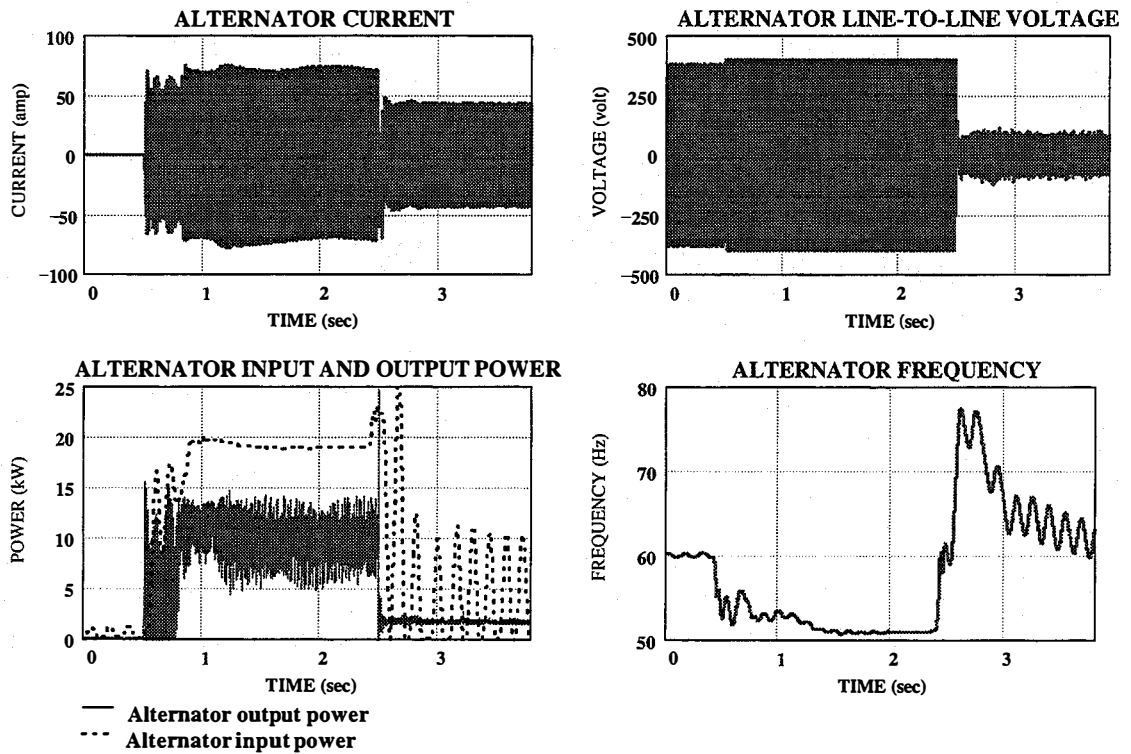


Figure 5.14. Alternator-connected “warm” start-up with 500- μ F series capacitor (alternator frequency—60 Hz)

5.3.4 Variable-Frequency Test

We varied the alternator frequency from 30 to 80 Hz to simulate a variable wind-speed regime. As we anticipated, the power to ice maker, temperatures, and ice production rate varied with the frequency as well. Figures 5.15–5.18 show results from this test.

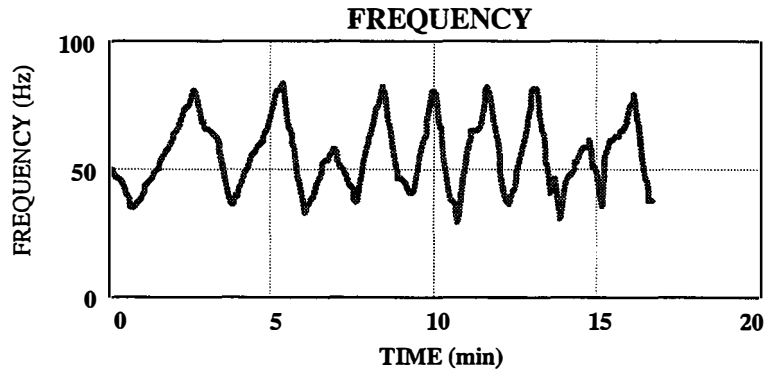


Figure 5.15. Alternator frequency during variable-frequency test

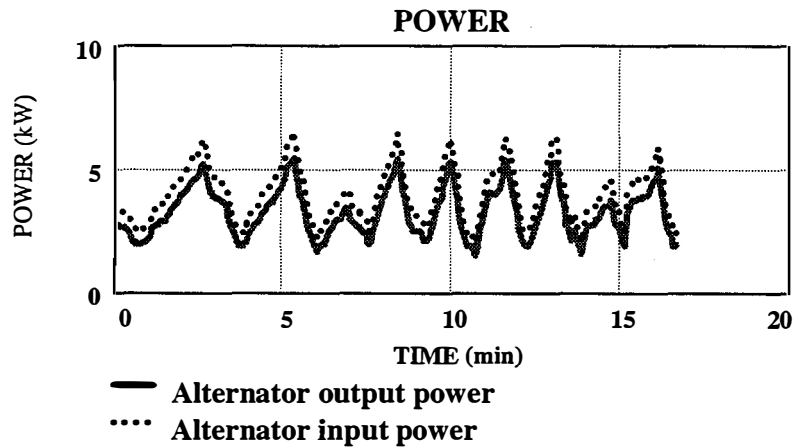


Figure 5.16. Mechanical and electric power during variable-frequency test

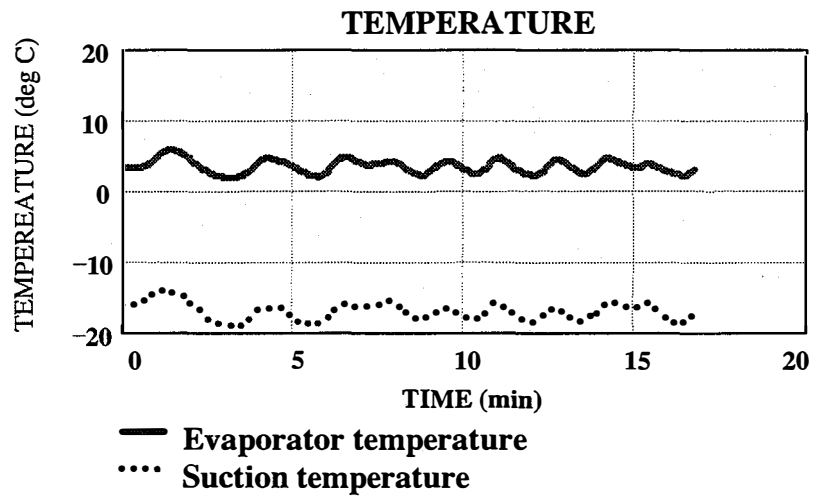


Figure 5.17. Evaporator and suction temperatures during variable-frequency test

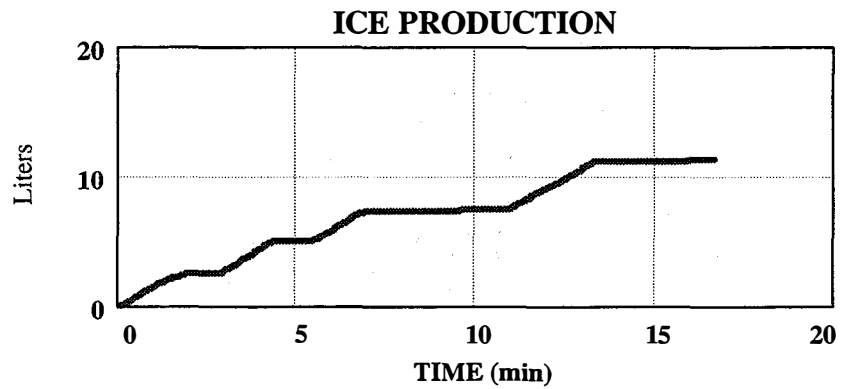


Figure 5.18. Cumulative ice production rate during variable-frequency test

5.3.5 Operating Problems Exposed during Testing

1. There is an incompatibility between the existing North Star control box and variable-voltage/speed operation. The existing contactor coil is rated for 230 VAC/60 Hz. Immediately after ice-maker start-up the alternator voltage decreases, causing the contactor to open. Then the voltage increases again, the contactor closes, and the cycle repeats. In order to carry out the test, we just bypassed the contactor. However, for variable-speed application another solution is needed (a DC contactor coil with an independent power supply, for example).

2. Another incompatibility was caused by the disk-driving motor. We had originally installed a 1/4-hp, single-phase capacitor start-up AC motor. Its starting capacitor caused problems during start-up at low frequencies, because it was tuned for 60 Hz. At lower frequencies, the motor did not start. Also, the single-phase motor imposed an unbalanced load on the alternator. So we replaced it with a three-phase motor (rated power—1/3 hp). After that, we did not have any problem with disk motor start-up. Moreover, the system became more balanced.

3. The small water pump located in the reservoir is also driven by a single-phase AC motor. At low frequencies the pump discharge pressure drops, and the amount of water sprayed on the disk decreases. This fact, in combination with higher suction temperature (and therefore higher disk temperature) at lower frequencies (see below), causes poor ice quality. The ice layer is thinner and brittle. At 30 Hz the pump is not able to spray any water at all, though the ice maker starts up at this frequency.

4. The disk-drive control timer was malfunctioning, causing the disk to rotate intermittently. We bypassed the timer in order to have continuous ice production. We do not know how the stock timer will respond to varying voltage and frequency.

5. At high frequencies (70–75 Hz) there is an intense mechanical vibration of both fans. At frequencies higher than 75 Hz vibration disappears. However, the fan motors start heating very intensively. The vibration can be avoided by changing the mechanical design of the fan blades and drive shafts. Using power factor correction capacitors on the compressor motor leads to more severe vibration, which appears at about 68 Hz and continues at higher frequencies.

6. The refrigeration circuit should be periodically checked for leaks. A loss of refrigerant reduces the ice maker's performance, particularly at higher frequencies.

A central issue is that any modification to the electrical configuration of the system, particularly involving the addition of capacitors, must be thoroughly thought through while carefully considering all possible ramifications. We performed all of our modeling and bench-scale testing using a single motor load, whereas the North Star ice maker has five different motors with very different characteristics. We added capacitors to the system so that they interact with all of the motors in the system, with very undesirable results.

5.4 Analysis of Ice Production as a Function of Wind Speed

We used the dynamometer test results to analyze the system's steady-state performance as a function of wind speed. For that purpose, we combined the measured power on the alternator shaft with the family of rotor power curves at different wind speeds (Figure 5.19). The hypothetical rotor power curves were obtained from the C_p curve for the 10-kW Bergey wind rotor. We obtained the ice production versus wind-speed curve (Figure 5.20) by determining the locus of intersections between this family of curves and the alternator shaft power versus

frequency curve, because at steady-state, the power output by the rotor must be completely absorbed by the generator. As shown in Figure 5.20, the ice production rate increases almost linearly with wind speed. The cut-in wind speed is high (about 6.7 m/s), a result of the ice maker's poor performance at low frequencies. The range of operational wind speeds for tested configuration is limited by a 6.6–10 m/s interval. The high limit is explained by certain operational problems at higher frequencies, as described in the previous section. We used this curve for approximate cost analysis.

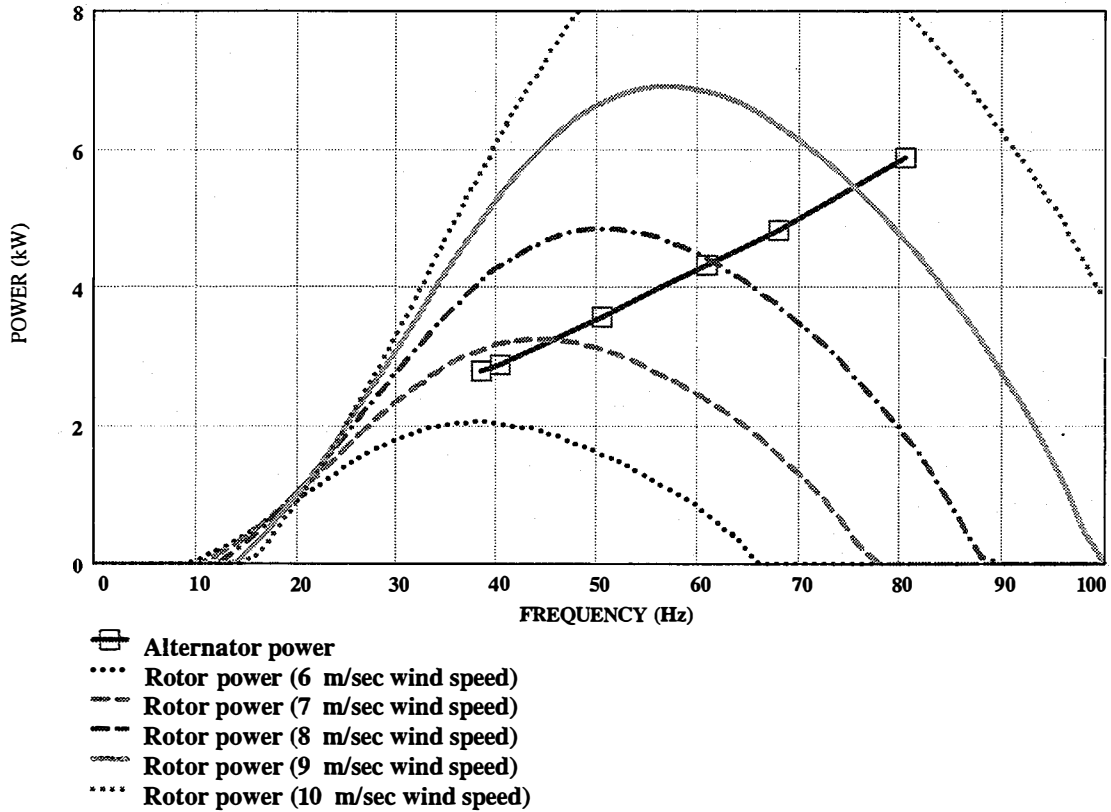


Figure 5.19. Alternator and wind rotor power

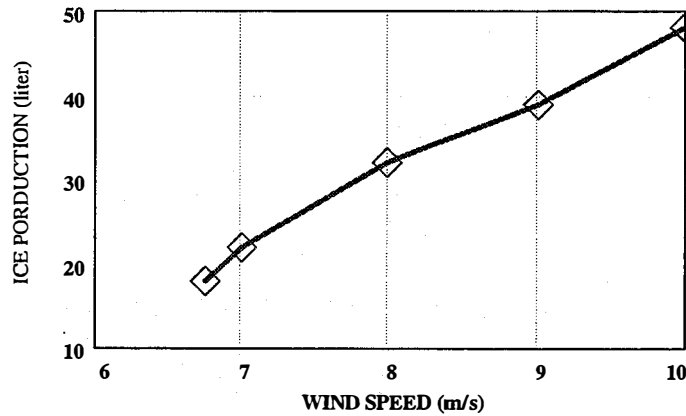


Figure 5.20. Ice production versus wind speed

5.5 Phase 3 Conclusions

The two-month testing process revealed a set of problems that make the ice-making system configuration unusable for variable-frequency/voltage operation. The North Star ice maker's start-up characteristics can probably be significantly improved by adding series motor start capacitors; however, great care must be taken to size them properly and to avoid interaction with other motors in the system. The ice production rate increases with frequency, although at higher frequencies the excessive vibration and motor overheating could potentially destroy the unit.

Our testing raised several design questions that should be answered before the North Star ice maker is developed further.

1. What are the characteristics of the expansion orifice in the disk assembly?
2. Is the orifice tuned for a certain compressor speed and/or refrigerant mass-flow rate?
3. How would the refrigeration system performance vary with changing compressor speed?
4. Why doesn't the disk operate while submerged in a water bath?
5. Could the unit be supplied with a thermostatically controlled expansion valve? How would its characteristics differ from those of the fixed-orifice design?

PART III: CONCLUSIONS AND FUTURE PLANS

6. Design Considerations for a Variable-Frequency Ice-Making System

This chapter provides technical information on variable-frequency ice-making systems. Section 6.1 reviews the known problems and proposed solutions for variable-voltage/frequency operation of a constant-voltage/frequency commercial ice maker. Section 6.2, which provides some general specifications and goals, could be used as the starting point for a complete technical specification of a commercial ice maker that will be powered by a PMA wind turbine.

6.1 Problems with Running Commercial Ice Makers on Variable-Frequency AC

We identified four basic problems with running commercially available ice makers on variable-frequency alternating current. They are: (1) PMA overloading during start-up, (2) mechanical vibrations at high frequencies, (3) poor quality of ice at low frequencies, and (4) control system failure. Restricting the operating-frequency range to within a narrow range of approximately 60 Hz is not a solution because, first, it would not solve the start-up problem, and second, it would make the system uneconomical. Therefore, we shall try to solve these problems rather than avoid them. The following sections discuss potential solutions for these problems.

6.1.1 The Start-Up Overload Problem

The start-up overload problem is that upon initial energization of the ice-maker compressor motor, the wind turbine generator cannot deliver the large start-up current needed to accelerate the compressor motor. The result could be overheating of the compressor motor or PMA, or stalling out of the wind turbine rotor. Solutions range from mechanically unloading the compressor motor so that it can accelerate adequately to electrically dampening the in-rush currents with devices such as series capacitors. As demonstrated in Phase 3, an oversized generator can also provide a viable solution.

For all three of the above-mentioned solutions, two things are certain: some additional expense will be required and some of the solutions will be impossible to implement on some ice makers. For example, using an oversized wind turbine could increase costs by thousands of dollars, making the system uneconomical. For ice makers that incorporate closed or hermetic compressors, some of the mechanical unloading schemes would not be possible.

Currently, electrical solutions appear to be the cheapest and easiest to implement for the start-up problem. The series capacitor solution that we investigated has its problems, however. Unbalanced loading of the ice maker's three phases resulting from the presence of various single-phase motors and control circuits, coupled with the series capacitors, can result in electrical resonances over much of the operational frequency range. Such resonances could have damaging effects on the ice maker and wind turbine. If series capacitors are used, then balanced loading is required between the three phases. This would require that all ice-maker loads be either all single phase or all three phase. A three-phase compressor motor with single-phase condenser fan motors is not acceptable.

Of the mechanical-unloading schemes, the options are friction or fluid clutches, forced-pressure equalization of the compressor ports, and different types of compressor, such as scroll or centrifugal, in which its pressure loading is proportional to its speed.

6.1.2 Mechanical Vibrations at High Frequencies

Severe vibrations of the condenser fan blades occurred at about 70 and 80 Hz. We suspect that those fan speeds corresponding to 70 and 80 Hz matched the resonant frequencies of the fan blades. Indeed, the vibrations were so severe that we had to shut down the icemaker.

There are several ways to counter the vibration problem. Redesigning the condenser fan blades and shafts so that the resonant frequencies are higher than 100 Hz would be expensive, and might lower the efficiency of the ice maker. Using three-phase condenser fan motors instead of single-phase motors may provide another solution, as the former may be better suited to high-frequency operation. Of course, this hypothesis would have to be tested. A final solution would be to use a water-cooled condenser rather than an air-cooled condenser. This solution may have the most promise: pumps are generally less sensitive to speed changes than are fans. An added benefit of using the water-cooled condenser is that the ice maker's performance will be less sensitive to changes in the ambient temperature and that corrosion may be easier to prevent.

6.1.3 Poor Quality of Ice at Low Frequencies

The North Star D-12 ice maker that was tested extensively at NREL did not produce high-quality ice at frequencies below the rated 60 Hz. The ice was very wet and the ice type was often not flake. In other words, a slushy mixture was produced that wouldn't be suitable for most purposes. The primary problem was that the temperature of the refrigerant in the evaporator disc varied with the speed of the compressor, a problem that wasn't identified until Phase 3 testing. The Phase 1 variable-frequency tests did not hold the ice maker at low frequency long enough to actually observe a reduction in ice quality. However, those tests did reveal an almost immediate increase of the evaporator (or suction) temperature when the alternator frequency was reduced.

We identified a few solutions to the evaporator-disk temperature problem. First, there is the possibility of regulating the evaporator temperature when the compressor speed changes. This will require devices such as thermostatically controlled valves that monitor the evaporator temperature. Another possibility is using thermal storage around the evaporator surface to reduce the heat transfer to the refrigerant. If the warm-up time for the evaporator surface were much longer than the duration of wind lulls, then the ice quality would be "smoothed out." In other words, continual starting and stopping of the system will not be tolerated. Another approach would be to find a wind resource that remains at a high enough level for a considerable time period each day to maintain the icemaker at or above rated frequency. Although some viable ice making sites may have such a wind resource, this should not be considered a solution to the problem of poor ice.

A related problem at low frequency is the reduction in water flow rate over the evaporator disk. However, this has more to do with reduced ice quantity than ice quality. The reduced quantity of ice is accounted for in the ice production versus frequency (or wind-speed) curves. Solving that problem would require less dependence on an active pumping device—perhaps a partially or fully submerged evaporator surface would do. Another possibility would be to supply water to the evaporator surface from a large, elevated reservoir. This would keep the supply pressure approximately constant.

6.1.4 Control System Failures

The final ice-maker problem that is attributable to variable-frequency operation is the failure of the control system, which for most commercial ice makers is energized from the icemaker's main power source. If that source of power produces less than rated voltage, then some of the components may stop functioning altogether. In particular, many of the contactors will fail to open or close under those conditions. If the source of power produces more than rated voltage, then there is the possibility of fuses and circuit breakers being blown or circuits being overloaded.

One way to solve this problem is to separate the power supply for the control system from the variable-frequency main power supply. Because most control circuits require very little energy, a small battery could be used as the power supply. If the control circuit cannot easily be changed over to DC, then a small inverter would be needed. Keeping the battery charged may require a custom-made charger because most commercially available AC battery chargers also require a constant-voltage/frequency power source.

6.2 “Strawman” Specification for a Commercial Ice Maker Powered by a PMA Wind Turbine

The following subsections form a “strawman” for a technical specification of a commercial ice maker powered by a PMA wind turbine. Suggested entries based on the system tested in Phase 3 by NREL (i.e., BWC 12-kW PMA alternator and North Star D-12 flake ice maker) are included in brackets. Based on the preceding discussion, it is understood that some modifications of existing equipment would be required in order to meet such a specification.

6.2.1 Power Source Characterization

- A delta-wound permanent magnet alternator with 3-phase output will provide power to the ice maker. (Note: A detailed technical specification should also include a description of the steady-state and dynamic properties of the alternator in the form of graphs; the operational envelope of the alternator should be shaded on these graphs.)
- The open-circuit line-to-line voltages will be as high as 600 VAC.
- The required closed-circuit frequencies will range from 30 to 100 Hz.
- The required closed-circuit line-to-line voltages will range from 100 to 300 VAC.

6.2.2 Ambient and Water Source Conditions

All performance goals are based on the following ambient and water source conditions:

- Ambient temperature: 40°C (104°F)
- Relative humidity: 90%
- Elevation: sea level
- Water source temperature: 28°C (82°F)
- Water source salinity: 300 to 30,000 ppm
- Water source pressure: unspecified.

6.2.3 Ice Maker Characterization

- Ice type: flake
- Refrigeration system: electric, vapor-compression
- Refrigerant: non-chlorofluorocarbon
- Condenser: air or water cooled.

6.2.4 Performance Goals

All of the following performance goals apply to the entire operational envelope:

- The ice maker will start up satisfactorily from a “warm” or “cold” condition without overloading the alternator. (A “warm” condition means that the evaporator temperature is greater than 5°C [41°F] and a “cold” condition means the reverse.)
- The instantaneous RMS currents in the three phases of the main power supply to the ice maker do not differ by more than 10%.
- The minimum rate of ice production will not be less than 25% of the rated, constant-frequency ice production of the ice maker.
- The maximum temperature of the ice will be -2°C (28°F).
- The character of the ice will not significantly differ from the rated, constant-frequency character of ice. (“Character of ice” is defined as the temperature, shape, thickness, and texture of the ice.)
- The ice maker will have an expected lifetime of at least 30,000 operational hours with preventive maintenance intervals of 6 months.

7. The Present and Future of Wind-Electric Ice-Making

Wind-electric ice making is currently in the developmental stage. The future of this technology depends on: (1) the potential market, (2) the cost of ice comparisons, and (3) the sustainability of developing-country installations. Although a worldwide market study has not yet been conducted, there are strong indications that a sizeable potential market does exist. The cost-of-ice comparisons are favorable for this technology and are discussed in Section 7.1. The sustainability issue has both technical and institutional dimensions. On the technical side, the system can be sustainable if the variable-speed issues discussed in Chapter 6 are addressed. Furthermore, sustainability gains may be derived from the elimination of electronic power converters such as rectifiers and inverters, which are often the source of failure in hybrid systems. Of course, institutional factors may be equally important to sustainability. Section 7.2 includes a list of characteristics (including the local wind resource) pertaining to the economic and institutional situation of a village that favor cost-effective and sustainable wind-electric ice-making projects. The final section in this chapter reviews NREL's plans for advancing wind-electric ice-making from the developmental stage to implementation.

7.1 Estimated Cost of Ice for Wind-Electric Ice-Making Systems

The phrase "cost of ice" is used here to refer to the relative cost-effectiveness of different approaches to producing ice. It is based on life-cycle cost, which is the best-known basis for comparing project alternatives. The different approaches that have been considered are: (1) delivery of ice (presumably produced in a freezer run off of the local electric grid) from a neighboring town, (2) an on-site wind-only system, (3) an on-site wind-diesel system, (4) an on-site wind-inverter system, (5) an on-site wind-hybrid system, and (6) an on-site diesel-only system. Although other options do exist, this list represents the four major wind-electric options (wind-only, wind-diesel, wind-inverter, wind-hybrid) as well as the two major conventional options (grid and diesel-only). The term "diesel" refers to any combustion engine-generator that consumes a fossil fuel. Other fuels could be gasoline, liquefied petroleum gas, or natural gas.

In the wind-only system, the wind turbine is connected directly to the ice maker and there is no other source of power. All production of ice is counted, regardless of how it matches up with the demand for ice. This assumes that the resource-load matching and the ice storage are sufficient to prevent any melting of ice before it is used. The wind-diesel system is a switched system in which the wind turbine produces ice just as in the wind-only case and the diesel can power the ice maker directly whenever the wind is not sufficient to produce ice. Because the switching is assumed to be manual, it is improbable that the diesel could run every hour that the wind is below the cut-in speed. In this analysis we assumed that the diesel could not run for more than 75% of the hours that the wind turbine is not powering the ice maker. The wind-inverter system, which uses a battery-powered inverter to power the ice maker, produces ice whenever the battery's state of charge is sufficient. (Wind energy is the only source for charging the batteries.) The wind-hybrid system is the same as the wind-inverter system, but with the addition of a backup engine-generator. Several different sizes of battery bank were considered for the wind-inverter and wind-hybrid systems. With the diesel-only system, in which the ice maker is driven directly by the diesel generator at all times, ice production is limited only by how long the generator is run. Downtime resulting from scheduled and unscheduled maintenance was not factored into this analysis. The net effect of downtime would be to decrease production and increase the cost of ice.

The cost of ice was determined by using the simulation program Hybrid2, followed by a detailed life-cycle cost calculation. Hybrid2 was used primarily to determine the performance of the power system components such as the wind turbine, diesel generator, and battery bank. These

performance results were then loaded into a spreadsheet for the life-cycle cost calculations. All costs were annualized—the sum of which was divided by the total annual ice production—to arrive at the overall cost of ice. The following subsections (7.1.1 and 7.1.2) describe the Hybrid2 modeling and the cost-of-ice spreadsheet, respectively.

The results of the cost-of-ice calculations were plotted on graphs (see Figures 7.1 and 7.2) showing cost of ice as a function of ice production. The two figures represent different fuel costs. Each graph shows the costs of ice for five of the six considered approaches to ice making. The cost of ice for the sixth approach, delivery of ice from a neighboring town, was not known well enough to be included on these graphs. (That cost is thought to be around U.S.\$0.04 per nominal pound of ice in many Mexican villages, a figure that could perhaps be much higher if melting during transport is considered.) The average annual wind speed is also an imbedded variable in these graphs. In addition to each wind-speed case, there are two or three different wind regimes represented. That is, actual wind data were used from sites that varied in Weibull shape factor from 1.85 to 2.35, thus giving a good representation of worldwide coastal wind conditions. Appendix K includes all of the graphs and cost-of-ice spreadsheets for all of the fuel cost cases (\$1.00, \$1.25, \$1.50, \$1.75, and \$2.00 per gallon) that were examined.

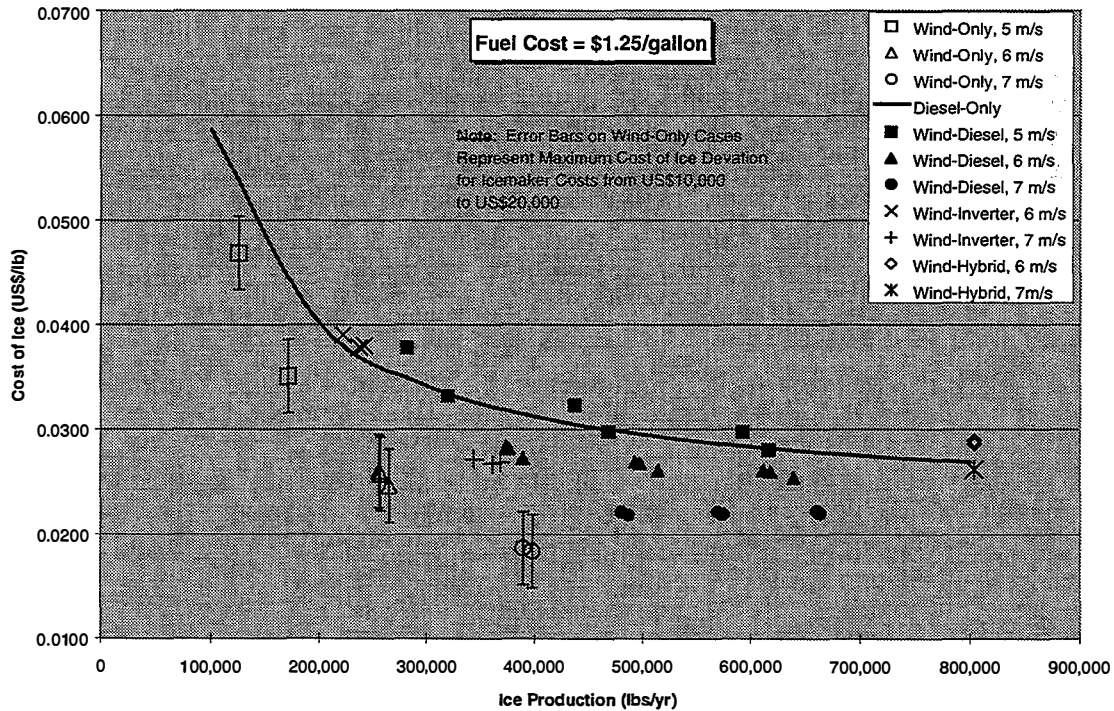


Figure 7.1. Cost of ice versus ice production for fuel cost = U.S.\$1.25/gallon

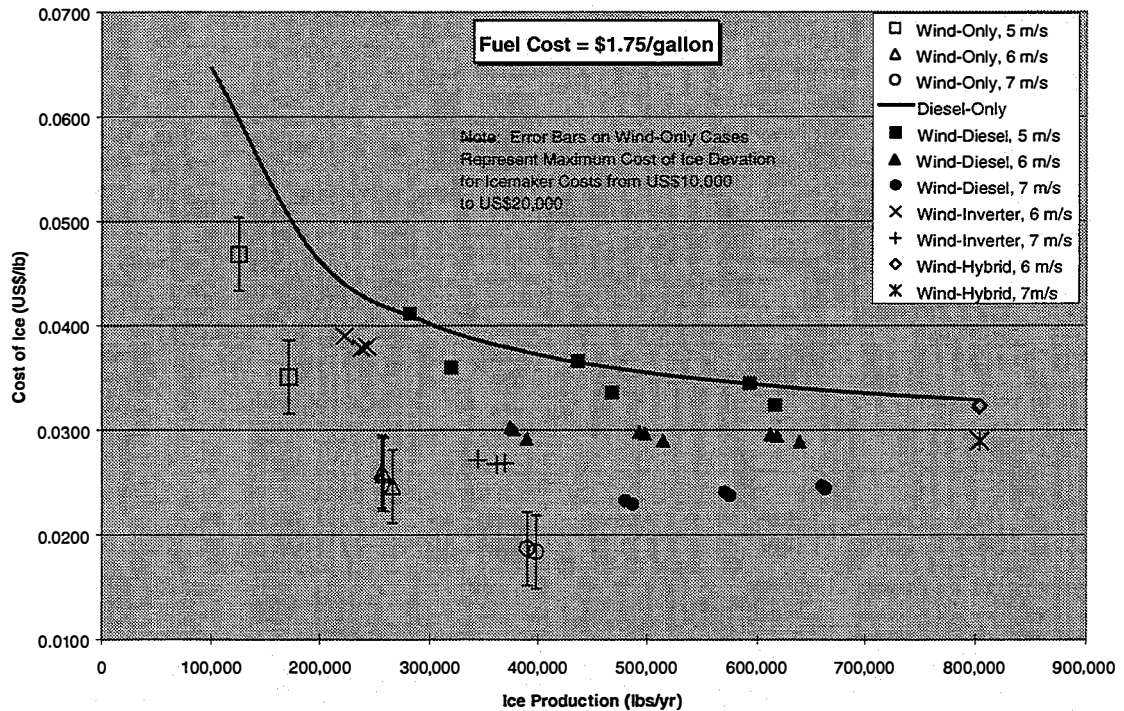


Figure 7.2. Cost of ice versus ice production for fuel cost = U.S.\$1.75/gallon

A careful examination of the cost-of-ice results reveals that the wind-only system, when the average annual wind speed is 6 m/s or higher, produces ice at or below the cost of all of the other considered alternatives—even when the fuel cost was as low as U.S.\$1.25 per gallon. The wind-only systems are more limited in their ice production, however. In order for those systems to produce more ice annually, multiple systems would be required. Because of the high capital cost of multiple systems, the availability of credit would strongly influence whether or not these systems could be purchased. Another limitation of the wind-only system is that it does not guarantee a certain amount of ice at a certain time. Excellent ice storage (i.e., minimal melting) and load-resource matching would help to minimize this limitation of the wind-only system. Any of the systems with a diesel generator have the advantages of being dispatchable (i.e., ice delivered on demand without the need for storage) and able to power other loads simultaneously because of the oversizing of the diesel generator. (The wind-inverter system also has this latter capability, but to a lesser degree.)

The factor that is most uncertain in this analysis is the cost of the ice-maker modifications. Because one or more modifications to an existing, commercially available ice maker will almost certainly be required for the directly connected systems (i.e., the wind-only and wind-diesel systems), the exact cost of the ice maker cannot be known at this time. The results that are presented here include a modification cost of U.S.\$5,000 which increases the ice-maker cost by 50%. Sensitivity studies have shown that even if the modification cost increased to U.S.\$10,000 the cost of ice would only increase by about U.S.\$0.0035. Consequently, the conclusion that the wind-only system is as cost effective as any of the other alternatives would not be affected significantly, even if the ice-maker modifications doubled the cost of the ice maker.

Thus, the following conclusions can be drawn from the cost-of-ice calculations:

- Given the benefit of having a diesel generator as a dispatchable power source and the slightly higher cost of ice of the wind-diesel systems, there is good reason for including diesel in the directly connected wind-ice-maker system.
- The wind-inverter system is not as cost effective as the wind-only system.
- The cost of the ice-maker modifications could as much as double the cost of the ice maker, and still the cost of ice for the wind-only and wind-diesel systems would likely be below the cost of ice that is transported from nearby towns to small fishing villages.
- The addition of value-added and import taxes (usually on the order of 15% to 30% of the total system cost) to any of the ice-making systems could potentially make the economics of on-site production of ice marginal.

7.1.1 Hybrid2 Performance Simulations

Hybrid2, a time-series simulation model for hybrid power systems, was used to predict the performance of all considered alternative systems with a wind-power component. The primary performance results from Hybrid2 were wind-generated ice production, diesel run time and fuel consumption, and expected battery life. The main inputs to Hybrid2 for these simulations are given below:

1. Ice Production from the Wind. A curve of predicted ice production versus wind speed resulted from the work of Phase 3. These data are shown in Table 7.1 as well as in Figure 5.20. The data for wind speeds higher than 10 m/s are an extrapolation of the data, taking into account the furling of the wind turbine. These data agree, for the most part, with the field tests from Phase 1. The rated capacity of the ice maker at 60 Hz and 230 VAC is 91.7 lbs./h. The vibration and heating problems that occurred at the higher frequencies (i.e., 70–80 Hz) have been neglected. We assumed that those problems would be addressed by the next-generation, directly connected ice maker. For the inverter-based systems, a BWC Excel-R wind turbine power curve was used.

Table 7.1. Ice Production versus Wind Speed for Directly Connected System

| Wind Speed (m/s) | Ice Production (lbs./h) | Wind Speed (m/s) | Ice Production (lbs./h) |
|------------------|-------------------------|------------------|-------------------------|
| 6.5 | 0 | 11 | 110 |
| 6.7 | 40 | 12 | 110 |
| 7 | 50 | 13 | 88 |
| 8 | 70 | 14 | 66 |
| 9 | 86 | 15 | 44 |
| 10 | 105 | 50 | 44 |

2. Wind Data. We used three data files of measured hourly average wind speeds. The three sites were Puaucho in Chile, Xcalac in Mexico, and Joanes in Brazil. All three are located in different coastal wind regimes representing Weibull shape factors from 1.85 to 2.35. All of the data files had one complete year of data. We scaled the data files to derive 5 and 6 m/s cases from the Puaucho data (4.98 m/s average); 5, 6, and 7 m/s cases from the Xcalac data (5.99 m/s average); and 6 and 7 m/s cases from the Joanes data (6.67 m/s average).

3. Ice-making Loads. The assumptions that governed the demand for ice are given for each system as follows: (1) wind-only: all wind above cut-in speed was converted to ice, stored, and eventually used with no particular pattern; (2) wind-diesel: same as for wind-only system, but with the diesel increasing ice production to any level (up to the practical limit) with no particular

use pattern; (3) wind-inverter and wind-hybrid: ice-making load was considered primary and was constant at 4 kW for every hour of the simulations. The ice maker produced 22.93 lbs. of ice for every kWh that it consumed, and it would produce 91.7 lbs. of ice per hour when operated directly from the diesel generator or the inverter.

4. Backup Generator. We used a 12-kW diesel generator because of the starting requirement of the ice maker. However, this size generator would probably still require a capacitor-assisted start of the ice maker. Supplemental loads would help to make the diesel systems more economical. A fuel curve representative of this size generator was used.

5. Dispatch Strategy. We used the following dispatch strategies regarding the diesel generator and battery bank: (1) wind-diesel: the diesel could run during any hour that the average wind speed was below the cut-in (around 6 m/s) up to a practical limit of 75% of the “wind-off” hours because of the manual switching that would be required between the wind turbine and diesel generator; (2) wind-inverter: the inverter would cease operation whenever the battery reached 20% state of charge; (3) wind-hybrid: same as the wind-inverter system with the additions that the diesel would start up when the battery reached 30% state of charge and shut off when the battery reached 80% state of charge. (The diesel was allowed to charge the battery bank and run the ice maker simultaneously.)

7.1.2 Cost-of-Ice Calculations

We calculated the cost of ice using standard life-cycle cost techniques. Costs of financing, maintenance, overhauls, replacements, and fuel were considered. We did not consider different rates of inflation, taxes, and salvage values. The detailed spreadsheets that we used for these calculations appear in Appendix K.

Table 7.2 gives the assumed capital costs for the five ice-making systems. The shipping and insurance costs, although lumped together as one cost, do include different contributions for the ice maker, diesel generator, wind turbine, and inverters. The battery costs include their shipping and insurance so that the additional cost for battery banks larger than eight Trojan L-16 batteries may be calculated accordingly. The inverter cost assumes that two Trace SW4024 inverters would be stacked in order to deliver the required 240 VAC to the ice maker.

The assumptions regarding operations and maintenance costs were as follows:

- The ice maker was replaced every 30,000 hours of use.
- The diesel generator was overhauled at a cost of \$3,600 every 20,000 hours of use.
- Annual scheduled ice-maker maintenance budget was \$500.
- Annual scheduled diesel generator maintenance budget was \$500.
- Annual scheduled battery maintenance budget was \$250.
- The cost of fuel varied from \$1.00 to \$2.00 per gallon.

Table 7.2. Estimated Capital Costs of Various Ice-Making Systems

| <i>Item</i> | Diesel-Only | Wind-Only | Wind-Diesel | Wind-Inverter | Wind-Hybrid |
|----------------------|--------------------|------------------|--------------------|----------------------|--------------------|
| Wind Turbine | 0 | 14,000 | 14,000 | 14,000 | 14,000 |
| Rectifier | 0 | 0 | 0 | 2,000 | 2,000 |
| Wind Turbine Tower | 0 | 7,000 | 7,000 | 7,000 | 7,000 |
| Inverters (2) | 0 | 0 | 0 | 6,000 | 6,000 |
| Batteries (8) | 0 | 0 | 0 | 1,550 | 1,550 |
| Ice Maker | 10,000 | 10,000 | 10,000 | 10,000 | 10,000 |
| Ice-maker Controller | 0 | 2,000 | 2,000 | 0 | 0 |
| Ice-maker Mods | 0 | 5,000 | 5,000 | 0 | 0 |
| Diesel Generator | 6,000 | 0 | 6,000 | 0 | 6,000 |
| Fuel Tank | 1,500 | 0 | 1,500 | 0 | 1,500 |
| Building | 3,000 | 3,000 | 3,000 | 3,000 | 3,000 |
| Balance of System | 2,000 | 2,500 | 3,000 | 3,500 | 4,000 |
| Shipping/Insurance | 1,090 | 2,110 | 2,740 | 2,610 | 3,240 |
| TOTAL | 23,590 | 45,610 | 54,240 | 49,660 | 58,290 |

The financial assumptions were as follows:

- The real discount rate was 8%.
- The economic life of the project was 20 years. (All components except the ice maker, diesel generator, and batteries were assumed to last for this time.)
- The loan interest rate was 10%.
- The loan period was 10 years.

7.2 The Characteristics of Good Sites for Directly Connected Wind Ice-Making Systems

The following is a checklist for the field surveyor looking for good sites to place a directly connected wind ice-making system. Of course, every site is not required to possess all of these attributes. Ideally, though, a feasibility analysis should be performed for each site that has at least a few of the attributes:

- The local cost of ice is greater than U.S.\$0.03 per pound or ice is not available at all.
- The community requires at least 2,000 pounds of ice per week, averaged over the entire year.
- The community requires no more than 7,000 pounds of ice per week, averaged over the entire year, for every U.S.\$50,000 in capital investment that is available.
- The community must have a wind turbine site that would provide an annual average wind speed at the hub height of at least 6 m/s.
- The wind resource should be somewhat “constant” (i.e., winds are sustained above 6 m/s for at least two hours at a time for much of the high-demand season).
- The community has a “good” correlation between the demand for ice and the wind resource. That is, the high-demand season should roughly correspond to the high-wind season.
- The community has good organization (i.e., someone in charge) and a relatively stable population (i.e., +/- 15% fluctuation around the annual average).
- The cost of annual ice-maker maintenance, including transportation and labor, should be “reasonable” (i.e., no more than about U.S.\$2,000).

- A source of water should exist for the ice maker and it must be reliable in the maximum quantity required by the ice maker (i.e., about 10 L/min, or 2.5 gal/min). Seawater or groundwater is preferred. Surface water may require purification.
- There should be a perception that an ice-making project will benefit the community in some way—for example, the economy, public health, or quality of life.

7.3 Conclusions and Future Plans

The North Star D-12 Ice Maker, which has been the focus of the Phase 2 and 3 investigations, would require extensive modifications to meet most of the goals for a variable-frequency ice-maker system that were given in Section 6.2. We also suspected that any commercially available ice maker would likely require some modification to meet those specifications. The cost-of-ice calculations in Section 7.1 have shown that directly connected wind-ice-making systems are cost competitive with most of the other ice-making options, even when modifications significantly affect the cost of the ice maker. It has also been shown that the wind-only system is more cost effective than the wind-inverter system. Of course, all of these conclusions are based on our belief that all of the technical obstacles can be overcome with a reasonable engineering effort.

Based on these findings, NREL believes that further development of directly connected wind-ice making systems could be a worthwhile joint business venture for a small wind turbine manufacturer and a commercial ice-maker manufacturer

8. Bibliography

- Ahachad, M.; Charia, M.; and Bernatchou, A. (July 1993). "Solar Absorption Heat Transformer Applications to Absorption Refrigerating Machines." *International Journal of Energy Research*; Vol. 17, No. 5, pp. 719-726.
- ASHRAE. (1992). "Chapter 35: Compressors." *1992 Systems and Equipment Handbook*.
- Berger International, Inc. (May 1986). "Renewable Energy Resources Field Testing Application Review for Field Test #6: Photovoltaic/Diesel Powered Ice Making Plant at Wadi El Raiyan." Prepared for U.S. Agency for International Development, PB87-155792.
- Boubakri, A.; et. al. (1992). "Experimental Study of Adsorptive Solar-Powered Ice Makers in Agadir (Morocco)—1. Performance in Actual Site." *Renewable Energy*; Vol. 2. No. 1.
- Condumex. (July 1993). "Eolo-Frio: Refrigeration Plant Using Wind Energy." Technical and commercial information.
- Davis, H.C. (1994). "Wind-Electric Ice Making for Developing World Villages." M.S. Thesis. Boulder, Colorado. Department of Civil Engineering, University of Colorado.
- Dixit, D.K. (1992). "Techno-Economic Evaluation of the Potential for Cold Storages in India." *Proceedings of Solar '92; June 15-18, 1992, Cocoa Beach, Florida*. American Solar Energy Society; pp. 209-211.
- Energy Concepts. (??). Marketing literature for the ISAAC solar-powered ammonia absorption refrigerator, Annapolis, Maryland, (301) 266-6521.
- Erickson, D. (July/August 1994). "Solar Icemakers." *Solar Today*; Vol. 8, No. 4, pp. 21-23.
- IEEE Standards Board. (1992). "IEEE Standard Test Procedure for Polyphase Induction Motors and Generators, IEEE Std. 112-1991." New York: IEEE.
- Raheman, H.; Gupta, C.P. (1989). "Development of a Solar-Energy-Operated Vapour-Absorption-Type Refrigerator." *Applied Energy*; Vol. 34, pp. 89-98.
- Rumondor, J. (1992). "Status Report—Rural Electric Cooperatives in Indonesia." *Proceedings of Productive Uses of Electricity in Rural Areas Workshop. November 15-19, 1982; Dhaka, Bangladesh*, pp. 66-71.
- Smith, Granville J. (??). "Productive Uses of Wind Power Ice Making Project Identification, Honduras, July 1994-July 1995." National Rural Electric Cooperative Association.
- Woollatt, D. (June 1993). "Factors Affecting Reciprocating Compressor Performance." *Hydrocarbon Processing*; Vol. 72, No. 6, pp. 57-64.

REPORT DOCUMENTATION PAGE

Form Approved
OMB NO. 0704-0188

Public reporting burden for this collection of information is estimated to average 1 hour per response, including the time for reviewing instructions, searching existing data sources, gathering and maintaining the data needed, and completing and reviewing the collection of information. Send comments regarding this burden estimate or any other aspect of this collection of information, including suggestions for reducing this burden, to Washington Headquarters Services, Directorate for Information Operations and Reports, 1215 Jefferson Davis Highway, Suite 1204, Arlington, VA 22202-4302, and to the Office of Management and Budget, Paperwork Reduction Project (0704-0188), Washington, DC 20503.

| | | | |
|--|--|---|---|
| 1. | 2. REPORT DATE July 1998 | 3. REPORT TYPE AND DATES COVERED Technical Report | |
| 4. TITLE AND SUBTITLE Wind-Electric Icemaking Project: Analysis and Dynamometer Testing Volume I | | | 5. FUNDING NUMBERS C: TA: WE805020 |
| 6. AUTHOR(S) Rick Holz, P.E., Vahan Gervorgian, Ph.D., Steve Drouilhet, P.E., Ed Muljadi, Ph.D. | | | |
| 7. PERFORMING ORGANIZATION NAME(S) AND ADDRESS(ES) National Wind Technology Center National Renewable Energy Laboratory 1617 Cole Blvd. Golden, CO 80401-3393 | | | 8. PERFORMING ORGANIZATION REPORT NUMBER |
| 9. SPONSORING/MONITORING AGENCY NAME(S) AND ADDRESS(ES) National Renewable Energy Laboratory 1617 Cole Blvd. Golden, CO 80401-3393 | | | 10. SPONSORING/MONITORING AGENCY REPORT NUMBER TP-500-24010 |
| 11. SUPPLEMENTARY NOTES | | | |
| 12a. DISTRIBUTION/AVAILABILITY STATEMENT National Technical Information Service U.S. Department of Commerce 5285 Port Royal Road Springfield, VA 22161 | | | 12b. DISTRIBUTION CODE UC-1213 |
| 13. ABSTRACT (<i>Maximum 200 words</i>) The wind/hybrid systems group at the national Renewable Energy Laboratory has been researching the most practical and cost-effective methods for producing ice from off-grid wind-electric power systems. The first phase of the project, conducted in 1993-1994, included full-scale dynamometer and field testing of two different electric ice makers directly connected to a permanent magnet alternator. The results of that phase were encouraging and the second phase of the project was launched in which steady-state and dynamic numerical models of these systems were developed and experimentally validated. The third phase of the project was the dynamometer testing of the North Star ice maker, which is powered by a 12-kilowatt Bergey Windpower Company, Inc., alternator. This report describes both the second and third project phases. Also included are detailed economic analyses and a discussion of the future prospects of wind-electric ice-making systems. The main report is contained in Volume I. Volume II consists of the report appendices, which include the actual computer programs used in the analysis and the detailed test results. | | | |
| 14. SUBJECT TERMS renewable energy; wind energy; icemaking | | | 15. NUMBER OF PAGES |
| | | | 16. PRICE CODE |
| 17. SECURITY CLASSIFICATION OF REPORT Unclassified | 18. SECURITY CLASSIFICATION OF THIS PAGE Unclassified | 19. SECURITY CLASSIFICATION OF ABSTRACT Unclassified | 20. LIMITATION OF ABSTRACT UL |